NASA CR-135113
TRW ER-7821F

PMR POLYIMIDE/GRAPHITE FIBER COMPOSITE FAN BLADES

BY
P. J. CAVANO
W. E. WINTERS

TRW EQUIPMENT

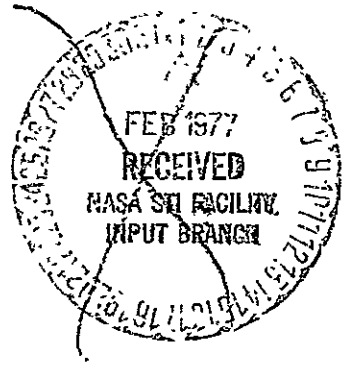

prepared for
NATIONAL AERONAUTICS AND SPACE ADMINISTRATION
NASA Lewis Research Center

Contract NAS 3-18939

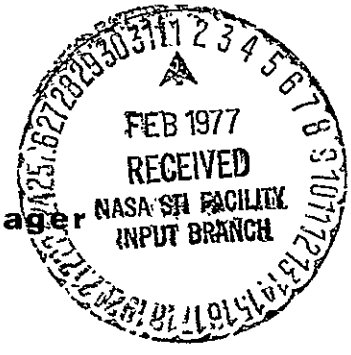

RAYMOND D. VANNUCCI, Project Manager

1. Report No.	2. Government Accession No.	3. Recipient's Catalog No.
NASA CR-135113		

4. Title and Subtitle	5. Report Date
PMR POLYIMIDE/GRAPHITE FIBER COMPOSITE FAN BLADES	December 15, 1976
	6. Performing Organization Code
7. Author(s)	8. Performing Organization Report No.
P. J. Cavano and W. E. Winters	ER-7821F
	10. Work Unit No.
9. Performing Organization Name and Address	11. Contract or Grant No.
TRW Inc. 23555 Euclid Avenue Cleveland, Ohio 44117	NAS3-18939
	13. Type of Report and Period Covered
12. Sponsoring Agency Name and Address	Contractor Report
National Aeronautics and Space Administration Washington, D.C. 20546	14. Sponsoring Agency Code

15. Supplementary Notes

Project Manager, R. D. Vannucci, Materials and Structures Division
NASA Lewis Research Center, Cleveland, Ohio

16. Abstract

Fourteen ultra-high speed fan blades, designed in accordance with the requirements of an ultra-high tip speed blade axial flow compressor, were fabricated from a high-strength graphite fiber tow and a PMR polyimide resin. Two of the blades contained glass roving hybridizing fiber. The PMR matrix was prepared by combining three monomeric reactants in methyl alcohol, and the solution was then applied directly to the reinforcing fiber for subsequent in situ polymerization, rather than employing a previously prepared prepolymer varnish. All prepreg employed on the program was prepared in-house using this technique. Six of the molded blades were completely finished by secondary bonding of root pressure pads and an electroformed nickel leading edge sheath prior to final machining. The results of the spin testing of nine PMR fan blades are given.

A two-phase material study prior to blade fabrication included an examination of neat resin tensile properties of the PMR resin at four formulated molecular weight levels. Additionally, three formulated molecular weight levels were investigated in composite form with both a high modulus and a high strength fiber, both as-molded and postcured, in room temperature and 232°C transverse tensile, flexure and short beam shear. Other preparatory work included an evaluation of five different mixed fiber orientation panels simulating potential blade constructions. Tests on these angle-plied laminates included flexure, short beam shear and tensile in both the longitudinal and transverse directions.

17. Key Words (Suggested by Author(s))	18. Distribution Statement
Polyimide Resin High Temperature Resin Graphite Fiber Composites In Situ Polymerization Hybrid Composites Jet Engine Fan Blade	Unclassified - Unlimited

19. Security Classif. (of this report)	20 Security Classif. (of this page)	21. No. of Pages	22. Price*
Unclassified	Unclassified	103	

* For sale by the National Technical Information Service, Springfield, Virginia 22151

FOREWORD

This document represents the final report of the work accomplished between 14 April 1975 and 15 August 1976 by TRW Incorporated for the National Aeronautics and Space Administration, Lewis Research Center, Cleveland, Ohio, under Contract NAS3-18939 on a program entitled, "PMR Polyimide/Graphite Fiber Composite Fan Blades." This program was conducted under the technical direction of Mr. Raymond D. Vannucci, NASA Project Manager.

Work on the program was conducted at TRW Materials Technology of TRW Equipment, Cleveland, Ohio. Mr. William E. Winters was the TRW Program Manager; the TRW Project Engineer was Mr. Paul J. Cavano.

Mr. Roy Hager was the NASA-Lewis Project Manager for the program which provided the fan blade spin test results discussed in the text. During the course of spin testing these blades at Pratt and Whitney Aircraft, East Hartford, Connecticut, several individuals were responsible; included were Messrs. H. Marman, D. Sulam and W. Gilroy.

PMR POLYIMIDE/GRAPHITE FIBER COMPOSITE FAN BLADES

by

P. J. Cavano and W. E. Winters

SUMMARY

The major objective of the program was to resolve a number of material, design and process problems, previously identified, that affect the fabrication, quality and performance of PMR polyimide resin matrix, graphite fiber reinforced ultra-high speed jet engine fan blades. This program employed elements of technology developed on two previous NASA programs, NAS3-15335 and NAS3-17772. The former program was concerned with the fan blade design, tool design and blade fabrication development, while the latter program emphasized optimization of the preparation and processing of the PMR polyimide resin matrix system. The PMR matrix system was prepared by combining three monomeric reactants in methyl alcohol and then applying the solution directly to the reinforcing fiber for subsequent in situ polymerization, rather than employing a previously prepared prepolymer varnish.

During the course of the program, fourteen ultra-high speed fan blades, designed in accordance with the requirements of an ultra-high tip speed axial flow compressor, were fabricated from a high-strength graphite fiber tow and the PMR polyimide resin. Two of the blades contained glass roving hybridizing fiber. Prepreg for all the blades, including the hybrid blades, was prepared in-house, providing close control of the ply thickness characteristic necessary in the fabrication of high precision composite blades. Six of the molded blades were completely finished by secondary bonding of root pressure pads and an electroformed nickel leading edge sheath prior to final machining of the root and tip contours to blueprint dimensions. The results of the spin testing of these blades and others are discussed.

A two-phase material study was conducted prior to fabricating the fan blades. These studies included an examination of neat resin tensile properties of the PMR resin at four different formulated molecular weight levels. Additionally, three formulated molecular weight levels were investigated in composite form with both a high modulus and a high strength fiber. The transverse tensile, flexure and short beam shear properties were determined at room temperature and 232°C using both as-molded and postcured specimens. Other preparatory work included an evaluation of five different ply orientation panels simulating potential blade constructions. Tests on these angle-plied laminates included flexure, short beam shear and tensile in both the longitudinal and transverse directions.

The objectives of the program were successfully achieved. The materials systems selected were shown to be quite suitable for the fabrication of fan blades of this type. The process methods employed were found to be appropriate for a manufacturing run of the size undertaken and capable of producing complex high quality, die molded aerospace hardware. The PMR matrix resin was found to be an easily processable system with a range of formulated molecular weight

compositions providing a spectrum of flow characteristics and excellent mechanical properties.

The introduction of the PMR resin matrix, the use of an interspersed ply stacking sequence, and the substitution of an alternate reinforcing fiber, along with other material and process modifications, produced a 137% improvement in the failure-initiation stress level of the blades in spin testing. Even with this magnitude of improvement, major design modifications appear necessary to achieve fan blade goals.

TABLE OF CONTENTS

TABLE OF CONTENTS (continued)

LIST OF TABLES

LIST OF FIGURES

LIST OF FIGURES (continued)

1.0 INTRODUCTION

This document constitutes the final report on NASA-Lewis Contract NAS3-18939, initiated 14 April 1975, and describes the work performed between that date and 15 August 1976. The major objective of the program was to resolve a number of material, design and process problems, previously identified, that affect the fabrication, quality and performance of PMR polyimide resin matrix, graphite fiber reinforced ultra-high speed fan blades. This program employed elements of technology developed on two previous NASA programs, NAS3-15335 and NAS3-17772 (1). The former program was concerned with the fan blade design, tool design and blade fabrication development, while the latter program determined the feasibility of, and reduced to practice, the techniques of complex component fabrication with the unique PMR polyimide resin system, which uses three monomeric reactants instead of a prepolymer varnish. After a material characterization phase, this program culminated in the fabrication of 14 ultra-high speed fan blades based on knowledge gained in the earlier programs and the material characterization efforts of the current program.

The program was divided into three basic phases described below.

Task I - Preliminary Material Studies

The objective of this task was to compare the room and elevated temperature (232°C) properties of three different formulated molecular weight (FMW) PMR resins, each on two different fiber types, both before and after postcure. Additionally, tensile properties of four neat resins (1100, 1300, 1500, 1900 FMW) were investigated. At the conclusion of this task, the single most appropriate FMW system was selected for study in the next phase.

Task II - Laminate Design and Final Material Studies

Using the selected PMR system and two different reinforcing fiber types (high strength and high modulus), a series of panels with various ply orientations and stacking sequences, representing candidate fan blade construction, were evaluated by mechanical testing at room temperature and 232°C with and without thermal cycling. These data were used to select the fiber orientation and type to be employed in the subsequent fabrication of fan blades.

Task III - Blade Fabrication and Evaluation

During this phase of the program, 14 fan blades were molded, including two hybrid blades containing glass fibers in addition to the selected graphite fibers. These blades were evaluated non-destructively by such methods as radiography, ultrasound, dimensional inspection and natural frequency testing. Further efforts involved the selection of adhesives and the development of bonding methods for application of root pressure pads and electroformed nickel leading edges. Six of the blades, with pressure pads and leading edges, were finish machined.

The program objective was completely fulfilled. The PMR polyimide was found to be safe, easy to handle, processable with relatively wide processing limits,

and suitable for the fabrication of complex hardware components. Spin test results of the ultra-high speed fan blades indicated that a 137% improvement in the failure-initiation stress level was achieved. Details of the materials, evaluation methods, processing techniques employed and results are described in the body of the following text.

2.0 MATERIAL AND PROCESS INVESTIGATIONS

The following sections discuss investigations prior to initiating the manufacture of the fan blades. Details are given on the fibers used, PMR resin preparation, prepregging techniques, test panel fabrication procedures, and the experimental results obtained.

2.1 Reinforcements

The two fiber types chosen were both tow materials from Hercules Incorporated; specifically, the two materials were Magnamite HM-S (high modulus) and A-S (high strength graphite fiber). The tow form was preferred because the untwisted tow can be spread in the prepregging operation to provide a specific, calculated per ply thickness. This requirement is important in manufacturing prepreg to be used in blade fabrication because it is necessary to exactly fill the die cavity with a fixed, predetermined number of plies of varying orientation. The wide range in properties between these fibers allowed for the observation of differences with the varying formulated molecular weight PMR systems. The vendor advertised property values for the two fibers are as shown below:

	A-S		HM-S	
Minimum Tensile Strength	2.8 GPa	410 ksi	2.3 GPa	340 ksi
Modulus	207-234 GPa	30-34 msi	345-379 GPa	50-55 msi

2.2 Resin Preparation

The monomeric reactant solution for the PMR systems was prepared by combining a diamine and two ester-acids in methyl alcohol. The specific compounds used are shown below:

Material	Abbreviation	Source
Monomethyl ester of 5-Norbornene-2, 3-dicarboxylic acid	NE	Burdick & Johnson
3, 3', 4, 4' - benzophenonetetracarboxylic dianhydride	BTDA	Aldrich
4, 4' - methylenedianiline	MDA	Eastman Kodak
Methyl alcohol (absolute)	-	Fisher

The required dimethyl ester of 3, 3', 4, 4' benzophenometetracarboxylic acid (BTDE) was prepared by refluxing benzophenonetetracarboxylic dianhydride (BTDA) with an excess of anhydrous methyl alcohol for a period of two hours after initiation of boiling. The BTDA was purchased commercially; the material was procured from Aldrich Chemical Company, Incorporated and is described as 96% pure with a two degree (^{o}C) melting point range. Esterification calculations were conducted on the basis of a 100% BTDA content and excess alcohol was added in sufficient quantity to yield a final 50 w/o solution of BTDE in methyl alcohol. Refluxing was accomplished in a 1000 ml flat-bottom glass reaction kettle (side

walls insulated) positioned on the platform of a heated magnetic stirring device. In this way, mechanical agitation of the solution could be maintained continuously during reflux.

After cooling of the BTDE solution, it was mixed with a previously prepared 50 w/o solution of 4, 4' methylenedianiline (MDA) and monomethyl ester of 5-norbornene-2, 3-dicarboxylic acid (NE) in methyl alcohol. The 50 w/o solution of the PMR-15 had a specific gravity of 1.000 and a viscosity in the range of 40 $N \cdot s/m^2$ (40 cps).

The various formulated molecular weight PMR systems evaluated were obtained by using the monomeric reactant stoichiometries shown below:

FMW	Moles of BTDE	Moles of MDA	Moles of NE
1100	1.257	2.257	2.000
1300	1.670	2.670	↓
1500	2.084	3.084	
1900	2.909	3.909	

The number of moles of the momomeric reactants in each of the monomeric solutions was governed by the following ratio:

$$n : (n + 1) : 2$$

where n, (n + 1) and 2 are the number of moles of BTDE, MDA and NE, respectively. The formulated molecular weight (FMW) is considered to be the average molecular weight of the imidized prepolymer that could have been formed if amide-acid prepolymer had been synthesized. The equation for FMW is:

$$FMW = n\ MW_{BTDE} + (n+1)\ MW_{MDA} + 2\ MW_{NE} - 2(n+1)\left[MW_{H_2O} + MW_{CH_3OH}\right]$$

where MW_{BTDE}, MW_{MDA}, etc. are the molecular weights of the indicated reactants and by-products. (2)

It is now common practice to designate the specific FMW system being discussed by eliminating the last two zeros from the FMW value and appending the remaining two digits to the PMR abbreviation. For example, a PMR system of a 1500 FMW becomes PMR-15. This convention is followed throughout this report.

2.3 Prepreg Preparation

Impregnation of the fiber was carried out by dry winding the fiber on a 1.5 m (5 ft) diameter drum and depositing the PMR solution onto the fiber surface with a precision metering device. The number of tows per inch was calculated with the following equation:

$$N = \frac{T\ V_f\ \rho_f}{W}$$

where: N = numbers of tows per inch
T = thickness per ply
V_f = fiber fraction
ρ_f = fiber density
W = fiber weight per unit length

Figure 1 shows the 1.5 m drum of the collimating unit that was used for the preparation of all prepreg on the program. The tow was wound with a slight tension created by an electrically operated spool brake. A roller and hoop arrangement spread the 10,000 filament tow so that an even fiber placement was achieved.

Prepreg thickness calculations were based on obtaining a finished molded ply thickness of 0.254 mm (10 mils) and a nominal fiber volume of 55-60 v/o. Total volatile content was brought to 10 to 12% by using a bank of infra-red lamps on the rotating material on the drum and a final treatment on a heated staging table.

2.4 Preliminary Material Studies

This portion of the program was devoted to a comparison of FMW's, in neat resin and composite form, at room temperature and 232°C. Table I summarizes the type of data collected in a test matrix. Experimental detail as well as evaluation results and conclusions are given below.

2.4.1 Neat Resin Evaluation

As an examination of the effect of PMR formulated molecular weight (FMW) on mechanical properties, an evaluation was made on neat resin moldings without reinforcement. While measurement of composite properties represents a characterization of fiber and matrix resin in concert, it was felt that the determination of strength, stiffness and ductility of the polyimide resin would assist in the final selection of the most appropriate molecular weight resin for fan blade fabrication and performance. Neat resin moldings were thus prepared at four FMW's and tested for tensile properties.

Monomer solutions were prepared as described above to produce polymers of 1100, 1300, 1500 and 1900 formulated molecular weight. Because the mechanical testing of unreinforced polymers is very sensitive to flaws or contamination, extreme care was taken in maintaining the material as free of foreign material as possible. The 50% methanol solutions were thus mixed and filtered through a Buchner filter before evaporation of the solvent in an air circulating oven. The containers of solution were placed on porous Teflon coated glass cloth and covered with a large inverted glass beaker to preclude dust particles settling into the resin.

The solutions were evaporated to dryness at 82°C (180°F) over a period of 71 hours. The solid form material was removed from the beaker, crushed, replaced in the beaker and imidized at 121°C (250°F) for three hours and two additional hours at 204°C (400°F). It was noted at this point that the 1100 FMW experienced additional foaming and the 1300 and 1500 FMW exhibited slight melting while the 1900 showed essentially no change during the 204°C exposure. The resins were then ground in a clean mortar and pestle and stored in clean sealed containers.

Moldings were prepared in a close fitting 6.4 x 25.4 cm (2-1/2 x 10 inch) die equipped with stops to insure uniform thickness of the resulting moldings. The procedure involved spreading the ground resin in the die cavity and inserting the cold tool, with stops, into a preheated platen press at 232°C (450°F). A 10 minute hold was maintained before applying pressure, in this case 13.8 MPa (2000 psi), then raising the temperature to 316°C (600°F). Resin was expelled until stops were reached. After the extruded resin gelled, the stops were removed and full pressure reapplied and held at 316°F (600°F) for one hour. Pressure and temperature were reduced simultaneously and the moldings removed from the tool. Half of each molding was postcured 16 hours at 343°C (650°F) with a rise to that temperature over an eight hour period.

Table II presents data on the moldings. It will be noted that, although the same thickness stops were used on all moldings, there is a significant increase in thickness with molecular weight while no differences are noted in specific gravity as calculated from weight and dimensions. Additional densification apparently occurred at lower FMW after gelation when full molding pressure was applied to the material. It is also interesting to note a slightly higher mold and postcure dimensional shrinkage with increasing FMW.

Visually, the moldings were smooth and appeared dense. The lower FMW moldings were slightly translucent to strong light which permitted examination for internal flaws, a few of which were identified. The 1900 FMW and none of the postcured moldings would pass light.

The moldings, representing eight conditions (four FMW's and postcure/no postcure), were used to make tensile specimens. A micro-specimen configuration was used which was 64 x 13 mm (2.5 x 0.5 inches) with a waisted 32 mm (1.25 inch) gage length form-ground to 10 mm (0.375 inch). To protect the surfaces from scratches, masking tape was adhered to the faces during grinding. Also, all specimen edges were hand polished (longitudinally) with 600 grit abrasive paper along the gage thickness to remove grinding lines which might create notches or stress risers during testing.

2.4.2 Composite Panel Evaluation

Using prepreg prepared as described above, laminates of these FMW's (1100, 1300, and 1500) were molded, postcured, ultrasonically inspected and machined into test specimens.

The molding cycle followed with each system varied only in the application of pressure. Both the A-S and the HM-S laminates of PMR-15 were prepared as follows:

a) Imidize prepreg stack 22 x 22 cm x 8 plies (8-1/2 inch x 8-1/2 inch) at 204°C (400°F) for two hours in oven.

b) Place stack in die preheated to 232°C (450°F).

c) Apply contact pressure and hold 10 minutes.

d) Apply 6.9 MPa (1000 psi) and set controllers for 316°C (600°F). This represents a temperature rise rate of 4.2°C/min. (7.5°F/min.).

e) Hold at 316°C (600°F) for one hour after part reaches 316°C.

f) Fan cool die to 260°C (500°F) and reduce pressure by one-half.

g) Fan cool die to 204°C (400°F) and reduce pressure to contact.

h) Introduce cooling water in platens to bring die to room temperature.

This same cycle was followed with the PMR-13 laminates except 3.5 MPa (500 psi) was used. The PMR-11/HMS-S laminate was done in the same way except 1.4 MPa (200 psi) was used after the 232°C hold period to limit flow. Just before the part reached 316°C, 6.9 MPa (1000 psi) was applied. The point of application of the additional pressure was determined by probing the expelled resin to ascertain gelation at the end of the gel period; the additional pressure was applied and a minute amount of added flow was experienced.

The technique of altering pressure (to compensate for the higher flow experienced with lower FMW's) with the various FMW's was done to maintain a relatively constant fiber volume in all laminates so that a direct comparison of mechanical test data could be made. The prepreg was all prepared in the same manner as anticipated for blade fabrication; i.e., the prepreg was calculated to yield 0.254 mm/ply (10 mils/ply) at a fiber volume of 57½ v/o and then an additional amount of resin was added to account for 3 w/o flow. Flow values on the laminates ranged from 1.2 w/o to 3.0 w/o.

Once the fabrication of all test laminates was completed, and the appropriate sections postcured for 16 hours at 343°C (650°F), laminates were ultrasonically inspected again after postcure and weight losses recorded. All the sonic C-scans on sections before postcure were completely clear with the exception of the expected edge effects. Some of the sections after postcure did disply minor, occasional indications, associated with the fiber orientation. No trend was observable with regard to formulated molecular weight (FMW), but it seemed that the A-S reinforced laminates did show a higher incidence of this effect. This might be related to the fact that bare A-S fibers will show some thermo-oxidative weight loss in thermal exposures as high as 343°C (650°F), while the HM-S material is quite stable.

It is felt that this latter fact accounts for the higher weight losses in postcure noted with the A-S laminates vs. the HM-S laminates. The values recorded are shown in the table below.

Laminate Weight Loss in Postcure (%)

	HM-S	A-S
1100 FMW	1.2	1.6
1300 FMW	1.2	1.7
1500 FMW	1.2	1.8

From these postcured laminates, specimens were machined for triplicate determinations to fulfill the conditions shown in table I. Test techniques and specimens designs were conventional. The short beam shear specimens were run at a span-to-depth ratio of 4:1 and the three point flexure specimens at approximately 35:1. The transverse tensile specimens were tabbed specimens with a pin loading arrangement. The straight-sided specimens had an overall length of 88.9 mm (3.5 in.) with a 50.8 mm (2 in.) gage length and a width of 12.7 mm (0.5 in.).

2.4.3 Evaluation Results and Discussion

Table III displays the results of the neat resin tensile tests. The conclusions that seem clear after a review of these data include:

a) The strain-to-failure values demonstrate a relatively high level for a high temperature cross-linked polyimide system.

b) Postcure degrades both strength and elongation but seems to have no effect on the modulus of the system.

c) With the exception of the 1500 FMW material, values for the range of FMW's studies seems closely grouped indicating no particular trend. The 1500 data do seem anomalous, and it is not known whether the 1500 represents a real deviation or, more probably, if some experimental problem was encountered that is not apparent. Further data would have to be gathered before these values were accepted as typical of the system.

All of the data from the composite testing from the Preliminary Materials Studies are shown in tables IV, V and VI. A review of the data shown in table IV, Transverse Tensile Results, leads to the conclusions given below:

a) The fiber system plays a larger role in determining properties than the various FMW systems studied.

b) The A-S fiber composites, when compared to the HM-S, show a higher strength and a higher strain-to-failure at room and elevated temperature and a slightly higher elastic modulus at room temperature.

c) Postcure reduces room temperature strength with all systems; at 232°C the HM-S strength shows no change, while the A-S shows a minor increase. Postcure seems to reduce the strain-to-failure values of the A-S composites at room temperature and appears to increase them slightly at 232°C. Strain-to-failure with the HM-S does not seem affected by postcure, nor does modulus with either system.

d) In comparing the FMW's, the room temperature strength of the nonpostcured resin, with both fibers, increases slightly with increasing FMW. After postcure, the 232°C values of the HM-S are relatively constant, and the A-S shows a lower value for the 1100 FMW compared to the other two FMW's. The room temperature values after postcure do not show any significant difference among the FMW systems.

Table V displays all the short beam shear values collected. The conclusions that follow from a review of these data are:

a) The fiber controls shear strength. All the A-S average values are higher than any of the HM-S average values for any condition examined. The HM-S values are closely grouped and little difference is seen with regard to postcure or FMW.

b) Postcure seems to offer no advantage with the HM-S fiber in the temperature range studied. With the A-S fiber, the postcure improved the elevated temperature performance but degraded the room temperature values. The 1500 FMW with the A-S fiber shows the greatest gain in 232°C (450°F) performance with the postcure employed.

c) No definitive trend is seen with regard to FMW. The 1500 FMW displays the highest room temperature, nonpostcured values with the A-S fiber, although the 1100 FMW exhibits the highest value with the HM-S fiber.

d) In examining the data with regard to temperature performance, the fiber seems to play a large role. For instance, in comparing HM-S data, the 232°C (450°F) averages for all three FMW's are only slightly below those of the room temperature values. The A-S fiber composites show a much larger drop with tests at 232°C (450°F) but still remain above all of the HM-S averages.

An examination of the composite flexural data in table VI leads to the following conclusions:

a) As might be expected, the A-S strength values are all higher than any of the HM-S numbers. The moduli values for the two systems are in the appropriate range for the fibers used and the fiber volume chosen.

b) Postcure seems to have little effect on the room temperature flexural properties of HM-S fiber composites. The A-S system shows a significant drop in room temperature strength performance with the postcure employed, with the largest differential seen with the 1500 FMW. Conversely, the postcured A-S/1500 system displays the greatest improvement in elevated temperature performance with the postcure.

c) In comparing FMW's using A-S fiber, the 1100 FMW shows the highest strength and modulus values at any condition. The FMW does not appear to have a significant effect with the HM-S fibers.

2.4.4 Preliminary Study Conclusions

In the preceding section, the conclusions listed were based only on the data collected for each of the individual test sequences. Considering all of these data together, the conclusions given below were drawn.

a) A strong, consistent trend was not observed that would allow recommendation of formulated molecular weight PMR system.

b) Postcure should not be employed unless required by anticipated, specific conditions such as extreme high temperature service, a need for exceptional dimensional stability, etc.

Application of these conclusions to the next phase of the program would indicate: a) the molding cycle used was appropriate, b) postcure would not be required, c) any of the three FMW's evaluated (PMR-11, -13, -15) could be used.

With regard to the latter conclusion, a basis was sought to identify characteristics that would indicate a preferred FMW. It is known (2)(3) that the 1100 FMW material can be made to yield more flow during molding than the higher FMW's which would be a decided advantage in the blade fabrication. On the other hand, more data, both in-house and industry-wide, have been collected on the 1500 FMW. It was decided therefore to initiate the next phase of the materials study program with a limited examination of altered processing cycles with the PMR-15 to determine if significantly greater flow could be obtained.

2.5 Laminate Design and Final Material Studies

As was noted above, the preliminary materials study resolved a number of questions regarding fabrication of the fan blades. In this phase, the effort involved an examination of altered PMR-15 mold cycles, an investigation of a number of simulated blade ply orientations, and a thermal cycling experiment to determine the effect of repetitive excursions from 232°C to room temperature. The details of these studies are given in the following sections.

2.5.1 PMR-15 Flow Studies

The objective of this series of experiments was to determine if an alternate imidizing/molding cycle could be identified that would provide significantly improved flow performance with the 1500 FMW system. The planned test matrix represented four major changes from the standard molding conditions previously described; these were:

a) Decreasing the insertion dwell time from 10 minutes to 5 minutes.

b) Introducing a 10 minute hold at 260°C (500°F) in the rise to 316°C (600°F) from 232°C (450°F).

c) Introducing a 20 minute hold at 288°C (550°F) in the rise to 316°C (600°F) from 232°C (450°F).

d) Using a temperature rise rate of 16.7°C/minute (30°F/minute) from 232°C (450°F) to 288°C (550°F) with a 10 minute hold at 288°C temperature.

All panels were 102 x 102 x 2 mm (4 x 4 x 0.080 inches) and were oven imidized. The same die was used for each experiment to insure the same clearances for resin flow. The panels were all molded at 6.9 MPa (1000 psi), held 10 minutes at 316°C (600°F) and demolded hot. The results of these trials are shown in Table VII.

As can be seen from Table VII, the majority of the panels with altered cycles displayed inferior surface conditions. The "flawed" surface condition noted in the table indicates that the panels had blisters or surface depressions. The only panels showing a good surface, besides those molded in a standard manner (Lam. No. 1 and 2), were those molded with a delay in temperature climb at 288°C (550°F). It was felt that the minor increase in flow attained with these cycles did not warrant

the risk involved in altering a standard molding cycle that had been employed so often in the past with complete success. It seems clear that altered molding cycles with the PMR-15 formulated molecular weight system cannot significantly increase the characteristic flow behavior of the PMR-15, and that there are attendant quality risks in attempting to gain minor flow improvements. For this reason, it was planned to continue to use the standard molding cycle, which employs a 10 minute hold at the 232°C (450°F) insertion temperature with only contact pressure and to use the PMR-11 system to obtain the resin flow required in blade manufacture.

2.5.2 Ply Orientation Panel Studies

This task consisted of fabricating and evaluating five laminates with various ply orientation arrangements using both HM-S and A-S fibers and the PMR-11. The laminate constructions, simulating to some degree the orientations encountered in typical blade designs, for the 21.6 x 21.6 x 0.6 cm (8-1/2 x 8-1/2 x 1/4 inch) panels are shown in table VIII.

The five panels described in table VIII were fabricated with the cycle (chosen to simulate a blade molding process) shown below:

a) The prepreg stack was imidized at 204°C (400°F) for two hours in a tool. The cold prepreg stack was placed in a cold tool and a thin metal plate added. This plate represented a pressure of 689 Pa. (0.1 psi) on the part. The tool was placed between the cold platens of a press and the temperature set in the following manner; 54°C for 20 minutes, 88°C for 20 minutes, 121°C for 20 minutes and 204°C for 135 minutes. The slow heat-up cycle was used to prevent any possible disruption of fiber orientation due to the expulsion of condensation volatiles.

b) The tool was cooled to room temperature by introducing cooling water in the press platens and the part removed.

c) The imidized stack was placed in die preheated to 232°C (450°F).

d) Contact pressure was applied and held 10 minutes.

e) A pressure of 1.4 MPa (200 psi) was applied and the controllers set for 316°C (600°F). This represented a temperature rise rate of 4.2°C/minute.

f) Twenty minutes after raising the controllers to 316°C, the pressure was increased to 6.9 MPa (1000 psi). This technique of step-wise pressure application limits resin flow to a nominal level. With these laminates, a nominal flow of about 3 w/o was obtained.

g) The 316°C temperature was held for 1-1/2 hours.

h) The die was fan cooled to 260°C and the pressure reduced by half.

i) The die was further fan cooled to 204°C and the pressure reduced to contact.

j) Water was introduced into the platens to bring die to room temperature and the part removed.

A special high lead-oxide containing, single-end glass roving was used as a radiographic tracer for monitoring potential fiber placement disruption during processing. The glass filaments were adhered to the surface of three plies per laminate during layup using a small amount of PMR-11 solution as a binder. The glass filaments were placed on 19.1 mm (3/4 inch) centers along the fiber orientation of the selected plies. A plus ply, a minus ply and a zero degree ply were chosen for each laminate as shown in table VIII.

All panels were X-rayed after molding to observe fiber movement. Figure 2 represents a typical X-ray clearly showing the glass fiber tracers. As can be seen, no significant orientation loss in this plane was experienced. Some gentle curving is apparent, but this is felt to be the result of original placement rather than movement during molding. Figure 3 is a photograph of a longitudinal section, along the zero degree fibers, showing no significant fiber displacement. The zero degree longitudinal fibers, then, showed no disruption in either plane along the major load bearing axis.

The panels were found to be essentially void-free through the use of an ultrasonic inspection technique. Samples were also taken from each panel for microscopic examination; these confirmed the sonic results. A total of 30 mechanical test specimens were machined from each laminate for determinations of flexural strength, interlaminar shear strength, and transverse tensile strength at both room temperature and 232°C (450°F) as shown in the test matrix in table IX. Specimen dimensions and span-to-depth ratios employed are shown in table X.

An examination of all of the specimens before test revealed that many of the specimens from constructions IV and V (shown in table VIII) exhibited small laminar cracks originating at the corners of the rectangular specimens. The laminar cracks seemed to be associated with the interface of the core/shell constructions. None of the specimens from construction I, II or III exhibited any cracking. Since the same machining practices were observed with all specimens and the as-molded panels were free of stress cracks, as determined by X-ray, it was deduced that the machining operation altered the residual stress patterns in the panels which lead to the cracking.

The 3.8 cm (1.5 inch) long short beam shear specimens displayed the most cracks, although they could be observed in lesser numbers in the tensile and flexure specimens. The majority of these cracks were 3.2 to 6.4 mm (1/8 to 1/4 inch) long. A typical example can be seen in figure 4 showing a 7X magnification of one end of a short beam shear specimen from construction IV (table VIII). After test a number of specimens were examined to determine the exact location of the crack. This was done by a microscopic examination of polished sections and prying open the precracked specimens. Figures 5 and 6 are 40X photographs of specimens from constructions IV and V. In each case, the outside laminate ply can be seen at the bottom of the photograph. As can be seen, the cracks were intralaminar in nature, i.e., the failure occurred, not between two plies, but in the center of a 0.25 mm (10 mil) ply, and in both cases in an HM-S ply. The failure was observed within the fifth ply (-30°) of construction number IV and in the fourth ply (-10°) in construction number V.

It was felt that the presence of these stress cracks made the ply orientation/fiber type arrangement in constructions IV and V less than desirable for blade application. However, for completeness, it was necessary to compare the mechanical data collected on these panels. Since the specimens were precracked before test, there was some question about the validity of the data; therefore, the following rationale was developed to eliminate apprehension about making property comparisons using these data.

In the tensile specimens, the cracks were at the outer corners, under the gripping tabs, and it was improbable that the cracks would affect the tensile results. In the case of the flexure bars, the specimens were 21.6 cm (8-1/2 inches) long and the small cracks were far removed from the locus of failure in the center of the specimen. With regard to the short beam shear specimens, the failure mode of the 90° specimens was, as expected, bending failure through the center of the specimen and, therefore, not influenced by cracks at the corners of the specimens. In the case of the 0° short beam shear specimens, the effect of the cracks can be best judged from the shear strength data collected on these specimens and shown in table XI. Firstly, the data are closely grouped, not to be expected if the cracks, of varying size and frequency, influenced the data. Next, construction IV shear results are the same as construction III results; these laminates had the equivalent materials and orientations in the center plane (maximum test stress location) and construction III specimens were not cracked. Therefore, the cracks can be shown not to have contributed to premature failure in the cracked construction IV specimens. It is therefore concluded that the data collected on cracked specimens do reflect real differences in material behavior and are valid for comparison purposes.

All of the data collected on all five laminate constructions are shown in table XI. As a convenience, the highest test value average obtained for each type of test is boxed. Quite clearly, the type II construction was superior in almost every property and was an easy first choice for examination in a blade demonstration. In examining the other constructions, types IV and V were eliminated on the basis of residual stress, as discussed above. The type I construction appeared to be a second overall choice, although the type I laminate values indicated significantly lower 0° shear strength than the type III construction.

2.5.3 Thermal Cycling Evaluation

Since the type II construction from table VIII was obviously superior, as indicated by the data in table XI discussed above, it was decided to repeat the testing of a type II laminate after repetitive thermal cycling from room temperature to 232°C (450°F). In addition to providing a duplication of results from a panel of the chosen orientation, the introduction of the thermal cycling would, to some degree, simulate the thermal stress condition created in a fan blade in actual service.

The PMR-11/A-S laminate was fabricated in the same manner as the previous angle-ply laminates in this series, except 0.12 mm (5 mil) prepreg was used instead of the 0.25 mm (10 mil) material previously employed. By using the thinner prepreg and the same number of plies (24), the resultant laminate would still be balanced and symmetrical in construction but would be half as thick.

This was done since it was felt desirable to test the longitudinal tensile strength, and the thick laminate previously used would have such a large cross section that it would have been difficult to retain the bonded tensile gripping tabs during testing and, additionally, the load required to induce failure in such a large specimen might have exceeded the capacity of the Instron testing machine.

Thermal cycling was accomplished by wrapping the 21.6 x 21.6 cm (8-1/2 x 8-1/2 inch) laminate in a glass cloth with a light steel plate on top and putting this package into a preheated oven at 232°C (450°F). A thermocouple was attached to the laminate to monitor the temperature. A total rise time of 25 minutes was required to reach 232°C and the laminate was then held for an additional 25 minutes at this temperature. At the end of the hold period, the package was removed, the laminate unwrapped and allowed to come to room temperature. The cooling period was 60 minutes. This cycle was repeated 10 times.

The laminate was X-rayed, ultrasonically inspected, weighed, measured for thickness change, and checked for distortion before and after thermal cycling. No change was observed in any of these tests except weight loss, in which a change of 0.4% loss was measured.

The laminate was then machined into mechanical test specimens as shown in figure 7. The results collected are shown in table XII along with the results from the previous laminate of this construction so that a convenient comparison can be made. As can be seen, the results from the two laminates compare quite well, with the thinner panel (number VI) generally showing significantly higher values. Previous work on a limited basis, both internal and funded (1), indicated that the use of the thinner ply does produce slightly higher values in angle-ply (±10 degrees) tensiles. It seems logical to assume that the thinner ply permits a more evenly distributed fiber arrangement which might lead to a more uniform load pattern in the composite.

The results of this final angle-plied panel confirmed the selection of the type II construction, indicated that no ill effects were sustained as a result of the thermal cycle imposed on the panel, and suggested that the use of the thinner prepreg led to improved mechanical properties. These additional conclusions represented further information to be employed in the fabrication of the fan blades manufactured in the last phase of this program.

2.6 Material and Process Selections for the Fan Blade

A review of all the information collected on material and process studies conducted during the first two phases of the program provided a number of conclusions pertinent to the fabrication of the fan blade. To briefly summarize, data from the first phase indicated that for the service temperature expected with the ultra-high speed blade, no postcure of the PMR composite was required. The comparison of 1100, 1300 and 1500 formulated molecular weight systems showed that the PMR-11 could be used to gain the inherently higher resin flow with no compromise on mechanical properties. The comparison of HM-S and A-S fiber reinforcement clearly revealed higher strength properties with the A-S tow. This latter characteristic was very important since the blade performance is known to be strength (tensile and shear) limited. The experimental work of the second phase

of the materials study confirmed the choice of the PMR-11/A-S system and indicated that the use of 0.127 mm (5 mil) prepreg vs. the 0.254 mm (10 mil) produced higher mechanical test values. The mechanical tests on the five panel orientations evaluated showed the type II, i.e., $(+40,0,-40,0)_n$, to be the preferred one. The thermal cycling experiment seemed to indicate that the spin test service conditions would not induce stress cracks or delaminations due to thermal expansivity mismatches. And finally, it was confirmed that a mold cycle, employing a 232°C insertion temperature, would be satisfactory in terms of producing acceptable properties. These conclusions form the basis for the initiation of the ultra-high speed fan bladed fabrication discussed in the next section of the report.

3.0 ULTRA-HIGH SPEED BLADE MANUFACTURE

The concluding phase of the program involved the fabrication and characterization of 14 ultra-high speed fan blades. The blade was designed on contract NAS3-15335. It was the objective of that program to develop and evaluate the aerodynamics of a jet engine fan stage operating at blade tip speeds of 671 m/s (2200 ft/sec), which represented a significant advancement in airfoil and airflow technology. Owing to the high stresses developed by the ultra-high speeds, a monolithic metal blade would be unsatisfactory and a graphite/polyimide was selected as the material of construction because of its high specific strength and stiffness and high temperature capability.

TRW was a subcontractor on NAS3-15335, charged with the design and build of necessary tooling, the development and implementation of a quality assurance plan, and the fabrication and delivery of blades. The blade itself has an overall length of approximately 28 cm (11 inches) and a chord width at the tip of 22 cm (8.5 inches). As can be seen in figure 8, the experimental airfoil has an unusual configuration. The text below describes the steps taken with the PMR-11/A-S material to fabricate and characterize 14 fan blades of the design discussed.

3.1 Materials of Construction

Efforts completed during the first portion of the program established the 1100 FMW variation of the PMR polyimide resin series as the preferred choice; this system was used for all blades fabricated on the program. The early study work also dictated the use of A-S fiber reinforcement. The A-S lot (53-5) used to fabricate blade S/N's T-12 through T-24 had a tensile strength of 3.2 GPa (463 ksi) and a modulus of 244.8 GPa (35.5 msi). These values compare to 2.9 GPa (421 ksi) tensile strength and 218.6 GPa (31.7 msi) modulus for lot 37-3 used in blade S/N T-11 and all panel work on the program. The lot used previously on two ultra-speed blades (fabricated on a separate procurement, designated S/N T-9 and T-10) had a tensile strength of 3.1 GPa (450 ksi) and a modulus of 240.6 GPa (34.9 msi).

Other materials of construction used in the fabrication of the fan blades are listed in table XIII. Some of these, such as the titanium root pressure pads and the aluminum root wedges, were the materials used on NAS3-15335, the original blade development program. Others, such as the leading edge pressure pad adhesives, were selected on this program and will be discussed in subsequent sections.

3.2 Fan Blade Fabrication

The following paragraphs will discuss each step in the balde fabrication starting with prepreg preparation and progressing through finish machining.

3.2.1 Prepreg Preparation

Using the PMR-11 and the A-S fiber, prepreg was prepared employing the same equipment and techniques described in Section 2.3. Target fiber volume was 57-1/2 v/o, which gave a cured resin solids content of 35.3 w/o; the target finished ply thickness used for all plies in blades T-11 through T-24H, was 0.124 mm (4.9 mils). This latter value was based on previous experience with

the designed blade ply shapes which indicated that a value just under 0.127 mm (5 mils) was best suited to fill the die cavity without inducing excessive resin flow and, hence, potential fiber movement. The monomer solution was applied at a 25 w/o concentration to achieve uniform wetting of the thin prepreg.

Three sheets of prepreg were prepared at one time in a single drum-load and fully consumed for each blade. Three quality control measures were employed to insure the uniformity and utilition of the prepreg. First, the weights of fiber and monomer solution used for each prepreg were compared with the calculated goals. Second, an areal density was obtained for each sheet by using samples (two per prepreg sheet) cut with a round die cutter from each sheet and the cured weight of this sample compared with a calculated nominal. And finally, a resin flow test was conducted on a 5.1 x 15.2 cm (2 x 6 inch) 10-ply laminate made up of plies from each of the three prepreg sheets to be used for one blade. This latter test, in addition to yielding a flow number for comparison with other prepreg lots, provided a cured laminate so that the response to the chosen cure cycle could be confirmed.

Data from all of these tests are summarized in table XIV. It is felt that these data reflect a uniform material produced by a closely controlled process. Some variability is, of course, to be expected due to such things as the precision of the solution metering device, but the most probable cause for error is the roll-to-roll variation in the fiber properties such as density and weight per unit length.

Prepreg for the two hybrid blades was prepared using basically the same techniques. Prepreg thickness was targeted at the same value as was the fiber volume. The cured resin solids content dropped, with the addition of the glass hybridizing fiber, from 35.3 to 33.6 w/o due to the higher density glass. A total of 20 w/o of the graphite fiber was replaced with S-glass 12 end roving. This was physically accomplished by first laying down the dry graphite fiber on the drum at a reduced spacing, i.e., at a value of 1.3 tows/cm (3.3 tows/inch) vs. 1.6 tows/cm (4.1 tows/inch) for the non-hybrid material. On top of this graphite fiber, the 12 end glass roving was laid down at 0.9 tows/cm (2.3 tows/inch). After both fibers were in place, the monomer solution was metered onto the material in a 25 w/o solution.

Figure 9 is a photograph of this type of prepreg on a winding drum (not the one used on this program) showing the general appearance of the hybrid prepreg. Data collected on the hybrid prepreg for the two hybrid blades fabricated, designated S/N's T-23 and T-24, are shown in table XIV.

3.2.2 Ply Preparation and Layup

Table XV lists the orientation of each of the plies used to lay up the fan blade. The number and configuration of the plies, used on all blade fabricated, were originally established on NAS3-15335. The stacking sequence shown, a totally interspersed arrangement, deviated from the original program in which a core/shell arrangement was specified; note the extreme left column in table XV in which the original core/shell arrangement is noted. This change was based on the observation on NAS3-15335 that stress cracking was occurring in the core, and occasional

core/shell delamination was noted at the interface. The interspersed sequence shown minimizes residual stress. The $\pm 40^{o}$ orientation was the result of efforts conducted in the early portions of this program, which showed high strength and no stress cracking.

The ply numbers carrying an "a" and "b" designation in table XV were originally 0.254 mm (10 mil) plies. This would result in a ply sequence as shown in table XVI, as used for example on S/N's T-9 and T-10. Due to the work on this program indicating an improvement in strength with the thinner ply material, all of the plies were made 0.127 mm (5 mil). A cost savings was effected by cutting out paired plies at one time. For example, plies 19a and 19b have the same shape but different orientations. By mating two sheets of prepreg, each with the required orientation, plies 19a and 19b could be cut and laid up at one time.

Another cost saving was introduced by employing disposable ply templates for the ply cutting on each blade. This was done by first arranging the original computer drawn Mylar (opaque) ply templates on a sheet of transparent Mylar with the template stacking lines parallel to one another and parallel to the planned zero degree prepreg fibers. This assembly was then put through an ozalid type machine which produced a blueprint with each of the individual templates shown. This blueprint was then adhered to the prepreg sheet outer separator film with an adhesive cement. All plies were then cut out by cutting through the blueprint and the underlying prepreg. Figure 10 shows a sheet of prepreg with the blueprint cemented to the surface. The system worked quite effectively and provided a ply of reproducible size. This technique of using a disposable ply template is obviously not suited for the manufacture of extended production runs but does provide an economical technique for small quantities of parts where the cost of steel rule dies is prohibitive.

After cutting all the plies for a single blade, four of the plies were provided with X-ray tracers so that potential fiber movement could be monitored through subsequent processing. This was done by using a single-end glass roving with a high lead oxide content. The glass roving was laid down on 1.9 cm (3/4 inch) centers along the graphite prepreg fiber axis and adhered with a thin coat of the PMR-11 solution. The four plies thus treated were numbers 27 (-40 degrees), 38 (0 degree), 48 (+40 degrees) and 60 (0 degree).

As can be noted in table XV, the ply stacking sequence lists show a concave and a convex blade half. These terms refer to the two halves in which the blade was laid up on the two lay-up tools shown in figure 11. These were available from NAS3-15335 and are of a cast epoxy construction.

Also indicated in table XV are the six aluminum root wedges interspersed with the prepreg layup at the root of the blade. Figure 12 shows the six wedges ready for adhesive treatment. These wedges were originally machined with a relief on each side to accommodate a separate film adhesive specified for this blade construction. Previous work (3) had been done that indicated that the PMR resin system,when coupled with an appropriate primer, was completely suitable for use as the adhesive in the integral molding of the root wedges; the PMR resin was therefore used as a wedge adhesive on each blade.

The 6061-T6 aluminum wedges were prepared by etching in a standard chromic-sulfuric acid solution for treating aluminum for bonding. All surfaces were then

sprayed (the same day as etched) with a very light coat of BR-34 adhesive primer from Bloomingdale Division of American Cyanamid and dried as recommended. The wedges were then brush coated with a PMR-11 solution and a piece of unimidized 0.127 mm (5 mil) prepreg laid into the relief machined in the wedges to accept the film adhesive previously used. These prepared wedges were then inserted into the prepreg layups at the appropriate locations.

Once the wedges and all of the plies were prepared, the lay-up process was started. Plies were laid down on the cast epoxy tools shown in figure 11 in the order given in table XV. Figure 13 is a closeup of a ply being placed on the lay-up stack; one of the two ply positioning points is shown in the figure. After positioning, the disposable ply template and the top separator sheet were discarded and the lay-up surface was ready for the next ply. Figure 14 shows a completed half of a blade layup.

Drape and tack of the PMR-11/A-S material, even in the case of the double plies, was excellent and no difficulty was experienced in tacking one ply to another and in forming the ply to the shape of the lay-up tool. At the conclusion of the layup of each half, the two halves were weighed and visually inspected in preparation for the next operation.

3.2.3 Blade Molding Cycle

The finish molding of the PMR-11 matrix system was broken into two discrete steps. First, the prepreg layup was imidized; this is the step where ring closure takes place and water and methyl alcohol are given off. The layup was then cooled, inspected and put into a 232°C tool for the final molding under pressure. The complete cycle was the same as used for the angle-plied panels molded during the materials evaluation phase and is described in detail below.

Figure 15 shows the molding die used for both imidization and molding. Figure 16 shows the molding press used with a view of the temperature controllers and recorder. Heating was accomplished with electrical cartridge heaters in the tool with four controllers. These separate controllers were used as follows: one controller for the punch, one for the die, one for the leading and trailing edge die rails, and one for the tip and root rails. The temperature recorder monitored two thermocouples at each of the four stations given. To minimize thermal loss to the press, both top and bottom press platens, on which the die base and punch were secured, were also heated. The platens were controlled by units integral to the molding press.

The layup was sandwiched between porous Teflon and several plies of glass cloth bleeder material and placed in the die at room temperature. A shot-bag, representing a pressure of 1.0 kPa (0.15 psi) was placed on top and the temperature increased gradually. This was done to eliminate any potential fiber movement during that portion of the cycle during which the volatile by-products were released. The thermal cycle used was as follows:

Temperature		Time
°C	°F	Minutes
54	130	20
88	190	20
121	250	20
204	400	120

At the conclusion of the last hold period, the temperature was reduced to room temperature by external fan cooling and the use of cooling water in the platens.

The imidized preformed layup was easily handled, and no significant distortion of surface ply orientation was observed. Figures 17 and 18 show both a full graphite fiber reinforced and a hybrid blade after imidization before final molding. The imidized parts were dry-fitted into the cold die to check ease of subsequent installation (no stock removal was required) and put to one side in readiness for final molding.

Final molding was accomplished by first bringing the die set to 232°C (450°F). When the temperature had equilibrated, the root end rail of the die was removed, the imidized part installed, and the end rail replaced. Contact pressure was applied and the part was held for 10 minutes, starting from the time of insertion. At the end of this period, 1.4 MPa (200 psi) was applied and the die brought to 316°C (600°F) over a 20 minute period. This pressure, 1.4 MPa, was adequate to bring the press down to a pre-determined location, indicated by removable stops set to produce the appropriate blade thickness. At the end of the 20 minute temperature increase to 316°C, the pressure was increased to 5.5 MPa (800 psi), and the part held at this temperature and pressure for 90 minutes. At the end of this time the die was cooled by fan cooling the external die surfaces until the punch and die were at 260°C (500°F) and the pressure was reduced to 1.9 MPa (270 psi) and fan cooling continued until the punch and die thermocouples indicated 204°C (400°F). At this point the pressure was reduced to contact and cooling water introduced into the press platens. Cooling was continued until die and punch temperatures were below 54°C (130°F).

Table XVII gives the information collected during the processing of the fan blades; two items are worthy of note. First, the percent flow values can be seen to be very low and to fall within a very narrow band. It is known that the PMR-11 system is capable of more flow, but resin expulsion was deliberately restricted by using a moderate pressure during the early stages of the cure cycle. More flow than this was not required to close the die to the proper size since the prepreg thickness control was good and the ply shapes and number used very closely approximated the volume required to fill the die cavity.

The kind of minor modifications needed to "fine tune" the process can be seen from the extra prepreg material added with blades T-19 through T-22, as shown in the footnotes to table XVII. Two behavior patterns were observed in the manufacture of blades T-11 through T-18. One was that, if the tool closed to stops too rapidly under the 1.4 MPa pressure first applied to the blade during molding, the surface quality of the blades would be poor, and that this type of behavior was related to the weight of the die charge going into imidization. Since a number of blades of the same kind were manufactured in a continuous run, it was

possible to establish that a charge weight of below 760 gm would lead to a blade with sonic defects or an undersize condition. A second fact noted was that a number of blades showed an ultrasonic indication pattern at the very tip. For these reasons, extra material was added as shown in table XVII in an attempt to eliminate these types of defects. The defects observed will be discussed further in the section below on blade characterization.

3.2.4 Leading Edge Sheath

Since the subject fan blade was a test item and was not to be subjected to full service conditions with expected foreign object damage, only a simple leading edge protector was needed. The design called for an electroformed nickel sheath with a thickness of 0.08 mm (0.003 inch). The finished sheath was 2.2 cm (7/8 inch) by 20.0 cm (7 and 7/8 inch) long.

Using a scrap blade made of epoxy/fiberglass, the leading edge section of the blade was cut off and machined to the correct size. This was then used as a model to cast a female silicone rubber tool. A filled tooling-epoxy was cast, under vacuum, into this silicone rubber tool to provide a series of disposable epoxy leading edge mandrels for electroforming. These mandrels were provided to United Nickel Corporation, Wooster, Ohio for their use in the electroforming operation. A series of two different thickness nickel sheaths were obtained; the first of the correct drawing size and a second set of twice this thickness for use in molding into the blade a relief for the subsequent secondary bonding of the sheath.

In preparing a blade layup that was to ultimately be fitted with the leading edge sheath, two plies were altered. These were numbers 4 and 72, which were both below the outer ply covering the entire surface. Material was cut from each of these plies to correspond to the configuration of the sheath. The blade layups were imidized in the normal manner described above. However, in preparation for the final molding, a heavy gage sheath, treated with a silicone mold release, was fitted on the layup leading edge and inserted into the molding tool along with the layup. After molding, the dummy nickel sheath was easily removed, leaving a relief of the correct configuration with enough depth to accommodate both the final sheath and an adhesive thickness of about 0.08 mm.

After a brief literature search, the adhesive selected for bonding the nickel sheath was ADX-3111.1 from the Hysol Division of the Dexter Corporation. This is a two-part paste adhesive cured with a liquid amine. The system has a pot life of approximately six hours and has the consistency of a thick honey. Shear strength at room temperature is given as 5100 psi and 1600 psi at 400°F. Besides the good strength and high temperature resistance, another characteristic that made the system appealing was that these properties might be obtained by curing for two hours at 82°C (180°F), thus minimizing the problem of differential thermal expansivities between the nickel and the composite material.

The composite surface was prepared for bonding by light sanding and solvent washing. The choice of this method was based on work done by Crane, et. al. (4) in which various peel plies and acid treatments were compared to sanding. None of the techniques was found to yield better performance than the sanding method.

Two different surface preparation techniques were employed for the nickel

leading edges. On all but one of the blades bonded, a common adhesive bonding etch was used, a five second dip in concentrated nitric acid. On S/N T-12 blade, the nickel leading edge was prepared for bonding by etching for five seconds in a chromic acid/hydrochloric acid solution. The reason for the use of two different standard etches was to observe any potential performance differences in service, since the adhesive bonding of pure nickel is traditionally very difficult.

After etching both the prepared composite surface and the nickel inner surface were spread with adhesive and the two parts mated. The blade with the nickel leading edge in place was inserted into the cold blade-molding tool and a pressure of approximately 69 kPa (10 psi) (over the total blade surface) was gradually applied over about a 20 minute period to extrude any excess resin and to conform the leading edge insert and adhesive precisely to the required blade contours. At the end of this period, the temperature was raised to 82°C (180°F) and held for two and one half hours. After removal from the die, the excess adhesive was carefully removed from the previously mold release treated surface of the blade.

3.2.5 Pressure Pad Bonding

The final operation before machining of the blades was the installation of the titanium root pressure pads. The pad bonding operation was accomplished by using the fixture shown in figure 19 with a finish molded blade in place. The pads can be seen at the junction of the airfoil and the root angle.

The rough machined 6Al-4V titanium pads were first stress relieved at 566°C (1050°F) for two hours to minimize residual stresses that might cause dimensional instability in later bonding or machining operations. The pads were then etched in a nitric/hydrofluoric acid solution and passivated in a trisodium phosphate/potassium fluoride/hydrofluoric acid solution (5) immediately prior to bonding.

The adhesive chosen for this application was the same as that used for leading edge sheath bonding; i.e., the Hysol ADX3111.1. For pad bonding, however, the adhesive was spread on 104 glass scrim cloth and staged for thirty minutes at 66°C (150°F) prior to use. The scrim made the adhesive easier to handle and, it is felt, contributed to a more even load distribution in use. The staging operation advanced the resin slightly to give a higher viscosity needed in this bonding sequence. After light sanding and solvent cleaning of the composite surface, the pads were mated with the prepared adhesive and placed in a bonding fixture (figure 19) which provided pressure to the adhesive bond line and accurately positioned the pads with regard to height and transverse location. The assembly was then placed in an air circulating oven and held at 82°C (180°F) for two and a half hours. After cooling, the pad locations were confirmed with a dimensional inspection and the blade prepared for final machining.

3.2.6 Final Machining

Six molded blades were machined to final configuration to meet exacting dimensional tolerances. The general approach to achieving the dovetail root configuration was to perform the machining operations with the blade mounted in a shuttle box. The shuttle was fitted with tooling-epoxy pads conforming to the concave and convex airfoil contours. The pads were originally prepared using a master casting from the blade mold. The blade was thus precisely secured in the

shuttle, just above the root, providing adequate support against tooling loads. Variations in molded blade thickness were accounted for by measurements from the shuttle box to each face of the blade, halving the dimensional difference to establish a mean stacking line for each blade.

The shuttle with the blade in place was then mounted in a holding fixture for positioning during the various machining operations. Excess stock was first milled from the triangular root bottom and sides. The titanium bearing pad faces were form ground to a predetermined drop gage dimension to establish the "Z" plane location normal to the mean stacking line. Subsequent operations included root-side flat grinding, root bottom mill, root bottom radius mill (using a form cutter) and edge blending. With these surfaces completed, the leading and trailing edge root angle-ends were ground to dimension using a sine plate to precisely establish the required angle (40^{o}). After each operation, dimensions were taken using a micrometer or specially designed drop gage and recorded in a blade log.

The blade was then removed from the shuttle and mounted in a tip radius machining fixture located on the blade bearing pad surfaces and the root leading edge. Excess stock was first removed from the tip with a fine tooth band saw leaving about 3.2 mm (0.125 inch) for finishing. The blade tip radius, actually a conical surface, was diamond-wheel ground by pivoting the blade on an axis on the fixture representing the center line of the wheel into which the blade will ultimately be spun. The blade was finished by hand-blending the trailing edge radius (leading edge radius established with the nickel insert) and breaking the corners in the root and tip areas.

All critical dimensions were recorded on each blade during the machining operations. While not considered a practical approach for production, the shuttle box, special gaging and log book approach proved quite adequate and very useful in producing and documenting these high precision blades. Figure 20 shows the completely finished blade after machining.

3.3 Fan Blade Characterization

All of the fan blades molded were submitted to the same inspection techniques. These included radiography, ultrasonic inspection, dimensional checks, a visual examination, and natural frequency. Further, six of the blades were reinspected ultrasonically and radiographically after machining, and additionally, plotted at 5X magnification on an airfoil inspection unit at three radial sections. Details of all these inspections follow.

3.3.1 Ultrasonic Results and Surface Appearance

All blades were ultrasonically inspected over 100% of the airfoil surface. A through-transmission technique was used in which the blade was passed between two opposed transducers. The transducers were 12.7 mm (1/2 inch) diameter, 10 MHz units fitted with polystyrene, truncated cone-shaped shoes. The cones had a 12.7 mm (1/2 inch) diameter base and a 3.2 mm (1/8 inch) diameter tip which was in contact with blade through a liquid couplant. The blade was held against the lower shoe and the upper, opposed shoe was forced against the blade by a dead weight to insure intimate contact.

Ultrasonic indication patterns for all of the blades are shown in figures 21 through 36. Six of the 16 blades for which sonic patterns are shown were completely indication free. Five blades showed patterns only at the extreme tip. This is a non-critical region since approximately 10.2 mm (0.400 inches) of the length was removed in final machining, and, additionally, this is a very low stress area. Nonetheless, an attempt was made to determine the cause of the sonic indication. Using S/N T-14, a complete section was cut across the blade about 4.8 mm (3/16 inch) down from the tip and polished for microscopic examination. A considerable number of voids were observed in the area identified as sub-standard by the ultrasonic inspection. As a result of the identification of these voids, extra material, in the form of tip patches about the size of the sonic indications, were put in several of the subsequent blades, as noted above and indicated in table XVII.

A possible hypothesis for these tip indications is related to the movement of material during the final molding process into an area informally identified as the "bump." The bump referred to can be seen in the airfoil in figure 8. It represents a sharp deviation in the airfoil configuration and is in the center of the blade chord and up about 50 mm (1.97 inches) from the root pad. It is about 3 mm (0.118 inch) deep and has a length across the chord width of about 60 mm (2.36 inches). It is felt possible that fibers anchored in the root were drawn from the tip and forced down into this "bump" during molding. An examination of the radiographs of these blades showed that the leaded glass roving tracer, originally extended to the tip edge, had withdrawn about 6.4 mm (1/4 inch) towards the root. The areas of sonic indication at the tip did, in fact, correspond to the chordal location of the "bump" in the blade.

Another possibility is that the ply shapes for this portion of the blade are not quite precise. If this were the case, inadequate material would be available to fill the die cavity in this tip area. A phenomenon noted with almost all of the blades showing the tip indications is the occurrence of a small number of tiny surface blisters on the top 1/3 of the blade. This might indicate that full pressure was not present during the final molding, thus allowing evolved cyclopentadiene to form the observed blisters.

S/N T-13 (figure 25) had a large sonic indication area surrounding the "bump" in the center of the airfoil and gradually increasing towards the root. There is little doubt that the sonic indications shown with T-13 reflected a poor blade. While the convex side of the blade had a normal appearance, the concave surface of the blade (the side that was up in the molding tool) displayed several large patches of discolored grainy surface and irregularly shaped blisters were present. It is felt that these effects were probably due to a reduced pressure during molding on this section of the blade. Records kept during molding show that the punch came down on stops much earlier than any of the previous blades molded. With the load borne on the stops, it seems possible that the cyclopentadiene evolved during chain extension was not re-reacted with the polymer and came to the upper surface in the tool, causing the blistering and discoloration.

S/N T-15 had similar surface indications but lesser in degree to those seen on T-13 although T-15 had a clean sonic inspection. A review of the molding data on T-15 indicated that die closing time, while not as short as T-13, was fairly rapid. With this information in mind, the molding of all subsequent blades was carefully monitored for material charge weight, application of molding

pressure and closing time. As a result, the reoccurrence of the inferior surface conditions noted on T-13 and T-15 was eliminated.

S/N T-19 showed a sonic indication at the tip but covering a larger area than previously seen; the indication represented a semi-circular pattern extending from the tip about 2.54 cm (1 inch) (at its maximum) and in the center 8.9 cm (3.5 inches) of the blade chord. Additionally, S/N T-19 has an indication at the blade root area. This latter indication covers an area starting at the leading edge hook and extends to the center of the blade. The maximum height above the pressure pad is about 2.54 cm (one inch), tapering out completely at the center of the blade. No explanation is available for this sonic pattern; it was the first blade, out of all those fabricated to date, to show an indication in this area.

The sonic inspection of S/N T-20 revealed a large indication about 6.4 cm (2-1/2 inches) wide up the center for the full length of the blade. A section taken from the tip (within the area later machined off) was examined microscopically but did not yield any useful information about the cause of this indication. The indication looked suspiciously like the shape of one of the center plies, and it was hypothesized that a piece of Mylar separator may have been left in the blade during layup. The literature indicated that Mylar melts at 260°C and the blade was molded at 316°C so it seems unlikely that the presence of a sheet of the 0.05 mm (two mil Mylar) could easily be identified intact in the blade. More likely would be a slightly resin rich appearing area or a porous area in the shape of the Mylar ply separator. A small test laminate was fabricated with a strip of Mylar in the center and examined sonically and microscopically. The Mylar could not be identified sonically, and the photomicrograph did not show any clear indication of the separator film.

The two hybrid blades, S/N's T-23H and T-24H, both showed sonic indications up the center. It is felt that both conditions were due to inadequate material in this portion of the blade. While table XIV indicates that the prepreg areal density figures were within acceptable limits, the inclusion of the glass fibers, with less available history on density and length/unit length data, made the calculated values less reliable than those on straight graphite fiber prepreg. Additionally, a limited manufacturing run of only two parts did not permit the emperical modification of material charge weights possible. As will be noted, the addition of three extra plies to the second blade did appreciably reduce the sonic indication area. There is no reason to believe that the use of hybrid prepreg should in any way reduce the attainable quality of the blades, and it is felt that further modification of prepreg thickness or charge weight would yield blades with equivalent quality to the straight graphite fiber blades.

3.3.2 Dimensional Inspection

Table XVIII lists all the dimensions taken on each blade immediately after molding. The measurements were taken with pin micrometers at five locations. Three were taken across the tip, down 2.5 mm (0.100 inch) from the tip end of the blade. The leading edge measurement was taken 3.6 mm (0.140 inch) in from the edge and the trailing edge reading 2.5 mm (0.100 inch) in from the edge. The "tip maximum" reading occurs roughly in the center of the blade and registers the thickest portion of the blade at this station. The two root readings were taken 33.5 mm (1.320 inch) up from the as-molded root bottom and in from the edge

12.7 mm (0.500 inch). Gages were fabricated to identify these locations and pencil lines scribed on the blade to note the locations. Pin micrometers were then used to record the readings at the intersection of the scribed lines in each case.

As can be seen from the dimensions shown in table XVIII, most of the values are centered around the nominals although the ±0.127 mm (0.005 inch) tolerance band is exceeded. For example, at the root with a 13.8 mm (0.545 inch) nominal, the leading edge dimensions ranged from +0.203 mm (0.008 inch) to a -0.229 mm (0.009 inch) about the nominal, and the trailing edge ranged from a +0.305 mm (0.012 inch) to a -0.406 mm (0.018 inch). Note that the tip maximum values never reached the nominal; from this it was concluded that the tool cavity is undersized at this point.

Table XIX summarizes the data for the airfoil displacement and twist analyses conducted on all of the machined blades. These characteristics are shown: lean, tilt and twist. Lean and tilt, defined in the table notes in airfoil terminology, reflect the linear displacement of the stacking point in a tangential and axial direction, respectively, at each section compared to the true blade stacking line. The analysis is an indication of the location of the airfoil as established by the root and confirms the precision of machining of the root pressure pad angles and leading edge stop as the blade is located in the engine. Twist refers to angular displacement compared to the root centerline.

To conduct the analysis, the blade was secured in a fixture simulating precisely the disc slot. Using a turbine blade plotting machine, the test airfoil was plotted and traced at 5X magnification at three radial sections along with the locations of the true stacking point and the true root centerline. The sections used represent one close to the root (H-H), one near mid-span (P-P) and one near the tip (W-W). The traces were then compared to the master charts for these sections and the displacements established. It was not necessary to analyze the airfoil contours since the mold tool had been analyzed earlier at all radial sections and found to conform to design tolerances. The molded blade then represented a true reproduction of the mold cavity with the exception of minor thickness variations. The analysis then utilized a "best-fit" positioning between trace and master chart. The analysis also provides an evaluation of airfoil bow which may have occurred due to residual stresses or other distortions. As can be seen from the data in table XIX, all displacements are minimal and, in general, are closely grouped.

3.3.3. Radiographic Inspection

All of the blades were X-rayed after molding and the machined blades were reradiographed after this operation. A review of all the X-rays showed that there were no stress cracks and, while some movement of the glass tracers was observed, the amount of movement was not excessive or unexpected. Figure 37 is an X-ray positive, reduced in size, of a finish machined fan blade. The dark strip to the right is the electroformed nickel leading edge sheath. The dark object to the lower left under a corner of the blade is a spacer used with the X-ray of each blade to provide a uniform height of the blade from the film. In this way, the twist of the blade was held constant from one X-ray to another so that observation of the glass tracer fibers was standardized. The X-ray shown is typical in both the absence of stress cracks and location of the glass tracer fibers.

3.3.4 Natural Frequency

All of the data collected during natural frequency test of the fan blades in their as-molded condition are shown in table XX. In addition to the first bending, second bending and first torsion values, information was also gathered on logarithmic decrement characteristics of the blades. This is a measure of the system damping.

The tests were run by affixing three calibrated accelerometers across the tip of the blade. The blade, mounted in a special fixture, was then excited by an electromechanical shaker table to pick up the various resonant points. The logarithmic decrement was calculated from the following equation:

$$\delta = 2\pi \frac{f_2 - f_1}{f_n} = \text{log decrement}$$

where: f_n = frequency of the first bending mode.

f_1 = frequency at which accelerometer voltage is $(0.707)(f_n)$ below that of the f_n peak.

f_2 = frequency at which accelerometer voltage is $(0.707)(f_n)$ above that of the f_n peak.

3.4 Fan Blade Spin Testing

This section describes the materials and construction of nine ultra-high speed fan blades and their spin test evaluation. The blades were fabricated by TRW Equipment, Cleveland, Ohio, under several NASA-Lewis contracts including NAS3-17772 (1), this program and under separate purchase. The blade design was developed under contract NAS3-15335 (report in preparation) by Pratt and Whitney Aircraft, East Hartford, Connecticut, where the spin testing was also accomplished. It is the purpose of this section to summarize the various improvements in materials, composite design and processing methods during the evaluation of the blade and to correlate these factors with performance. For the purposes of clarity and completeness, a review is given of all of the PMR blades spin tested, not only those prepared on this program.

During the course of the development of the ultra-high speed blade, a new and unique type of polyimide resin designated PMR was developed by NASA-Lewis personnel which provided higher temperature capability, greater ductility and improved translation of fiber properties in graphite fiber composites than the composite matrix resin originally selected for the high speed blade. With the development of processing procedures for PMR graphite fiber composites, under the above mentioned contracts, that were appropriate for fan blade fabrication, it became appropriate to evaluate the PMR composite system in the very demanding application of the ultra-high speed fan blade. Several blades were thus fabricated over a period of time and submitted for evaluation, which included spin testing, low cycle fatigue and high frequency fatigue. The paragraphs below discuss in detail the evaluation of all the PMR blades spin tested.

3.4.1 Blade Construction

Table XXI defines the materials of construction and the composite ply orientation and thickness used for each of the blades evaluated. Blades S/N's T-1 and T-2 were of identical construction to the blades originally evaluated on NAS3-15335 with the exception of the substitution of PMR-15 polyimide resin as the composite matrix. The reinforcement was HT-S graphite fiber from Hercules Incorporated and the composite construction was of a shell/core design with the $\pm 40^{\circ}$ shell plies separated from the 0° core plies by a single pair of $\pm 20^{\circ}$ transition plies. Blade S/N T-4 was modified to incorporate a $\pm 30^{\circ}$ shell and an interspersed $(+10^{\circ}, 0^{\circ}, -10^{\circ}, 0^{\circ})_n$ core.

For blades S/N T-9 and beyond, A-S fiber was substituted for HT-S. The A-S provided a somewhat higher tensile and composite shear strength reinforcement with a slight reduction of fiber modulus, approximately 221 GPa vs. 248 GPa (32 vs. 36 msi). The higher flow PMR-11 system was substituted for the PMR-15. A major change in these blades included the use of a totally interspersed composite construction $(+40^{\circ}, 0^{\circ}, -40^{\circ}, 0^{\circ})_n$ instead of the shell/core design used on prior blades.

Several minor changes were also incorporated into blades S/N's T-9 and T-10 including:

- Increased ply length of 1.0-1.5 mm (0.040-0.060 inch) at both root and tip to better fill the die cavity.
- Reduced resin content by 3%.
- Reduced 0.254 mm (10 mil) core ply thickness by 5%.
- Replaced parts of three plies (nos. 20, 26, 56) which had been eliminated in previous blades to accommodate an oversize condition near the root.

Blades S/N's T-12 through T-22 were further modified by substituting 0.127 mm (5 mil) prepreg, which had demonstrated improved composite properties, for the 0.254 mm (10 mil) prepreg previously used. Also, these blades incorporated a 0.08 mm (3 mil) electroformed nickel leading edge sheath secondary bonded to the blade with a high temperature epoxy paste adhesive which was also used for the titanium root pressure pad.

3.4.2 Blade Evaluation Methods

Before shipment for spin testing, all blades were radiographically, ultrasonically and dimensionally inspected. The blades, upon arrival at PWA, were again radiographed and ultrasonically inspected prior to spin testing. Initial evaluation in the spin pit involved acceleration to 110% speed, in 10% increments starting at 60% speed, with ultrasonic evaluation after each increment. One hundred percent speed was at 15,200 rpm. Following initial spin-up tests, blades were subjected to fifty cycles of low cycle fatigue (LCF) by repeatedly spinning briefly to 100 to 105% speed with ultrasonic inspection after each 10 cycle increment.

With survival of LCF, the blades were then subjected to ten million cycles of high frequency fatigue (HFF) on a vibration table. Blades were excited at their first bending frequency mode with sufficient energy to achieve a ±2.5 mm (±0.1 in.) tip amplitude displacement. A final series of tests included an additional ten cycles in LCF at the same speed as the original LCF. Natural frequency measurements were made on the blade initially and after each major type of testing. First and second bending and first torsional modes were determined. It should be noted that the natural frequency data shown in table XXII were collected by Pratt and Whitney Aircraft on completely machined blades with leading edge guards in place. The variation between the frequencies for the same blades reported in both tables XX and XXII may be attributed to these differences. In addition to these tests, visual examinations were made at each step of the evaluation.

3.4.3 Blade Evaluation Results

Three of these unusually highly stressed blades survived the entire testing procedure although not without internal damage and changes in natural frequencies. The results of the natural frequency tests are presented in table XXII. A number of observations can be made. The bending frequencies of the $\pm 30^{\circ}$ shell, $\pm 10^{\circ}$, 0° interspersed core of blade S/N T-4 were slightly higher than the basic design (S/N T-1) while the torsional frequency indicated no change. On the other hand, the $\pm 40^{\circ}$, 0° interspersed construction of blades S/N T-9 and T-10 coupled with the use of A-S fiber caused little change in any mode over S/N T-4. The use of the same construction for blades S/N T-12 through 22, but with 0.129 mm prepreg in the core instead of 0.254 mm, produced significant frequency changes. Increases of 8.5% and 4.5% in first and second bending, respectively, were noted while a 4.8% drop in torsional frequency was observed. Of interest is the reproducibility in the frequencies of like construction blades (S/N's 12, 14, 21, 22) with maximum deviation from mean values at each of the three vibrational modes of 0.7%, 0.7% and 1.2%, respectively.

Reduction in natural frequencies in all three modes was noted after the completion of each test evaluation series. Major changes occurred in the original spin-up to 100 or 105% speed and in the first 50 cycles in LCF. Largest reductions were noted in the first bending mode, ranging from 5-7%. Only minor frequency changes resulted from HFF ranging from 0.1 to 2.6% in all modes while essentially no additional damage was incurred in the final 10 cycles in LCF. It is interesting to note that the total change in first bending for blade S/N T-10, from before test until final evaluation, was only 20 hertz or 7.8%, even though serious delamination was noted even after original spin-up to 110% speed.

Spin test history for each blade is tabulated in table XXIII. Figures 38 through 54 exhibit, pictorially, the results of PWA ultrasonic and visual inspection at various stages in the evaluation. While a large number of maps were prepared, only those showing significant changes have been reproduced here.

Blade S/N T-1 exhibited a small narrow ultrasonic indication (figure 38), as fabricated, which was presumed to be a delamination. This indication expanded to the root area after spin-up to 90% speed and blade failure was experienced at 100% speed.

Blade S/N T-2 survived the entire testing procedure beginning with an as-fabricated indication (figure 39) which grew steadily through initial spin-up and 30 cycles of LCF (figure 40). No further change was noted through HFF and 10 additional cycles of LCF. The performance of S/N T-4 was similar to T-1 although the ultrasonic C-scan was clear initially. Likewise, S/N T-9 was clear initially but delaminated at 100% speed across the full chord width, above the root, as shown in figure 41.

Blade S/N T-10, originally clear, survived the full test procedure and was ultrasonically clear through 100% speed. Local, minor fiber lifting was observed at the tip and mid-span on the leading edge after 80% speed (figure 42). At 100% speed a crack appeared in the root leading edge face in the composite between aluminum root wedges (figure 43). At 110% delamination occurred similar to the previous blade (figure 44). It was, however, further tested with no change noted in LCF and only slight expansion of the delaminated area observed after HFF (figure 45). No additional delamination occurred in the final LCF although some additional fiber lifting was noted (figure 46) and one pressure pad was lifted for a 5 cm length. A view of the low pressure face is illustrated in figure 46 along with the high pressure side of the airfoil showing all indications. The survival of this blade was surprising since it was deviated in machining; the root leading edge face was machined 2 mm (0.080 inch) short, placing the blade in the spin arbor significantly displaced from the true stacking axis.

The performance of blade S/N T-12 was similar to blade T-9 and T-10 except delamination occurred at 105% speed (figure 47). No further evaluation was conducted on this blade.

Blade S/N T-14 went through the entire testing procedure. Figure 48 illustrates an ultrasonic clear blade but some minor imperfections were observed on the leading edge sheath prior to test. Otherwise, the blade was sound except that the tip end was machined 2 mm (0.080 inch) short. Figures 49, 50 and 51 illustrate visual indications occurring during initial spin-up although no ultrasonic indications were noted through 110% speed, a decided improvement over previous blades. However, after 50 cycles LCF at 105% speed, delamination was experienced (figure 52). An additional small piece (25 cm length) of the leading edge guard was lost in HFF at the tip on the low pressure face, but no additional damage was incurred in the final 10 cycles in LCF.

For blade S/N T-21, no ultrasonic indications were observed during spin-up but, at 100% speed, blade failure occurred at the location indicated in figure 53. The performance of S/N T-22 was similar to several previous blades exhibiting delamination at 100% speed as shown in figure 54.

Blade S/N T-2, which had survived the entire test procedure, was sectioned and observed microscopically at Pratt and Whitney. Examination of the sections confirmed the presence of fabrication residual-stress radial cracking in the core which had been observed previously in radiographs. The number of radial cracks had, in fact, increased significantly. Of more concern was the serious amount of delamination between the shell and core members and within the core. The microscopic analysis identified a shear type failure, induced predominantly by the high stresses of spin testing, but intensified by the core/shell residual stress concentration in the composite. Otherwise, the blade was sound with no porosity

observed, although some fiber dislocations were observed. This latter observation lead to the use, in subsequent blades, of high density fibers strategically located for radiographic identification for fiber orientation maintenance. Processing procedures were also modified to achieve minimum fiber displacement in fabrication. The technique significantly improved blade quality.

From the test results, it is apparent that failure occurs or is initiated at, or near the contour discontinuity in the airfoil about 5 cm (2 inches) above the root at mid-chord (sometimes described as the "bump" area) or at the severe leading edge curvature above the root. In the high stress loading environment of high speed spinning, these sharp contour changes appear to induce a shear stress condition beyond the capability of the laminated composite construction.

3.4.4 Blade Spin Test Summary

It was demonstrated that sound, high quality, complex fan blades could be reproducibly fabricated using PMR-11 polyimide reinforced with A-S type graphite fiber. Very significant performance improvements were demonstrated through the use of this material combination, improved processing techniques and composite construction compared to the first NAS3-15335 blades. The average speed at which delamination initiated was increased from 65% of full speed for original contract blades to 100 to 105%. On the basis of centrifugal loading, this represents an increase in failure initiation stress of 137%. However, with the current design, the blade must be considered marginal for full operation in the stress environment intended. Operation somewhat below 100% of full speed, 671 m/sec (2200 ft/sec) tip speed, is fully practical.

The totally interspersed composite construction was found to eliminate residual stress cracking and the 0.127 mm (5 mil) core laminae provided improved performance over the 0.254 mm (10 mil) in the original blade design. For the totally interspersed orientation investigated $(+40^{o}, 0^{o}, -40^{o}, 0^{o})_{n}$, increases were noted in blade bending vibrational modes with some reduction in torsional frequency. Natural frequencies can, however, be tuned by varying fiber orientation angles and/or the ratio of radial oriented to angle-plied material.

In conclusion, the PMR-11/A-S combination provides one of the highest strength and shear capability, low density composite materials of construction available at this time. Ultrasonically sound, ultra-high speed blades fabricated with this material have demonstrated only marginal survivability. Further blade performance improvements for this application must, therefore, be sought through improved airfoil and root retention designs. Additional considerations should include such factors as root wedge material selection and, looking forward to jet engine operation, the incorporation of a leading edge protection scheme that not only survives the spinning environment, but provides the necessary degree of erosion and foreign object damage protection.

4.0 PROGRAM CONCLUSIONS

Specific conclusions on such things as processing details and material properties are presented in the body of the text. The conclusions below represent broader statements related to the program objective and the more general characteristics of the PMR polyimide composite system evaluated.

1. The objectives of the program were completely fulfilled. The materials systems selected, including the reinforcement, the use of the PMR resin as both composite matrix and wedge adhesive and the pad and leading edge epoxy adhesives were shown to be quite suitable for the fabrication of high quality, void-free fan blades. The process methods employed, including the drum winding of prepreg, the use of disposable ply templates, molding and inspection techniques, were found to be appropriate for a manufacturing run of the size undertaken and capable of producing complex, high quality, die molded, aerospace hardware. Spin testing of the fan blades revealed that, despite the achievement of an increase of 137% in the failure-initiation stress level, the present configuration is only marginally survivable and further design changes would be required to gain performance improvements.

2. The PMR resin was found to be an easily processable, high temperature, matrix resin which exhibited high strain-to-failure for a crosslinked polyimide and a range of formulated molecular weight compositions providing a spectrum of flow characteristics with equivalent mechanical properties.

3. The use of the PMR system and the A-S graphite fiber tow, coupled with a totally interspersed ply stacking sequence in a $(+40^{o}, 0^{o}, -40^{o}, 0^{o})_{n}$ fiber orientation, provided the best combination of mechanical properties and composite structures without residual stress cracks. Thermal cycling of this system up to $232^{o}C$ did not produce any deleterious effects such as introduction of stress cracks or degradation of mechanical properties.

5.0 RECOMMENDATIONS FOR FURTHER WORK

It has been shown that die molding procedures are available for producing high quality aerospace hardware with the PMR polyimide matrix system. Further work should be pursued with alternate reinforcements and additional fabrication methods, e.g., autoclaving. Further definition of PMR composites produced with these alternate reinforcements and fabrication methods should include investigations of environmental resistance and long term characteristics such as fatigue and thermo-oxidative stability. If further ultra-high speed fan blade work is undertaken, the present configuration and design should be reviewed.

TABLE I

PRELIMINARY MATERIALS STUDY TEST MATRIX

			1100 FMW	1300 FMW	1500 FMW	1900 FMW
Room Temperature and 232°C Test	HM-S Fiber	Not Postcured	Short Beam Shear Flexural Transverse Tensile	Short Beam Shear Flexural Transverse Tensile	Short Beam Shear Flexural Transverse Tensile	-
		Postcured	Short Beam Shear Flexural Transverse Tensile	Short Beam Shear Flexural Transverse Tensile	Short Beam Shear Flexural Transverse Tensile	-
	A-S Fiber	Not Postcured	Short Beam Shear Flexural Transverse Tensile	Short Beam Shear Flexural Transverse Tensile	Short Beam Shear Flexural Transverse Tensile	-
		Postcured	Short Beam Shear Flexural Transverse Tensile	Short Beam Shear Flexural Transverse Tensile	Short Beam Shear Flexural Transverse Tensile	-
Room Temperature Test	Neat Resin	Not Postcured	Tensile	Tensile	Tensile	Tensile
		Postcured	Tensile	Tensile	Tensile	Tensile

TABLE II

PMR NEAT RESIN MOLDING DATA

FMW	1100	1300	1500	1900
Mold Shrinkage (Linear), %	1.08	1.27	1.24	1.36
Average Thickness, mm	1.4	1.6	1.7	1.8
in.	0.057	0.063	0.065	0.069
Specific Gravity[a]	1.29	1.28	1.29	1.29
Weight Loss in Postcure, %	3.6	3.8	4.0	3.8
Postcure Shrinkage (Linear), %	0.56	0.69	0.97	0.89

[a] Calculated from weight and dimensional data.

TABLE III

NEAT RESIN ROOM TEMPERATURE TENSILE STRENGTH RESULTS

	1100 FMW	1300 FMW	1500 FMW	1900 FMW
Non-Postcured				
(S.I. Units)				
Stg., MPa	73.8	81.4	45.5	75.8
Strain, %	2.6	3.4	1.5	2.7
Modulus, GPa	3	3	3	3
(U.S. Units)				
Stg., ksi	10.7	11.8	6.6	11.0
Strain, %	2.6	3.4	1.5	2.7
Modulus, msi	0.5	0.5	0.5	0.5
Postcured				
(S.I. Units)				
Stg., MPa	49.6	59.3	38.6	60.7
Strain, %	1.6	2.1	1.1	2.0
Modulus, GPa	3	3	4	3
(U.S. Units)				
Stg., ksi	7.2	8.6	5.6	8.8
Strain, %	1.6	2.1	1.1	2.0
Modulus, msi	0.5	0.5	0.6	0.5

NOTE: All values represent average of at least three determinations.

TABLE IV

PMR COMPOSITE TRANSVERSE TENSILE STRENGTH RESULTS

			1100 FMW			1300 FMW			1500 FMW		
			Strength	Strain %	Modulus	Strength	Strain %	Modulus	Strength	Strain %	Modulus
HM-S Fiber	Non-Postcured	RT	25 MPa 3.6 ksi	0.31	8.3 GPa 1.2 msi	27 MPa 3.9 ksi	0.31	9.7 GPa 1.4 msi	30 MPa 4.3 ksi	0.35	8.3 GPa 1.2 msi
		232°C	13 MPa 1.9 ksi	0.23	5.5 GPa 0.8 msi	12 MPa 1.8 ksi	0.22	5.5 GPa 0.8 msi	14 MPa 2.1 ksi	0.30	5.5 GPa 0.8 msi
	Postcured	RT	26 MPa 3.7 ksi	0.32	8.3 GPa 1.2 msi	25 MPa 3.6 ksi	0.33	8.3 GPa 1.2 msi	23 MPa 3.4 ksi	0.29	8.3 GPa 1.2 msi
		232°C	11 MPa 1.6 ksi	0.20	4.8 GPa 0.7 msi	13 MPa 1.9 ksi	0.16	5.5 GPa 0.8 msi	12 MPa 1.8 ksi	0.15	6.9 GPa 1.0 msi
A-S Fiber	Non-Postcured	RT	66 MPa 9.5 ksi	0.78	9.7 GPa 1.4 msi	70 MPa 10.1 ksi	0.80	9.0 GPa 1.3 msi	85 MPa 12.4 ksi	0.91	9.7 GPa 1.4 msi
		232°C	18 MPa 2.6 ksi	0.33	5.5 GPa 0.8 msi	37 MPa 5.4 ksi	0.64	6.2 GPa 0.9 msi	30 MPa 4.4 ksi	0.54	5.5 GPa 0.8 msi
	Postcured	RT	60 MPa 8.7 ksi	0.64	9.7 GPa 1.4 msi	62 MPa 9.0 ksi	0.76	9.0 GPa 1.3 msi	58 MPa 8.4 ksi	0.58	10.3 GPa 1.5 msi
		232°C	39 MPa 5.7 ksi	0.68	6.2 GPa 0.9 msi	39 MPa 5.6 ksi	0.80	5.5 GPa 0.8 msi	46 MPa 6.7 ksi	0.79	6.9 GPa 1.0 msi

Note: Values shown represent averages of three determinations in most cases.

TABLE V

PMR COMPOSITE SHORT BEAM SHEAR STRENGTH RESULTS

			1100 FMW	1300 FMW	1500 FMW
HM-S	Non-Postcured	RT	51 MPa 7.4 ksi	50 MPa 7.1 ksi	45 MPa 6.5 ksi
		232°C	41 MPa 6.0 ksi	41 MPa 6.0 ksi	34 MPa 5.0 ksi
	Postcured	RT	41 MPa 5.9 ksi	47 MPa 6.8 ksi	40 MPa 5.8 ksi
		232°C	34 MPa 4.9 ksi	41 MPa 5.9 ksi	34 MPa 4.9 ksi
A-S	Non-Postcured	RT	114 MPa 16.6 ksi	124 MPa 18.0 ksi	130 MPa 18.9 ksi
		232°C	57 MPa 8.3 ksi	60 MPa 8.7 ksi	52 MPa 7.6 ksi
	Postcured	RT	123 MPa 17.8 ksi	108 MPa 15.7 ksi	114 MPa 16.6 ksi
		232°C	68 MPa 9.8 ksi	61 MPa 8.8 ksi	72 MPa 10.5 ksi

Note: Each value represents the average of three determinations.

TABLE VI

PMR COMPOSITE FLEXURE STRENGTH TEST RESULTS

			1100 FMW Strength	1100 FMW Modulus	1300 FMW Strength	1300 FMW Modulus	1500 FMW Strength	1500 FMW Modulus
HM-S Fiber	Non-Postcured	RT	1077 MPa 156.3 ksi	163 GPa 23.6 msi	1116 MPa 161.8 ksi	162 GPa 23.5 msi	1117 MPa 162.0 ksi	149 GPa 21.6 msi
		232°C	1116 MPa 161.8 ksi	170 GPa 24.6 msi	1038 MPa 150.6 ksi	166 GPa 24.1 msi	951 MPa 138.0 ksi	140 GPa 20.3 msi
	Postcured	RT	1100 MPa 159.5 ksi	170 GPa 24.7 msi	1091 MPa 158.2 ksi	158 GPa 22.9 msi	1107 MPa 160.5 ksi	153 GPa 22.2 msi
		232°C	951 MPa 137.9 ksi	157 GPa 22.8 msi	1056 MPa 153.2 ksi	156 GPa 22.6 msi	987 MPa 143.2 ksi	153 GPa 22.2 msi
A-S Fiber	Non-Postcured	RT	1785 MPa 258.9 ksi	110 GPa 16.0 msi	1705 MPa 247.3 ksi	103 GPa 15.0 msi	1741 MPa 252.5 ksi	106 GPa 15.4 msi
		232°C	1511 MPa 219.2 ksi	112 GPa 16.3 msi	1331 MPa 193.0 ksi	108 GPa 15.6 msi	1264 MPa 183.3 msi	105 GPa 15.2 msi
	Postcured	RT	1598 MPa 231.8 ksi	116 GPa 16.8 msi	1405 MPa 203.8 ksi	103 GPa 15.0 msi	1282 MPa 185.9 ksi	109 GPa 15.8 msi
		232°C	1595 MPa 231.4 ksi	112 GPa 16.3 msi	1246 MPa 180.7 ksi	98 GPa 14.2 msi	1508 MPa 218.7 ksi	107 GPa 15.5 msi

Note: Values represent average of three determinations in most cases.

TABLE VII

PMR-15 LAMINATE FLOW STUDY RESULTS

Lam. No.	Visual Appearance	Resin Flow	Imidization Conditions		Die Insertion Conditions[b]		Rise Delay Conditions		Rise Time To Hold	Rise Time to 316°C
		%	°C	Hours	°C	Min.	°C	Min.	Min.	Min.
1	Good	2	121	0.5	232	10	-	-	-	20
2	Good	2	↓	2	↓	10	-	-	-	20
4	Flawed[a]	8	↓	2	↓	5	-	-	-	20
6	Flawed	6	↓	2	↓	10	260	10	7	13
8	Flawed	5	↓	2	↓	10	288	20	13	7
8R	Good	6	↓	2	↓	10	↓	20	13	7
10	Flawed	7	↓	2	↓	10	↓	10	3[c]	7
12	Discolored & Grainy	2	↓	2	288	10	-	-	-	7
5	Good	4	204	1	232	0	288	10	13	7
5A	Flawed	4	↓	1	↓	0	288	5	13	7
7	Flawed	1	↓	1	↓	10	260	10	7	13
9	Flawed	1	↓	1	↓	10	288	20	13	7

(a) Flawed surface note indicates presence of blisters or surface depressions.

(b) Time of hold at temperature shown before pressure application.

(c) This rapid rise rate was accomplished by transferring die to a second press with platens preheated to 288°C.

TABLE VIII

ANGLE-PLY LAMINATE CONFIGURATIONS/FIBER TYPES

Ply No.	I	II	III	IV	V
1	+30/HMS (a)	+40/AS	+30/HM (a)	+30/HMS (a)	HMS
2	0/AS	0 (a)	-30	+10/AS	↓
3	-30/HMS	-40	+30	0	
4	0/AS	0	-30	-10	
5	+30/HMS	+40	-10/AS	-30/HMS	
6	0/AS	0	0	-10/AS	AS
7	-30/HMS	-40	+10	0	↓
8	0/AS	0	0	+10	
9	+30/HMS	+40	-10	0	
10	0/AS	0	0	-10	
11	-30/HMS	-40	+10	0 (a)	
12	0/AS (a)	0	0 (a)	+10	
13	0/AS	0	0	0	
14	-30/HMS	-40	+10	+10	
15	0/AS	0	0	0	
16	+30/HMS	+40 (a)	-10	-10	
17	0/AS	0	0	0	
18	-30/HMS	-40 (a)	+10	+10	
19	0/AS	0	0	0	
20	+30/HMS	+40	-10	-10	
21	0/AS	0	-30/HM (a)	-30/HMS (a)	HMS
22	-30/HMS (a)	-40	+30	-10/AS	↓
23	0/AS	0	-30	0	
24	+30/HMS	+40	+30	+10	
25				+30/HMS	

Same as Configuration IV

(a) Those plies designated had single end leaded glass fibers parallel to the ply orientation on 19.1 mm centers for use as radiographic tracers.

(b) Finish molded prepreg thickness to be 0.254 mm (10 mil).

TABLE IX

TEST MATRIX FOR ANGLE-PLY LAMINATES I THROUGH V

Property	Flexural Strength		Interlaminar Shear Strength		Transverse Tensile Strength
Loading Orientation	0°	90°	0°	90°	90°
Test Temperature					
RT	X	X	X	X	X
232°C (450°F)	X	X	X	X	X

Note: Three specimens/test condition

TABLE X

ANGLE-PLY PANEL SPECIMEN DIMENSIONS

	Length cm	Length inches	Width cm	Width inches	Span/Depth Test Ratio
0° Flexure	21.6	8½	1	3/8	25:1
90° Flexure	12.7	5			17:1
90° Tensile	12.7	5			-
0° Short Beam Shear	3.8	1½			4:1
90° Short Beam Shear	3.8	1½			4:1

Note: Thickness to be as molded: nominal 6.1 mm (0.240 inches).

TABLE XI

ANGLE-PLY PANEL MECHANICAL TEST RESULTS
(S.I. UNITS)

Construction Laminate No.	0°Flexure 22°C Stg. MPa	0°Flexure 22°C Mod. GPa	0°Flexure 232°C Stg. MPa	0°Flexure 232°C Mod. GPa	90°Flexure 22°C Stg. MPa	90°Flexure 22°C Mod. GPa	90°Flexure 232°C Stg. MPa	90°Flexure 232°C Mod. GPa	0°SBS 22°C Stg. MPa	0°SBS 232°C Stg. MPa	90°SBS 22°C Stg. MPa	90°SBS 232°C Stg. MPa	90° Tensile 22°C Stg. MPa	90° Tensile 22°C Mod GPa	90° Tensile 22°C Str. %	90° Tensile 232°C Stg. MPa	90° Tensile 232°C Mod. GPa	90° Tensile 232°C Str. %
I 743-32	580	77.2	526	66.9	100	10.3	95.1	8.3	35.9	40.7	13.1	13.8	51.7	9.0	0.8	54.5	9.0	0.4
	633	77.9	567	71.7	101	10.3	99.3	7.6	37.2	33.1	12.4	15.2	51.7	11.0	0.5	52.4	8.3	0.5
	623	77.2	541	71.7	101	10.3	97.9	8.3	42.1	33.8	13.1	13.8	51.0	9.7	0.7	54.5	9.0	0.4
Avg	612	77.2	545	70.3	101	10.3	97.2	8.3	38.6	35.9	13.1	14.5	51.7	9.7	0.7	53.8	9.0	0.4
II 743-38	1038	61.4	756	57.2	205	15.2	174.0	13.1	90.3	50.3	31.7	32.4	121.0	15.9	1.1	131.0	15.9	0.5
	908	60.7	711	55.8	225	15.2	184.0	13.1	82.7	54.5	33.8	32.4	119.0	15.9	1.1	125.0	14.5	0.6
	978	63.4	843	57.2	177	15.9	188.0	13.8	87.6	52.4	35.2	30.3	115.0	18.6	1.0	121.0	17.9	0.5
Avg	[975]	62.1	[769]	56.5	[203]	[15.2]	[182.0]	[13.1]	[86.9]	[52.4]	[33.8]	[31.7]	[119.0]	[16.5]	[1.1]	[125.0]	[15.9]	0.5
III 743-35	526	65.5	446	60.0	88.2	9.7	82.7	8.3	70.3	49.0	13.1	11.7	43.4	9.0	0.5	34.5	8.3	1.0
	577	64.8	503	59.3	96.5	9.7	81.3	7.6	70.3	49.6	13.1	11.7	51.0	9.0	0.6	35.9	9.7	0.4
	583	63.4	436	55.8	88.2	9.7	84.1	8.3	66.9	46.2	13.8	13.1	44.1	11.0	0.4	31.7	11.7	0.3
Avg	562	64.8	462	58.6	91.0	9.7	82.7	8.3	68.9	48.3	13.1	12.4	46.2	9.7	0.5	33.8	9.7	0.6
IV 743-36	750	82.0	701	76.5	68.9	9.7	59.3	8.3	69.6	47.6	15.2	8.3	38.6	9.0	0.4	30.3	8.3	0.9
	800	83.4	721	75.1	80.7	9.7	64.1	8.3	69.6	50.3	11.7	9.0	37.9	9.0	0.4	26.9	6.9	0.5
	714	83.4	734	75.8	70.3	9.7	66.9	8.3	68.9	46.2	11.0	10.3	40.7	11.0	0.4	31.7	9.0	0.4
Avg	755	82.7	718	75.8	73.1	9.7	63.4	8.3	69.6	48.3	12.4	9.0	39.3	9.7	0.4	29.6	8.3	0.6
V 743-37	653	97.9	616	88.9	71.7	9.7	75.1	8.3	48.3	49.0	11.0	10.3	35.2	9.0	0.4	31.0	9.0	0.8
	609	103.0	578	86.9	64.7	9.7	57.9	8.3	54.5	44.8	9.7	9.0	35.9	8.3	0.4	31.0	9.7	0.4
	620	97.2	550	87.6	80.7	9.7	71.0	8.3	45.5	43.4	9.0	9.0	38.6	9.0	0.4	27.6	6.9	0.5
Avg	627	[99.3]	581	[87.6]	72.4	9.7	68.3	8.3	49.6	45.5	9.7	9.7	36.5	9.0	0.4	29.6	8.3	0.6

NOTE: [ ] = highest average value

TABLE XI (continued)

ANGLE-PLY PANEL MECHANICAL TEST RESULTS

(U.S. UNITS)

Construction Laminate No.		0° Flexure 72°F Stg. ksi	0° Flexure 72°F Mod. msi	0° Flexure 450°F Stg. ksi	0° Flexure 450°F Mod. msi	90° Flexure 72°F Stg. ksi	90° Flexure 72°F Mod. msi	90° Flexure 450°F Stg. ksi	90° Flexure 450°F Mod. msi	0° SBS 0°SBS 72°F Stg. ksi	0° SBS 0°SBS 450°F Stg. ksi	90°SBS 90°SBS 72°F Stg. ksi	90°SBS 90°SBS 450°F Stg. ksi	90° Tensile 72°F Stg. ksi	90° Tensile 72°F Mod. msi	90° Tensile 72°F Str. %	90°Tensile 450°F Stg. ksi	90°Tensile 450°F Mod. msi	90°Tensile 450°F Str. %
I 743-32		84.2	11.2	76.3	9.7	14.5	1.5	13.8	1.2	5.2	5.9	1.9	2.0	7.5	1.3	0.8	7.9	1.3	0.4
		91.8	11.3	82.2	10.4	14.6	1.5	14.4	1.1	5.4	4.8	1.8	2.2	7.5	1.6	0.5	7.6	1.2	0.5
		90.3	11.2	78.5	10.4	14.6	1.5	14.2	1.2	6.1	4.9	1.9	2.0	7.4	1.4	0.7	7.9	1.3	0.4
	Avg	88.8	11.2	79.0	10.2	14.6	1.5	14.1	1.2	5.6	5.2	1.9	2.1	7.5	1.4	0.7	7.8	1.3	0.4
II 743-38		150.6	8.9	109.6	8.3	29.8	2.2	25.3	1.9	13.1	7.3	4.6	4.7	17.6	2.3	1.1	19.0	2.3	0.5
		131.7	8.8	103.1	8.1	32.6	2.2	26.7	1.9	12.0	7.9	4.9	4.7	17.3	2.3	1.1	18.1	2.1	0.6
		141.8	9.2	122.2	8.3	25.7	2.3	27.3	2.0	12.7	7.6	5.1	4.4	16.7	2.7	1.0	17.5	2.6	0.5
	Avg	[141.4]	9.0	[111.6]	8.2	[29.4]	[2.2]	[26.4]	[1.9]	[12.6]	[7.6]	[4.9]	[4.6]	[17.2]	[2.4]	[1.1]	[18.2]	[2.3]	0.5
III 743-35		76.3	9.5	64.7	8.7	12.8	1.4	12.0	1.2	10.2	7.1	1.9	1.7	6.3	1.3	0.5	5.0	1.2	1.0
		83.7	9.4	73.0	8.6	14.0	1.4	11.8	1.1	10.2	7.2	1.9	1.7	7.4	1.3	0.6	5.2	1.4	0.4
		84.6	9.2	63.2	8.1	12.8	1.4	12.2	1.2	9.7	6.7	2.0	1.9	6.4	1.6	0.4	4.6	1.7	0.3
	Avg	81.5	9.4	67.0	8.5	13.2	1.4	12.0	1.2	10.0	7.0	1.9	1.8	6.7	1.4	0.5	4.9	1.4	0.6
IV 743-36		108.8	11.9	101.7	11.1	10.0	1.4	8.6	1.2	10.1	6.9	2.2	1.2	5.6	1.3	0.4	4.4	1.2	0.9
		116.1	12.1	104.5	10.9	11.7	1.4	9.3	1.2	10.1	7.3	1.7	1.3	5.5	1.3	0.4	3.9	1.0	0.5
		103.6	12.1	106.4	11.0	10.2	1.4	9.7	1.2	10.0	6.7	1.6	1.5	5.9	1.6	0.4	4.6	1.3	0.4
	Avg	109.5	12.0	104.2	11.0	10.7	1.4	9.2	1.2	10.1	7.0	1.8	1.3	5.7	1.4	0.4	4.3	1.2	0.6
V 743-37		94.7	14.2	89.3	12.9	10.4	1.4	10.9	1.2	7.0	7.1	1.6	1.5	5.1	1.3	0.4	4.5	1.3	0.8
		88.4	14.9	83.9	12.6	9.3	1.4	8.4	1.2	7.9	6.5	1.4	1.3	5.2	1.2	0.4	4.5	1.4	0.4
		89.9	14.1	79.8	12.7	11.7	1.4	10.3	1.2	6.6	6.3	1.3	1.3	5.6	1.3	0.4	4.0	1.0	0.5
	Avg	91.0	[14.4]	84.3	[12.7]	10.5	1.4	9.9	1.2	7.2	6.6	1.4	1.4	5.3	1.3	0.4	4.3	1.2	0.6

NOTE: [ ] = highest average value

TABLE XII

THERMALLY CYCLED ANGLE-PLY PANEL RESULTS

Condition	Panel II			Panel VI		
	Not Postcured			Not Postcured, Thermally Cycled[a]		
Construction	$(+40,0,-40,0)_n$ 24 Plies 0.254 mm (10 mil) Prepreg			$(+40,0,-40,0)_n$ 24 Plies 0.127 mm (5 mil) Prepreg		
	RT	232°C	S/D[b] Ratio	RT	232°C	S/D Ratio
0° Flex						
Stg, MPa	975	770		1061	1017	
ksi	141.4	111.6	26:1	153.9	147.5	36:1
Mod, GPa	62	57		66	62	
msi	9.0	8.2		9.6	9.0	
90° Flex						
Stg, MPa	203	182		-	-	
ksi	29.4	26.4	17:1	-	-	-
Mod, GPa	15	13		-	-	
msi	2.2	1.9	-	-	-	-
0° SBS						
Stg, MPa	87	52		93	57	
ksi	12.6	7.6	4:1	13.5	8.2	4:1
90° SBS						
Stg, MPa	34	32		45	40	
ksi	4.9	4.6	4:1	6.5	5.8	4:1
90° Tensile						
Stg, MPa	119	125		156	163	
ksi	17.2	18.2	-	22.6	23.6	-
Mod, GPa	17	16		17	12	
msi	2.4	2.3	-	2.5	1.8	-
Strain, %	1.1	0.5	-	0.9	1.4	-
0° Tensile[c]						
Stg, MPa	-	-		776	797	
ksi	-	-	-	112.5	115.6	-
Mod, GPa	-	-		70	63	
msi	-	-	-	10.2	9.2	-
Strain, %	-	-	-	1.1		

(a) Thermally cycled 10 times from room temperature to 232°C.

(b) Span-to-depth ratio.

(c) Longitudinal tensile specimens were straightsided 22 cm (8½") long by 6 mm (1/4") wide by laminate thickness. Gage length was 114 cm (4½").

TABLE XIII

FAN BLADE MATERIALS OF CONSTRUCTION

	Material	Description
1.	Primary Reinforcing Fiber	A-S aerospace grade graphite fiber from Hercules, Inc.
2.	Hybridizing Fiber	12 end S-glass with 904 finish from Owens-Corning.
3.	Radiographic Trace Fiber	Single end lead glass LCG from Owens-Corning.
4.	Resin Matrix	PMR-11.
5.	Root Wedges	6061-T6 aluminum, AMS-4053.
6.	Wedge Adhesive Primer	BR-34 from American Cyanamid.
7.	Wedge Adhesive	PMR-11
8.	Root Pressure Pads	6Al-4V titanium, AMS-4928.
9.	Pressure Pad Adhesive	ADX-3111.1 two part epoxy paste from Hysol with 104 glass cloth scrim.
10.	Leading Edge Sheath	Electroformed nickel.
11.	Leading Edge Adhesive	ADX-3111.1 two part epoxy paste from Hysol.

TABLE XIV

BLADE PREPREG DATA

Blade S/N	A-S Fiber Lot	Prepreg Run No.	Calc. Prepreg w/o Resin, Avg.	Avg. Areal Density g/m^2	Avg. Areal Density % Dev.(a)	Test Laminate % Flow
T-9	43-2	745-23	37.0	195.3	-3.6	-
T-10	43-2	745-29	32.0	194.1	-4.2	-
T-11	37-3	743-61	36.2	198.4	+0.5	9
T-12	53-5	743-66	35.2	198.9	+0.2	8
T-13	↓	743-74	36.1	195.9	-1.3	12
T-14		743-79	36.5	191.1	-3.7	7
T-15		743-84	35.2	196.1	-1.2	9
T-16		743-88	35.3	204.0	+2.7	9
T-17		743-94	36.7	195.0	-1.8	12
T-18		768-3	35.7	191.3	-3.6	10
T-19		768-8	35.6	196.5	-0.9	15
T-20		768-13	35.0	206.0	+3.7	12
T-21		768-18	36.4	199.3	+0.5	13
T-22		768-24	35.8	196.1	-1.2	-
T-23H		768-30	33.2	205.5	-1.1	9.3
T-24H		768-34	32.9	203.8	-1.9	-

(a) Deviation from calculated nominal.

TABLE XV

0.127 mm (5 MIL) BLADE LAYUP STACKING SEQUENCE

	Convex Blade Half			Concave Blade Half		
	Ply No.	Orientation	Wedge	Ply No.	Orientation	Wedge
Tip	1	-60		75	+60	
	2	+60		74	-60	
Shell	3	+40		73	-40	
	4	0		72	0	
	5	-40		71	+40	
	6	0		70	0	
	7	+40		69	-40	
	8	0		68	0	
	9	-40		67	+40	
	10	0		66	0	
	11	+40		65	-40	
	12	0		64	0	
	13	-40		63	+40	
	14	0		62	0	
	15	+40		61	-40	
	16	0		60	0	
	17	-40		59	+40	
	18	0	←58269(1)	58	0	←58274(6)
Core	19a	0		57a	0	
	19b	+40		57b	-40	
	20a	0		56a	0	
	20b	-40		56b	+40	
	21a	0		55a	0	
	21b	+40		55b	-40	
	22a	0		54a	0	
	22b	-40		54b	+40	
	23a	0		53a	0	
	23b	+40		53b	-40	
	24a	0		52a	0	
	24b	-40		52b	+40	
	25a	0		51a	0	
	25b	+40	←58270(2)	51b	-40	←58273(5)
	26a	0		50a	0	
	26b	-40		50b	+40	
	27a	0		49a	0	
	27b	+40		49b	-40	
	28a	0		48a	0	
	28b	-40		48b	+40	
	29a	0		47a	0	
	29b	+40		47b	-40	
	30a	0		46a	0	
	30b	-40		46b	+40	
	31a	0		45a	0	
	31b	+40		45b	-40	
	32a	0		44a	0	
	32b	-40	←58271(3)	44b	+40	←58272(4)
	33a	0		43a	0	
	33b	+40		43b	-40	
	34a	0		42a	0	
	34b	-40		42b	+40	
	35a	0		41a	0	
	35b	+40		41b	-40	
	36a	0		40a	0	
	36b	-40		40b	+40	
	37a	0		39a	0	
	37b	0		39b	0	
			Center Ply	38	0	

TABLE XVI

S/N T-9 AND T-10 BLADE LAYUP STACKING SEQUENCE

Convex Blade Half			Concave Blade Half		
Ply No.	Orientation	Prepreg Thick.	Ply No.	Orientation	Prepreg Thick.
1	-60	0.127 mm (5 mil)	75	+60	0.127 mm (5 mil)
2	+60		74	-60	
3	+40		73	-40	
4	0		72	0	
5	-40		71	+40	
6	0		70	0	
7	+40		69	-40	
8	0		68	0	
9	-40		67	+40	
10	0		66	0	
11	+40		65	-40	
12	0		64	0	
13	-40		63	+40	
14	0		62	0	
15	+40		61	-40	
16	0		60	0	
17	-40		59	+40	
18	0	Wedge SKN-58269 (1)	58	0	Wedge SKN-58274 (6)
19	a +40 b 0	0.127 mm	57	a -40 b 0	0.127 mm
20	-40	0.241 mm (9.5 mil)	56	+40	0.241 mm (9.5 mil)
21	0		55	0	
22	+40		54	-40	
23	0		53	0	
24	-40		52	+40	
25	0	Wedge SKN-58270 (2)	51	0	Wedge SKN-58273 (5)
26	+40		50	-40	
27	0		49	0	
28	-40		48	+40	
29	0		47	0	
30	+40		46	-40	
31	0		45	0	
32	-40	Wedge SKN-58271 (3)	44	+40	Wedge SKN-58272 (4)
33	0		43	0	
34	+40		42	-40	
35	0		41	0	
36	-40		40	+40	
37	0		39	0	
			38	0	0.127 mm

TABLE XVII

BLADE MOLDING PROCESS DATA

Blade S/N	Composite Weight Before Imidization gms	Composite Weight After Imidization gms	Composite Weight After Molding gms	Weight of Wedges, gms	Flow, gms	Flow, %
T-9	765	700	695	279	5	0.7
T-10	754	696	688	276	8	1.1
T-11	763	697	690	275	7	1.0
T-12	758	694	687	277	7	1.0
T-13	753	686	676	274	10	1.5
T-14	759	685	681	275	4	0.6
T-15	752	691	683	275	8	1.1
T-16	765	697	692	275	5	0.7
T-17	743	678	674	276	4	0.6
T-18	766	694	688	275	6	0.9
T-19[a][b]	760	698	693	274	5	0.7
T-20[b]	773	708	702	273	6	0.9
T-21[a][b]	771	708	700	276	8	1.1
T-22[c]	764	706	699	273	7	1.0
T-23H	795	731	725	275	6	0.8
T-24H[d]	809	744	738	275	6	0.8

(a) An extra 0.127 mm full length, full width ply #38 was added.

(b) Semi-circular ply patch (~13 cm^2) was added in center of tip.

(c) Two extra 0.127 mm full length, full width #38 plies were added.

(d) Added two full width #38 plies, one full length ply #31a, and two tip patches.

TABLE XVIII

AS-MOLDED BLADE DIMENSIONS

(S.I. UNITS)

Blade S/N	Net Composite Weight, gms	Thickness Dimensions, mm[(b)]				
		Tip LE	Tip Max	Tip TE	Root LE	Root TE
Target	-	0.86	10.11	1.40	13.84	13.84
T-9	695	0.84	9.75	1.24	13.94	13.79
T-10	688	0.81	9.65	1.17	13.69	13.56
T-11	690	0.71	9.65	1.35	13.72	13.59
T-12	687	0.43[(a)]	9.65	1.32	13.77	13.74
T-13	676	0.48[(a)]	9.60	1.09	13.61	13.59
T-14	681	0.71[(a)]	9.65	1.17	13.74	13.61
T-15	683	0.51[(a)]	9.65	1.09	13.69	13.69
T-16	692	0.46[(a)]	9.68	1.07	13.82	13.72
T-17	674	0.25[(a)]	9.55	1.04	13.64	13.39
T-18	688	0.43[(a)]	9.70	1.19	13.84	13.72
T-19	693	0.48[(a)]	9.73	1.17	13.84	13.77
T-20	702	0.53[(a)]	9.88	1.27	14.05	13.97
T-21	700	0.46[(a)]	9.86	1.30	14.05	14.15
T-22	699	0.51[(a)]	9.78	1.19	13.79	13.92
T-23H	725	0.33[(a)]	9.63	0.94	13.72	13.56
T-24H	738	-	9.88	1.40	14.02	13.77

(a) Measurement taken within LE relief, therefore, 0.30 mm should be added to this value.

(b) All tolerances ± 0.13 mm.

TABLE XVIII (continued)

AS-MOLDED BLADE DIMENSIONS

(U.S. UNITS)

Blade S/N	Net Composite Weight, gms	Thickness Dimensions, inches[b] Tip LE	Tip Max	Tip TE	Root LE	Root TE
Target	-	0.034	0.398	0.055	0.545	0.545
T-9	695	0.033	0.384	0.049	0.549	0.543
T-10	688	0.032	0.380	0.046	0.539	0.534
T-11	690	0.028	0.380	0.053	0.540	0.535
T-12	687	0.017[a]	0.380	0.052	0.542	0.541
T-13	676	0.019[a]	0.378	0.043	0.536	0.535
T-14	681	0.028[a]	0.380	0.046	0.541	0.536
T-15	683	0.020[a]	0.380	0.043	0.539	0.539
T-16	692	0.018[a]	0.381	0.042	0.544	0.540
T-17	674	0.010[a]	0.376	0.041	0.537	0.527
T-18	688	0.017[a]	0.382	0.047	0.545	0.540
T-19	693	0.019[a]	0.383	0.046	0.545	0.542
T-20	702	0.021[a]	0.389	0.050	0.553	0.550
T-21	700	0.018[a]	0.388	0.051	0.553	0.557
T-22	699	0.020[a]	0.385	0.047	0.543	0.548
T-23H	725	0.013[a]	0.379	0.037	0.540	0.534
T-24H	738	-	0.389	0.055	0.552	0.542

(a) Measurement taken within LE relief, therefore, 0.012 inch should be added to this value.

(b) All tolerances ± 0.005 inch.

TABLE XIX

FINISHED MACHINED BLADE AIRFOIL DISPLACEMENT ANALYSIS

Section	Lean[a]			Tilt[b]			Twist (degrees)		
Blade S/N	H-H	PP	WW	H-H	PP	WW	H-H	PP	WW
T-9 mm	+0.38	+1.07	+1.14	+0.41	+0.38	+0.23			
in.	+0.015	+0.042	+0.045	+0.016	+0.015	+0.009	-	-	-
T-10 mm	+0.71	+0.36	+0.25	+0.66	-0.10	-0.28			
in.	+0.028	+0.014	+0.010	+0.026	-0.004	-0.011	-	-	-
T-12 mm	0	+0.38	+0.08	+0.13	+0.10	-0.25			
in.	0	+0.015	+0.003	+0.005	+0.004	-0.010	-	-	-
T-14 mm	0	+0.15	-0.10	+0.05	-0.25	-0.51			
in.	0	+0.006	-0.004	+0.002	-0.010	-0.020	-	-	-
T-16 mm	-0.10	+0.51	+0.05	+0.18	+0.30	-0.10	0.02°	0.35°	0.13°
in.	-0.004	+0.020	+0.002	+0.007	+0.012	-0.004	0°1'	0°21'	0°8'
T-21 mm	+0.08	+0.43	+0.66	+0.13	+0.08	+0.13	0.17°	0.08°	0.08°
in.	+0.003	+0.017	+0.026	+0.005	+0.003	+0.005	0°10'	0°5'	0°5'
T-22 mm	+0.25	+0.79	+1.02	+0.30	+0.43	+0.46	0.07°	0.18°	0.35°
in.	+0.010	+0.031	+0.040	+0.012	+0.017	+0.018	0°4'	0°11'	0°21'
T-24H mm	-0.13	+0.69	+0.66	+0.13	+0.30	0	0.07°	0.17°	0.35°
in.	-0.005	+0.027	+0.026	+0.005	+0.012	0	0°4'	0°10'	0°21'

(a) Lean: Distance from X Plane to Leading Edge (+) or Trailing Edge (-).

(b) Tilt: Distance from Y Plane Forward (O.D. +) or Aft (I.D. -).

TABLE XX

NATURAL FREQUENCY (HERTZ) OF FAN BLADES IN AS-MOLDED CONDITION

S/N	First Bending	Second Bending	First Torsion	Log Decrement
T-9	221	815	548	0.201
T-10	217	803	531	0.144
T-11	229	833	524	0.163
T-12	238	868	547	0.157
T-13	231	843	515	0.136
T-14	231	841	525	0.163
T-15	231	848	556	0.163
T-16	232	842	517	0.163
T-17	233	841	488	0.186
T-18	234	844	515	0.160
T-19	235	856	521	0.160
T-20	255	856	521	0.188
T-21	-	-	-	-
T-22	236	863	516	0.157
T-23H	216	782	475	0.088
T-24H	219	786	489	0.086

TABLE XXI

BLADE CONSTRUCTION

Blade S/N	Fiber	Resin	Ply Orientation, Degrees				Ply Thick., mm		Leading Edge
			Tip	Shell	Trans.	Core	Shell	Core	
T-1	HT-S	PMR-15	±75	±40	±20	0	0.127 (5 mil)	0.254 (10 mil)	None
T-2	HT-S	PMR-15	±75	±40	±20	0			
T-4	HT-S	PMR-15	±75	±30	±30	$(10,0,-10,0)_n$			
T-9	A-S	PMR-11	±60		$(+40,0,-40,0)_n$				
T-10									
T-12								0.127 (5 mil)	Yes
T-14									
T-21									
T-22									

TABLE XXII

BLADE NATURAL FREQUENCIES, HERTZ

	Blade S/N (speed)	1st Bending	2nd Bending	1st Torsion
Drawing Requirements		250 ± 13	840 ± 42	845 ± 42
Initial	T-1	248	932	804
	T-4	269	997	808
	T-9	261	985	813
	T-10	258	975	815
	T-12	284	1025	789
	T-14	281	1029	777
	T-21	283	1026	768
	T-22	280	1017	766
After 1st Spin	T-12 (105%)	265	987	762
	T-22 (100%)	267	995	748
After 50 Cycles Low Cycle Fatigue	T-2 (100%)	226	889	731
	T-10 (110%)	244	953	783
	T-14 (105%)	262	988	736
After 10^7 Cycles High Frequency Fatigue	T-2	220	884	727
	T-10	238	939	777
	T-14	257	986	735
After 10 Cycles Low Cycle Fatigue	T-10 (110%)	238	938	777
	(a)T-14 (105%)	264	975	738

(a)Taping down of loose edge protector may have affected these frequencies.

TABLE XXIII

BLADE SPIN TEST RESULTS

Blade S/N	As-Molded Sonic Quality	Ultrasonic Indications after First Excursion to Spin Speed Shown					LCF[a] (Speed)	10^7 HFF[b] Cycles	LCF 10 Cycles
		80%	90%	100%	105%	110%			
T-1	Indication	Pass	Delam.	Blade Failed	-	-	-	-	-
T-2	Indication	Delam.	Delam.Growth	Delam.Growth	N.T.[c]	N.T.	Small Delam. Growth (100%) 30 Cycles	N.C.[d]	N.C.
T-4	Clear	Pass	Pass	Blade Failed	-	-	-	-	-
T-9				Delam.	-	-	-	-	-
T-10				Pass	N.T.	Delam.	N.C.	N.C.	Delam.Growth
T-12				Pass	Delam.	-	-	-	-
T-14				Pass	Pass	Pass	Delam. (105%) 50 Cycles	L.E. Guard Missing at Tip	N.C.
T-21				Blade Failed	-	-	-	-	-
T-22				Delam.	-	-	-	-	-

(a) Low cycle fatigue.
(b) High frequency fatigue.
(c) Not tested in this mode.
(d) No change observed in ultrasonic inspection.

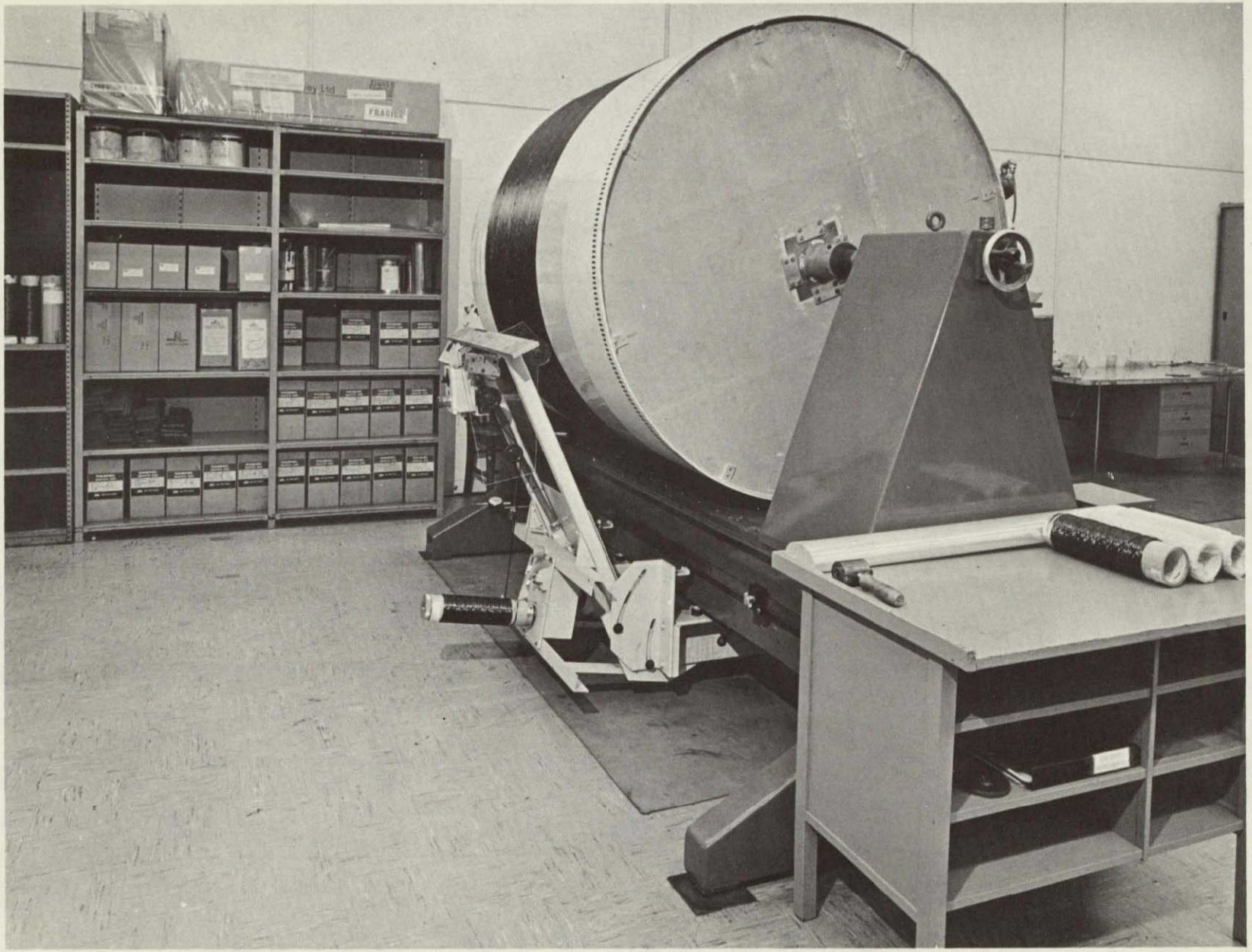

Figure 1. Fiber Collimating Unit Used for Prepregging.

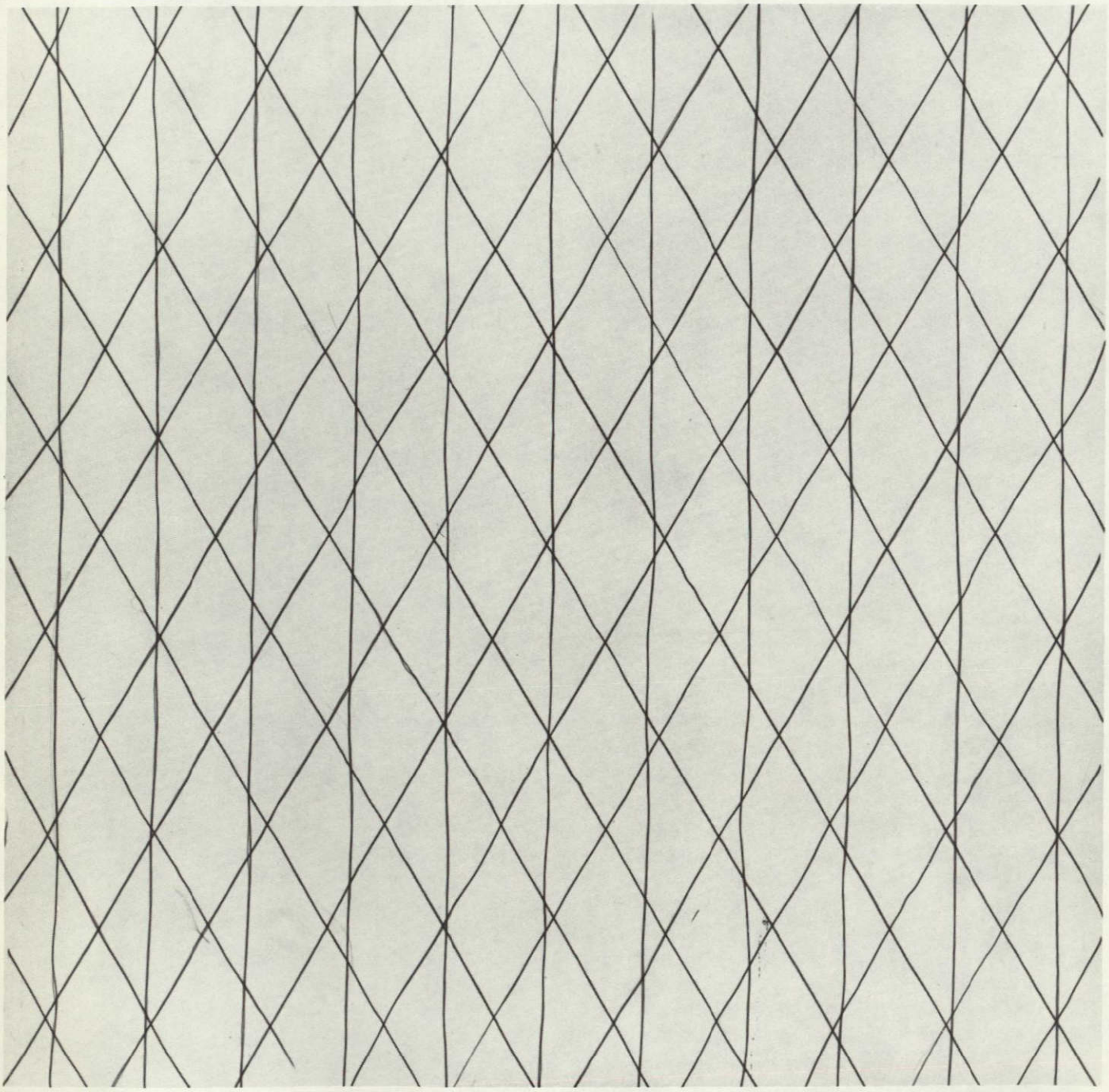

Figure 2. X-Ray of Construction III Panel Showing Leaded Glass Tracers.

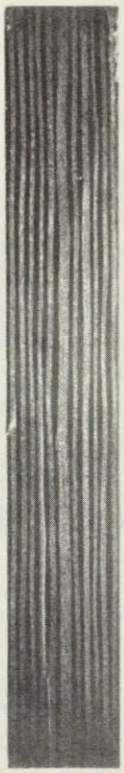

2.5X

Figure 3. Longitudinal Cross Section of Shear Specimen Showing Ply Parallelism in Construction III.

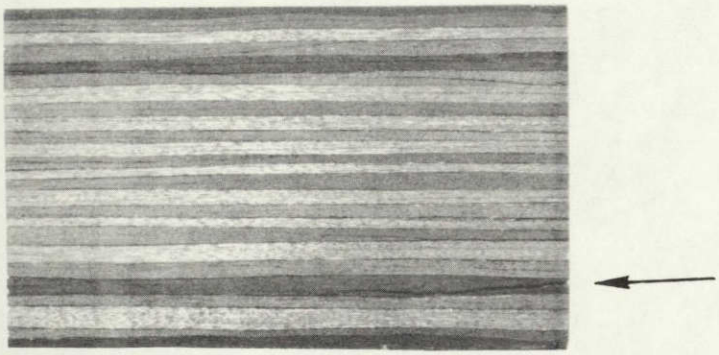

7X

Figure 4. Magnified Photograph of Shear Specimen Showing Stress Crack Location in Construction IV.

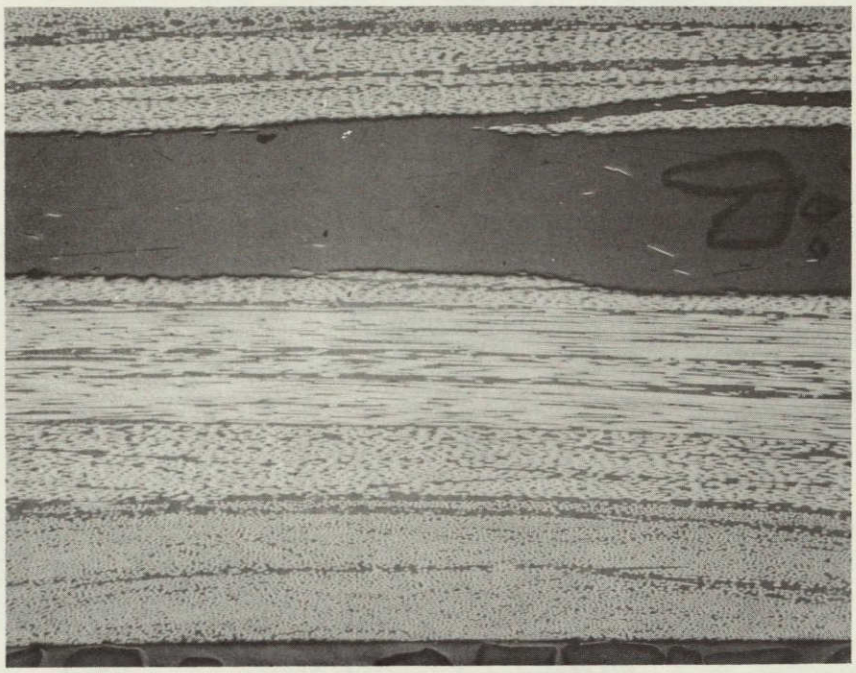

40X

Figure 5. Photomicrograph of Type V Laminate Construction Showing Stress Crack.

40X

Figure 6. Photomicrograph of Type IV Laminate Construction Showing Stress Crack.

7324-C

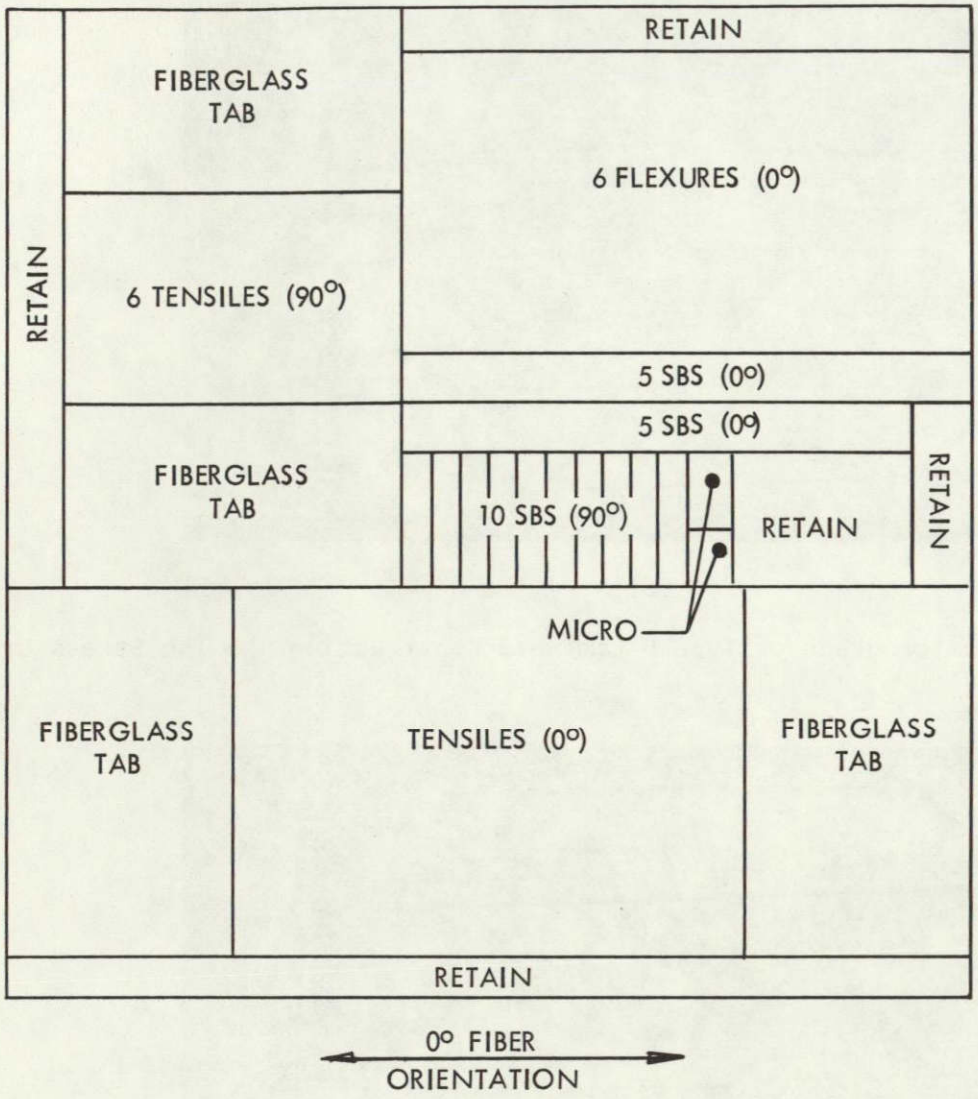

FIGURE 7 TEST SPECIMEN LAYOUT FOR LAMINATE VI.

Figure 8. Ultra-High Speed Fan Blade in Finished Machined Form.

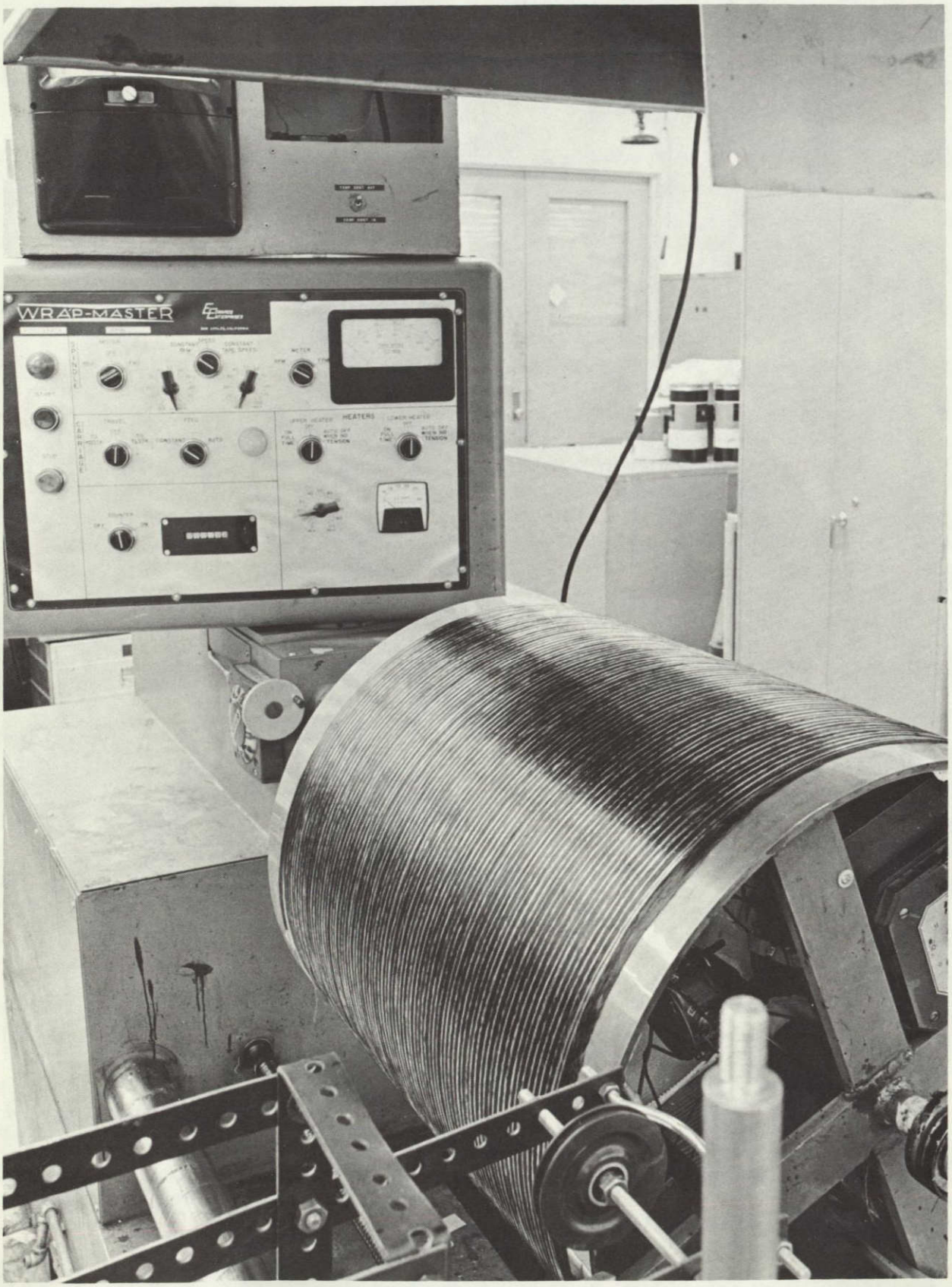

Figure 9. Glass/Graphite Hybrid Prepreg.

Figure 10. Blade Prepreg Ply Location Arrangement.

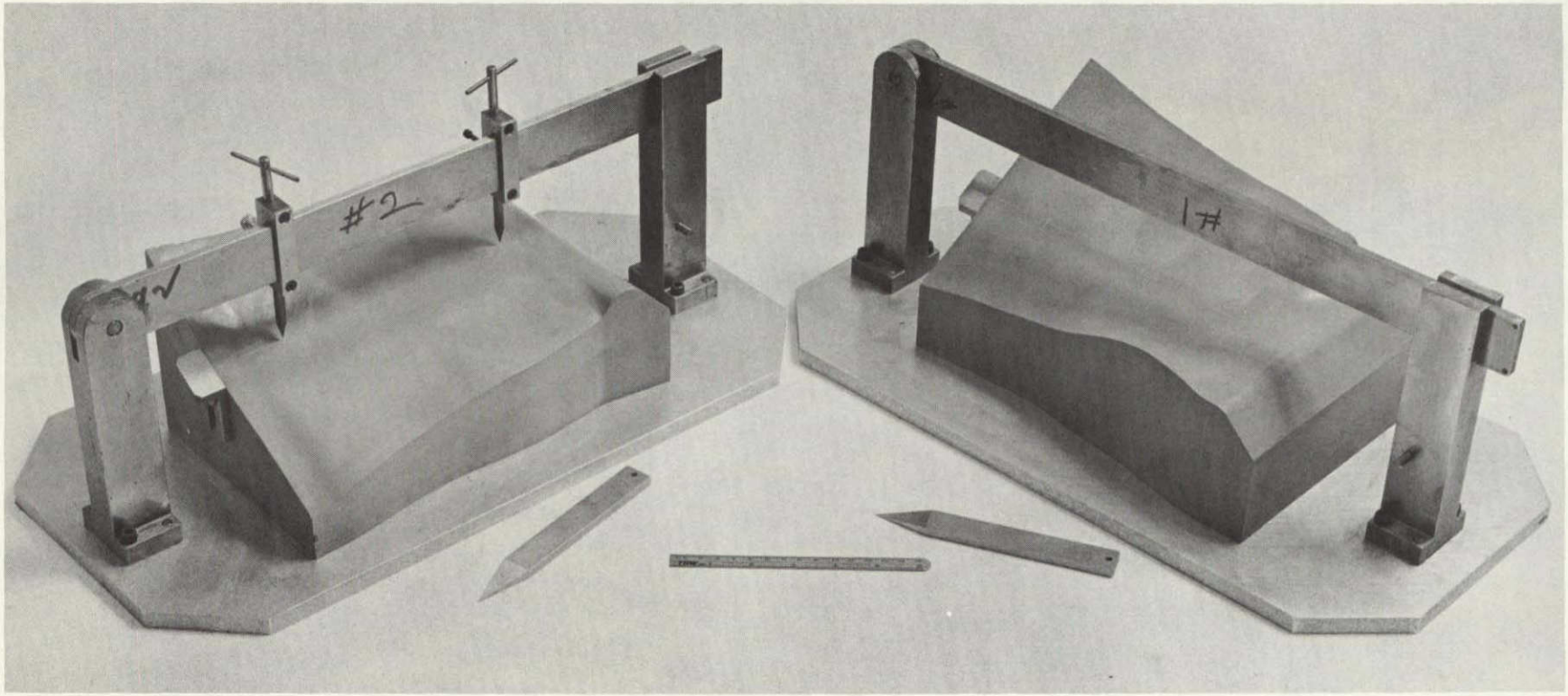

Figure 11. Blade Prepreg Layup Tools.

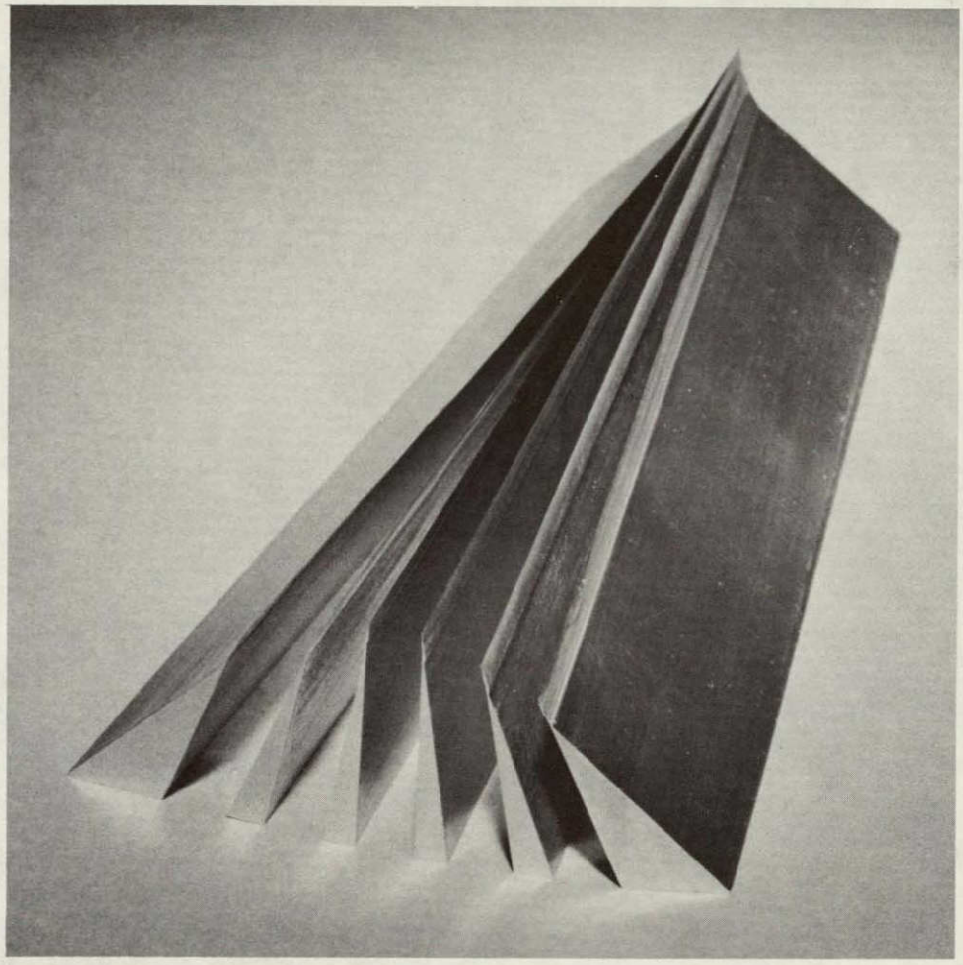

Figure 12. Blade Root Wedges Ready for Priming.

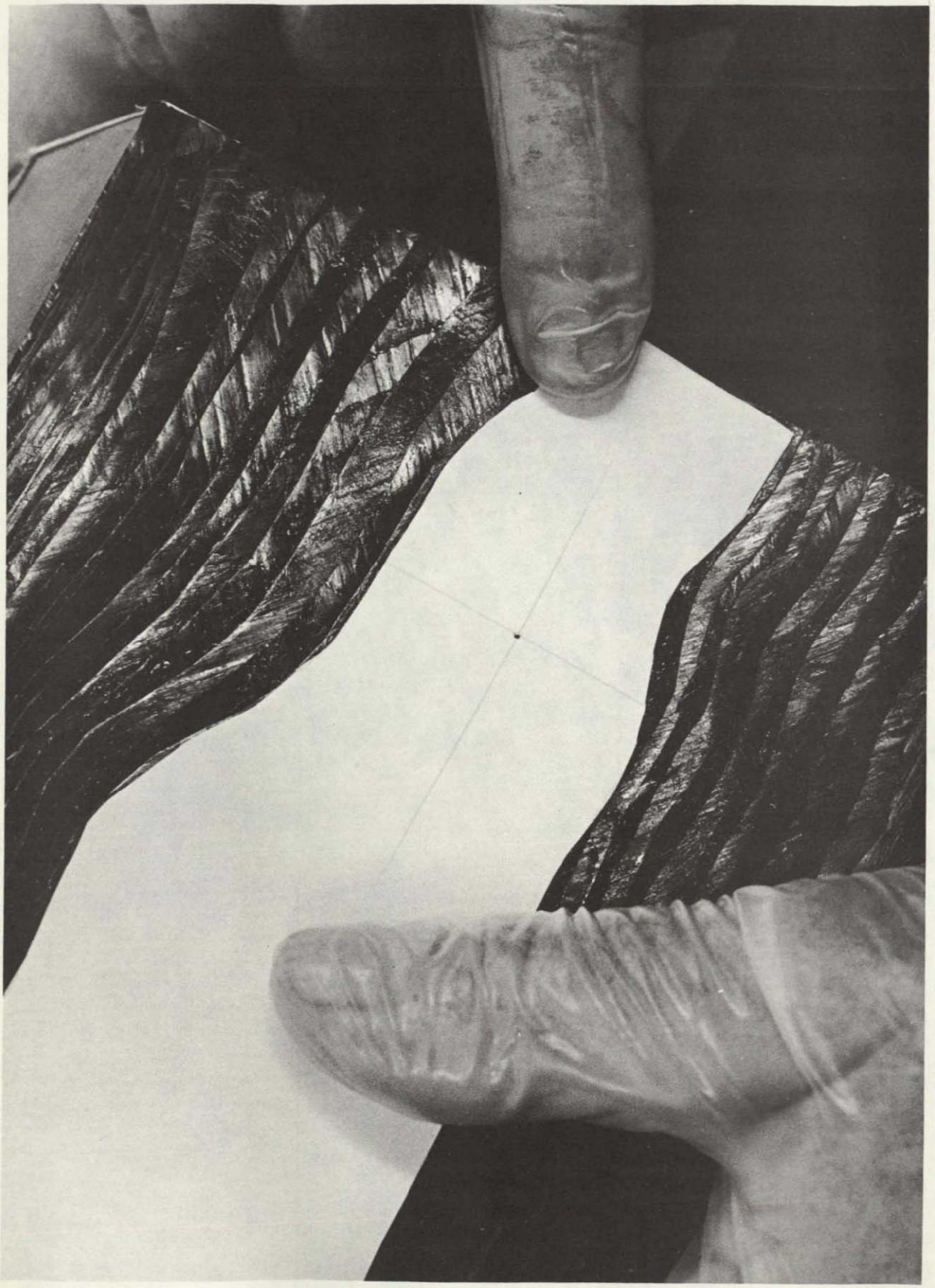

Figure 13. Blade Ply Being Placed on Layup Tool.

Figure 14. Half of Completed Blade Layup.

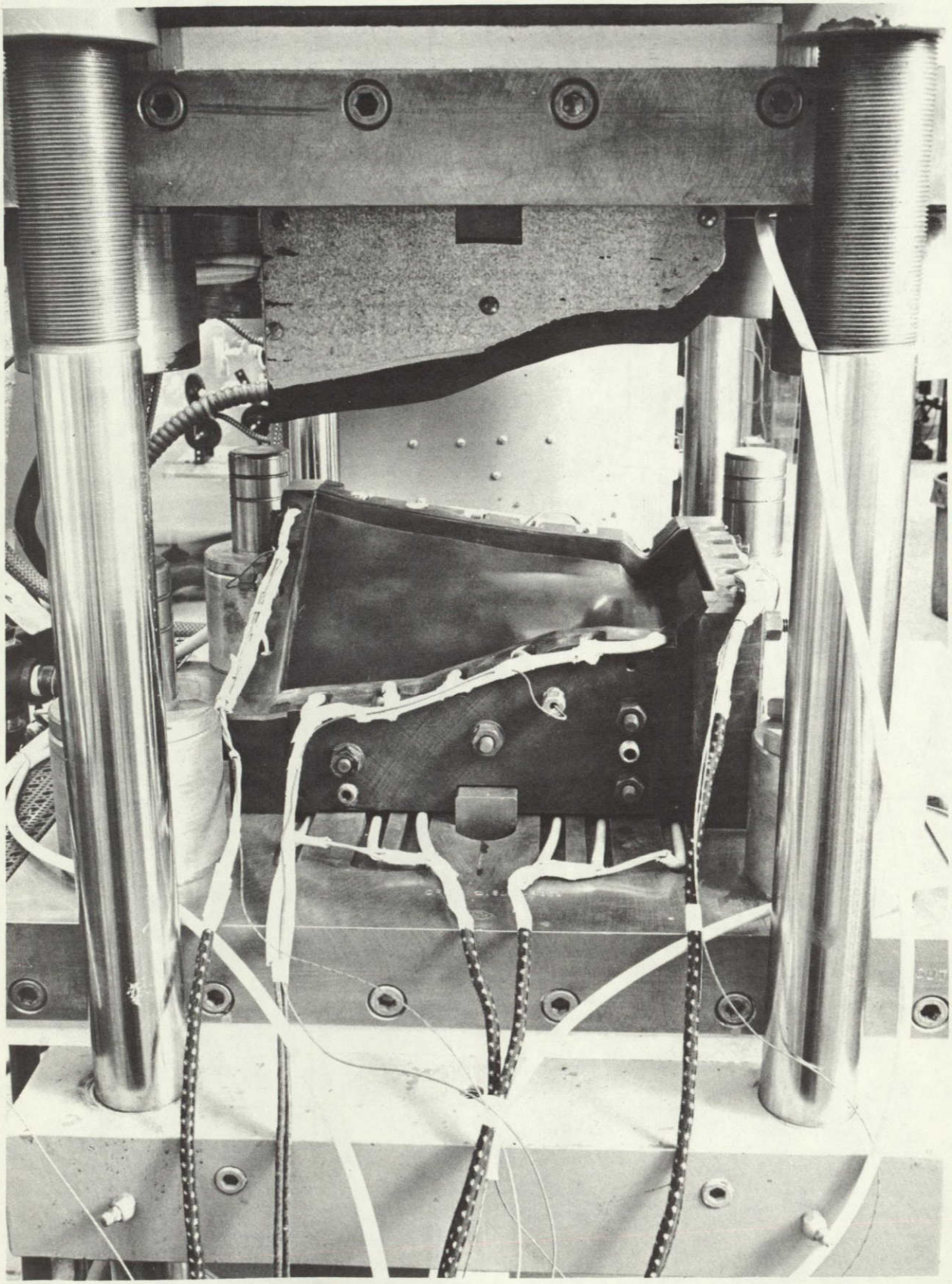

Figure 15. Blade Molding Die in Press.

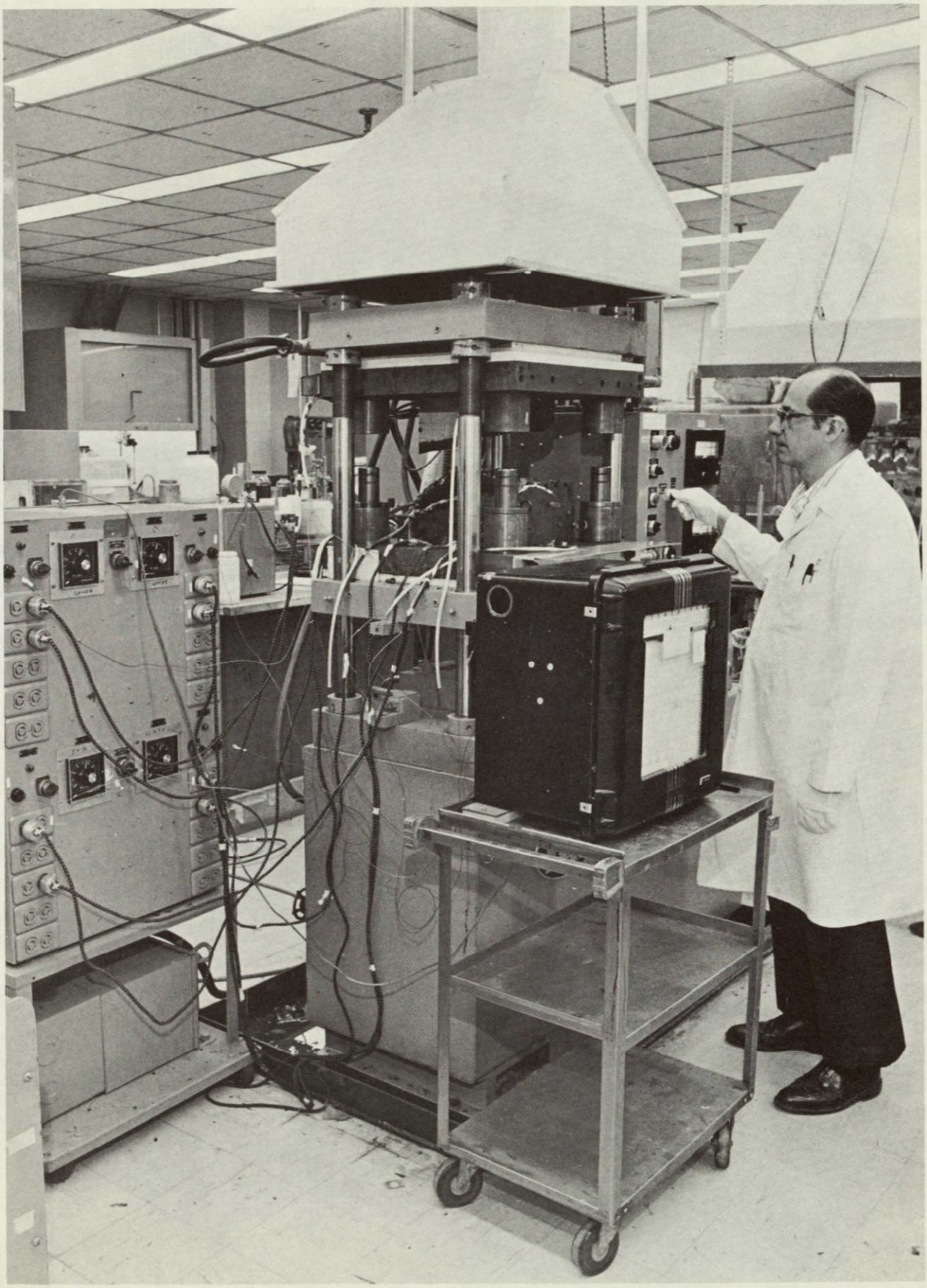

Figure 16. Blade Molding Press Showing Temperature Controller and Recorder.

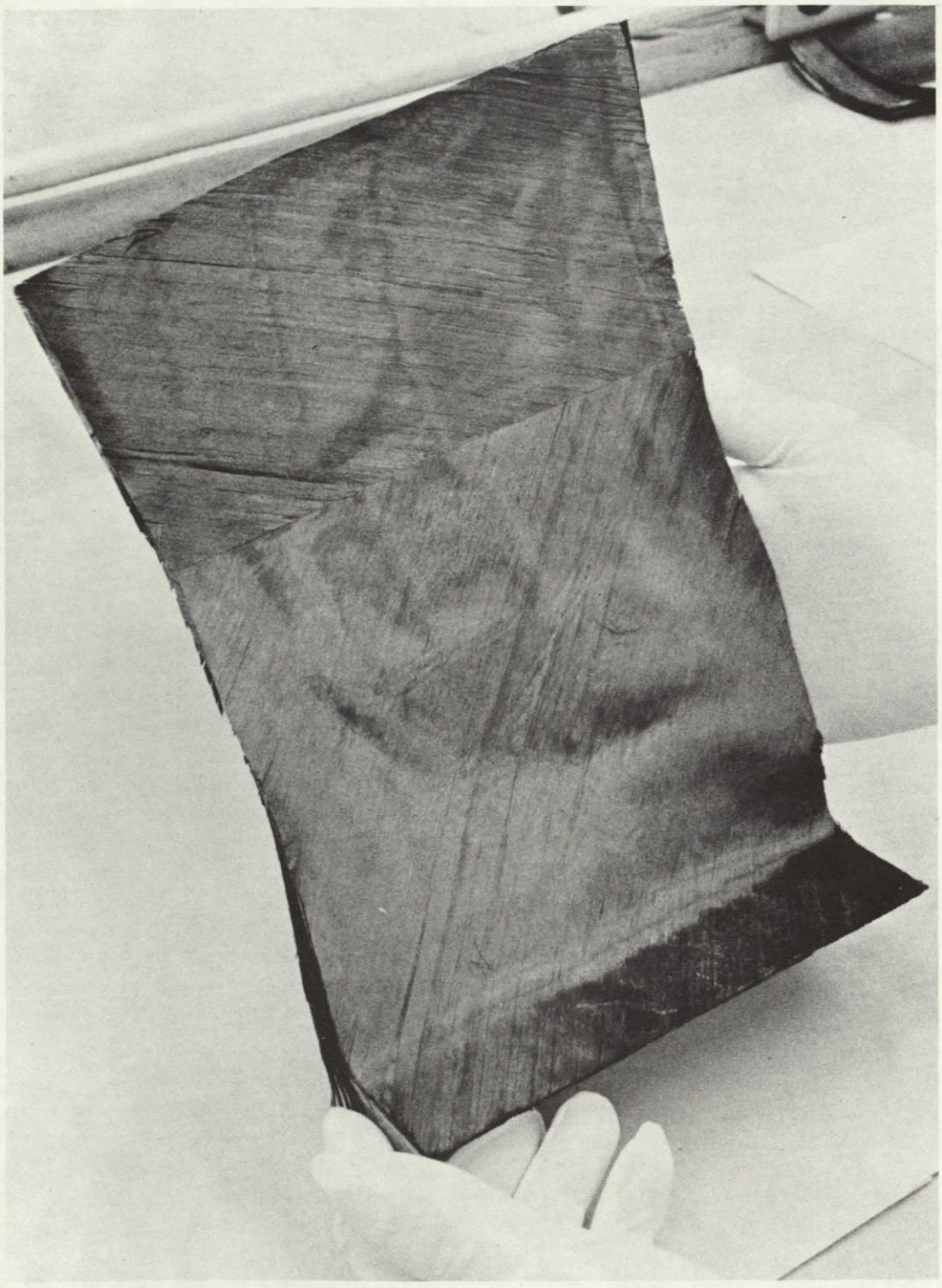

Figure 17. Blade Layup After Imidization.

Figure 18. Hybrid Blade After Imidization.

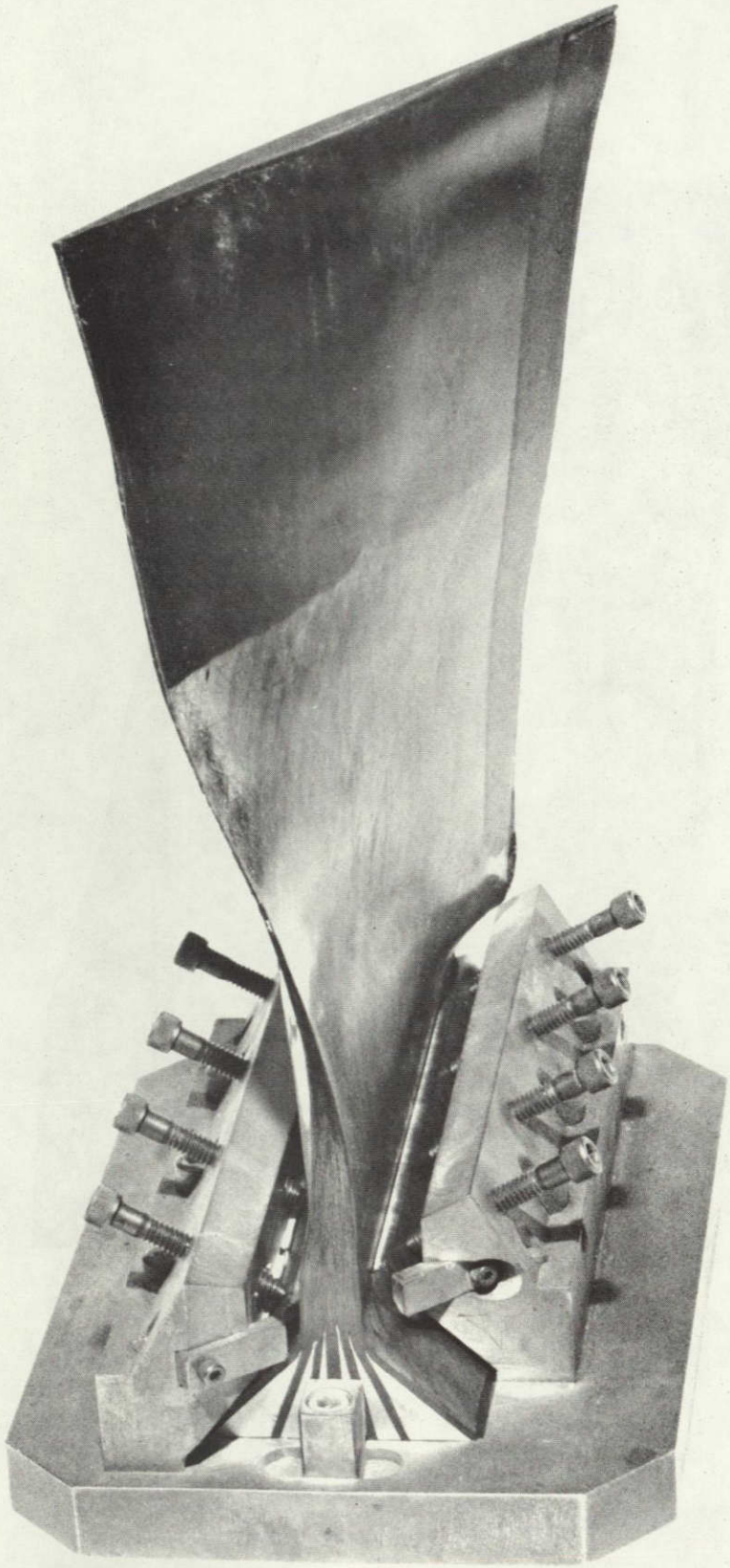

Figure 19. Final Molded Blade in Root Pressure Pad Bonding Fixture.

Figure 20. Completely Finished Ultra-High Speed Fan Blade.

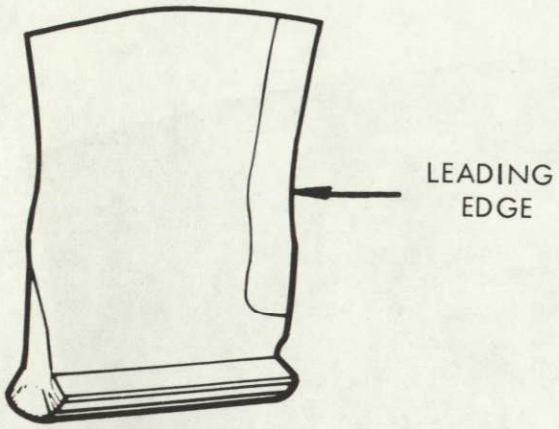

NO INDICATIONS

FIG. 21 S/N T-9

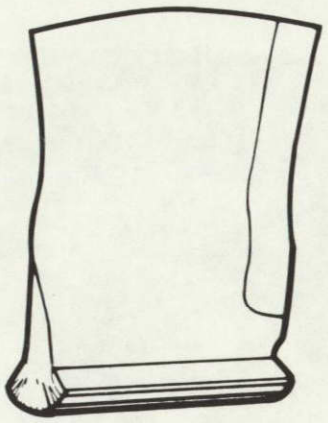

NO INDICATIONS

FIG. 22 S/N T-10

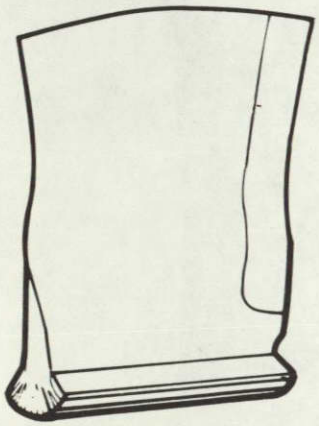

NO INDICATIONS

FIG. 23 S/N T-11

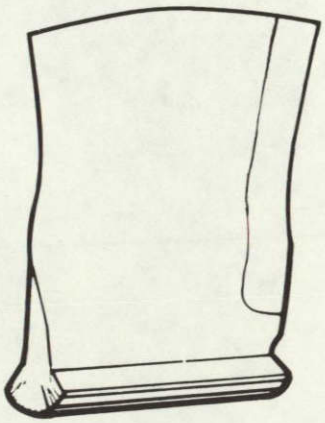

NO INDICATIONS

FIG. 24 S/N T-12

SONIC INDICATION PATTERN FOR BLADES

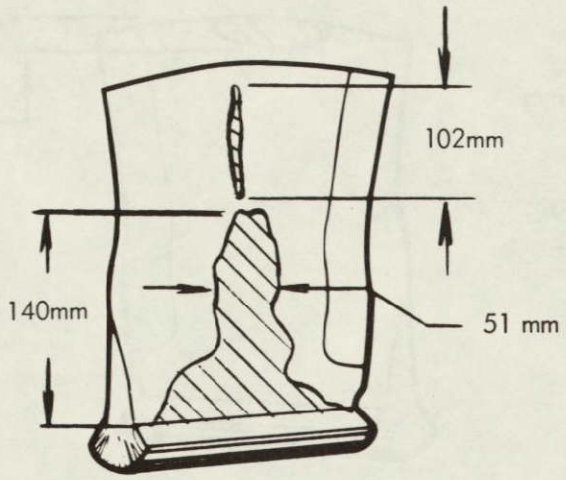

FIG. 25 S/N T-13

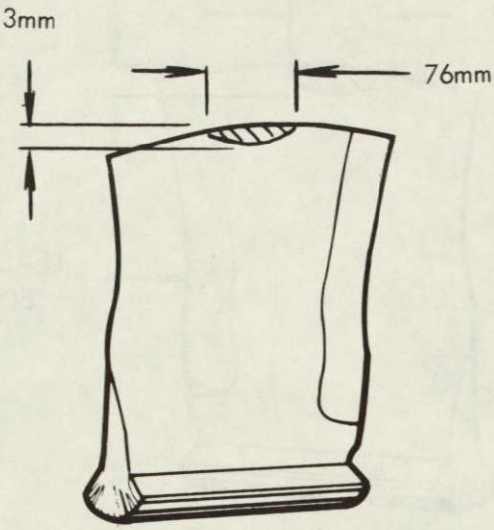

FIG. 26 S/N T-14

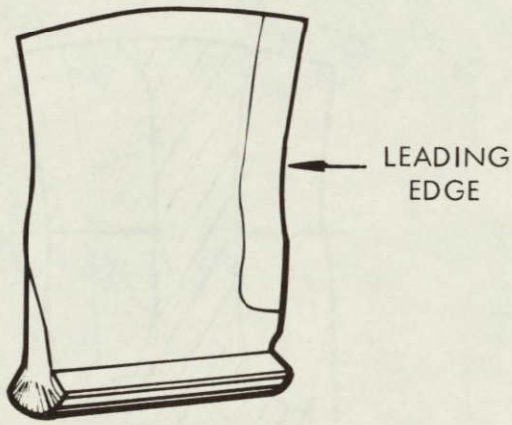

NO INDICATIONS

FIG. 27 S/N T-15

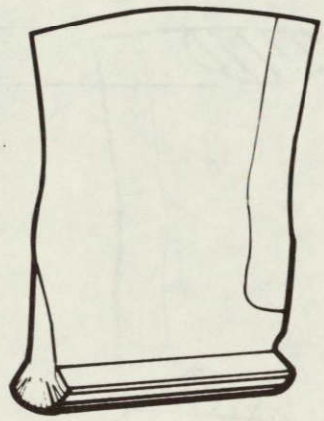

NO INDICATIONS

FIG. 28 S/N T-16

SONIC INDICATION PATTERN FOR BLADES

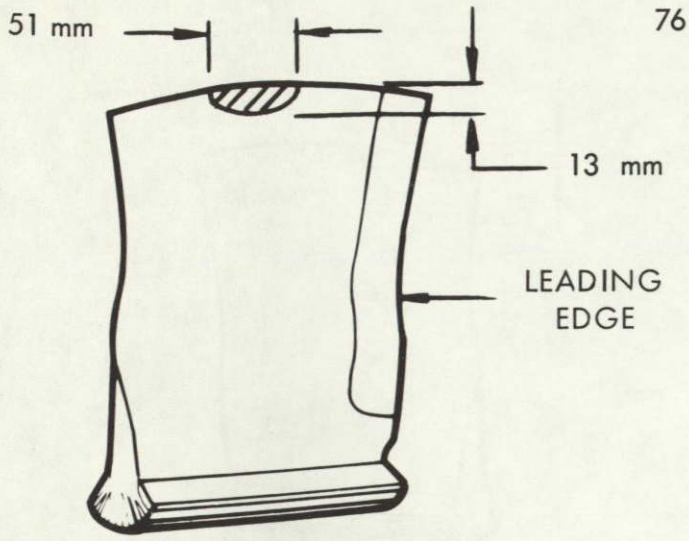

FIG. 29 S/N T-17

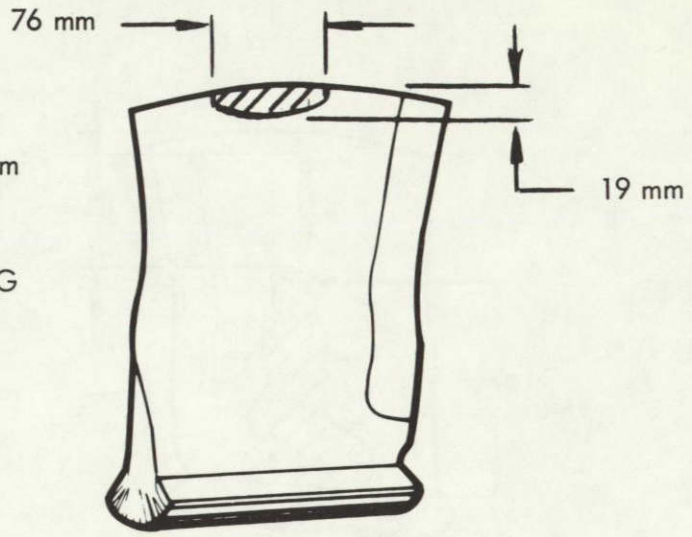

FIG. 30 S/N T-18

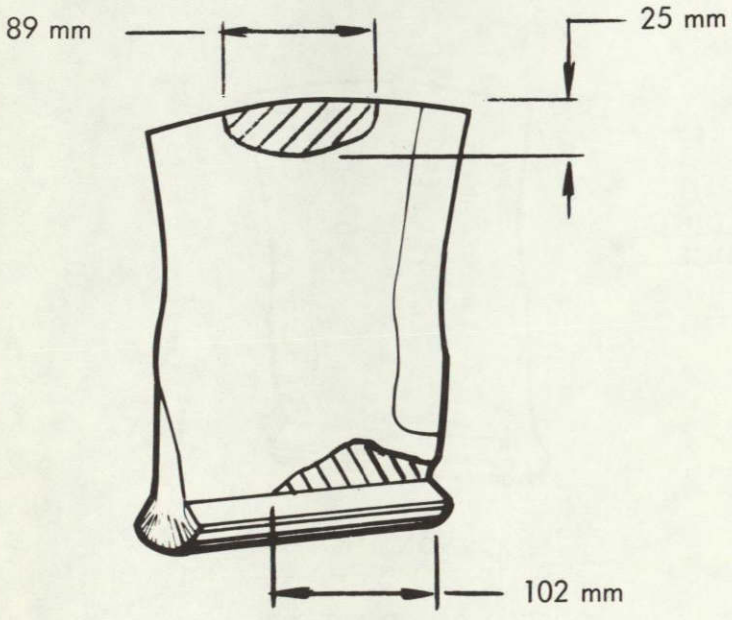

FIG. 31 S/NT-19

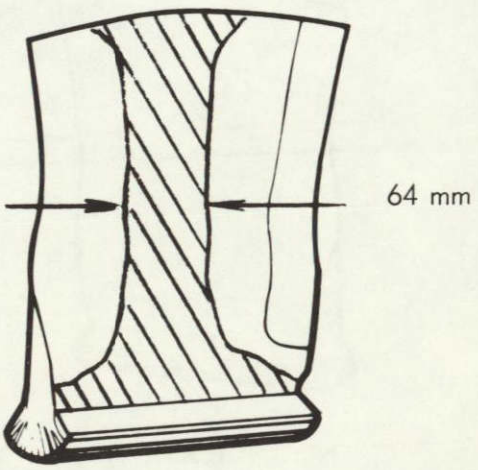

FIG. 32 S/N T-20

SONIC INDICATION PATTERN FOR BLADES

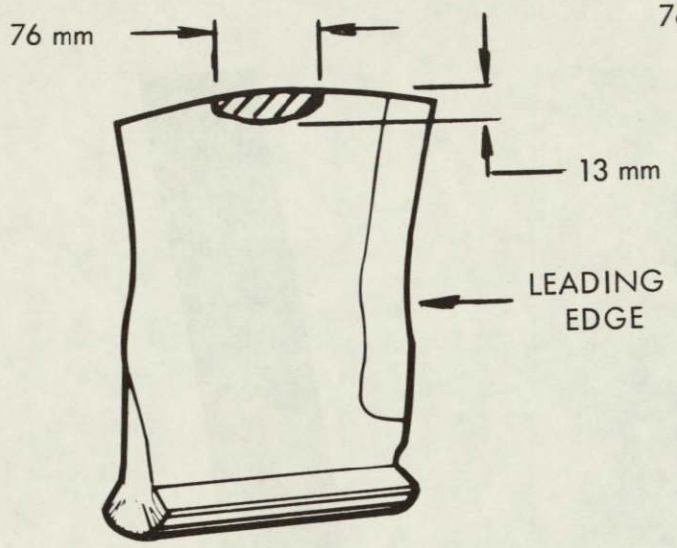

FIG. 33 S/N T-21

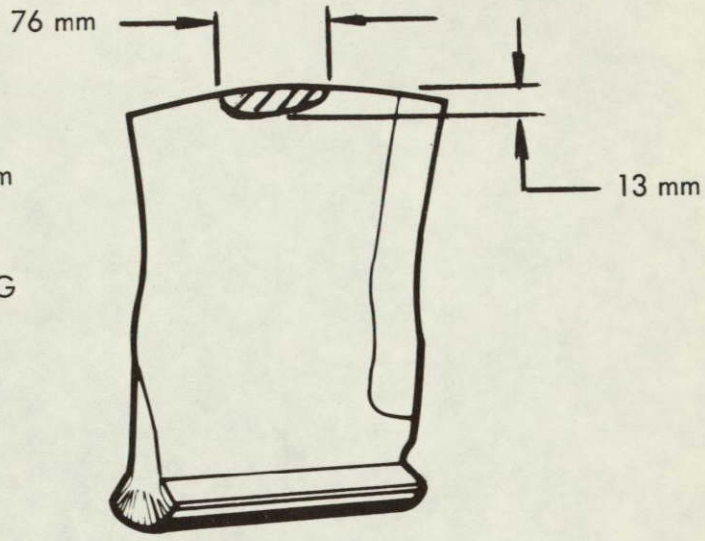

FIG. 34 S/N T-22

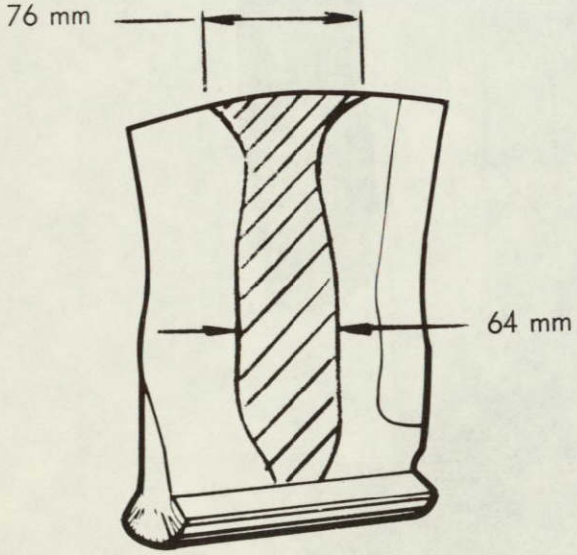

FIG. 35 S/N T-23H

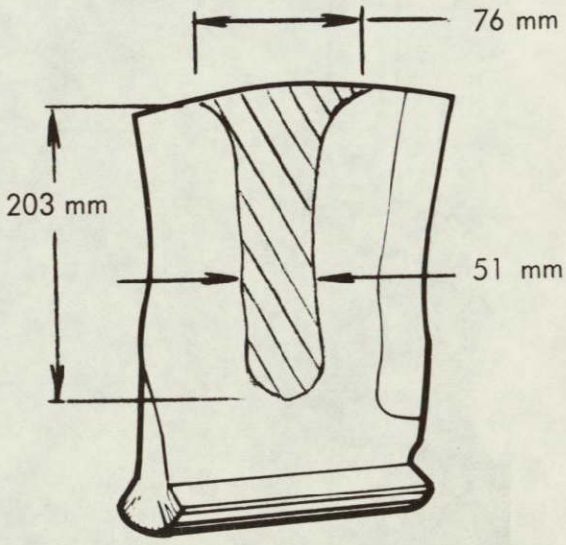

FIG. 36 S/N T-24H

SONIC INDICATION PATTERN FOR BLADES

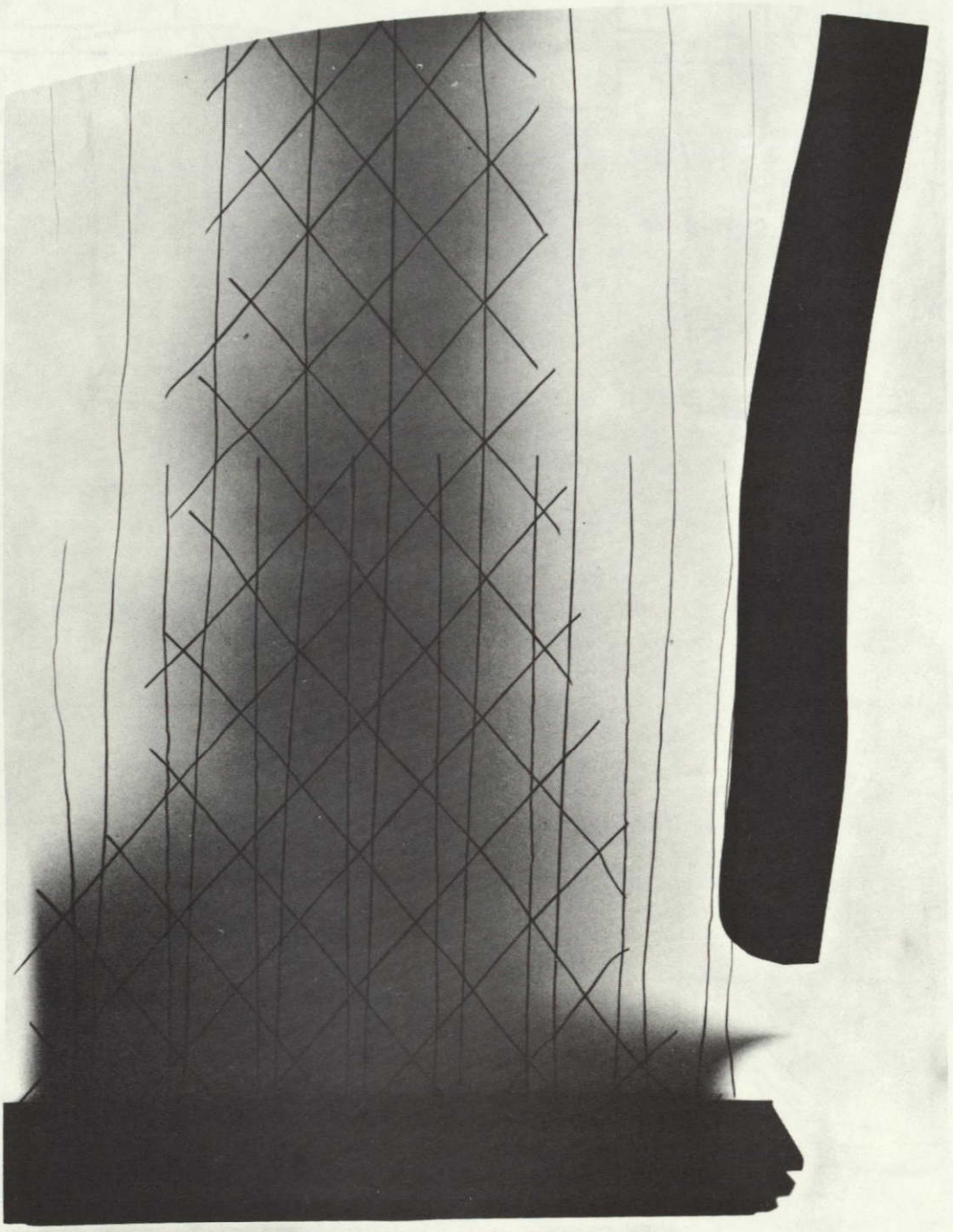

Figure 37. X-Ray Positive of Fan Blade (Reduced) Showing the Nickel Leading Edge and Glass Tracer Fibers.

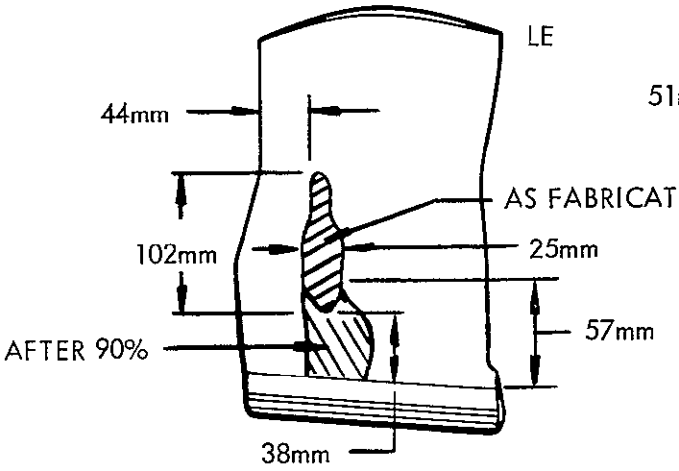

FIG. 38 S/N T-1

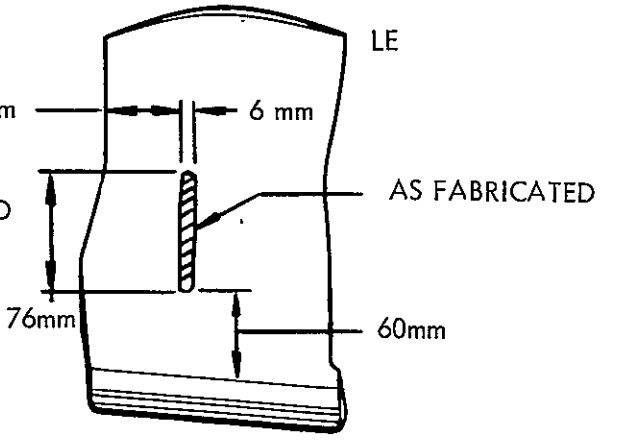

FIG. 39 S/N T-2

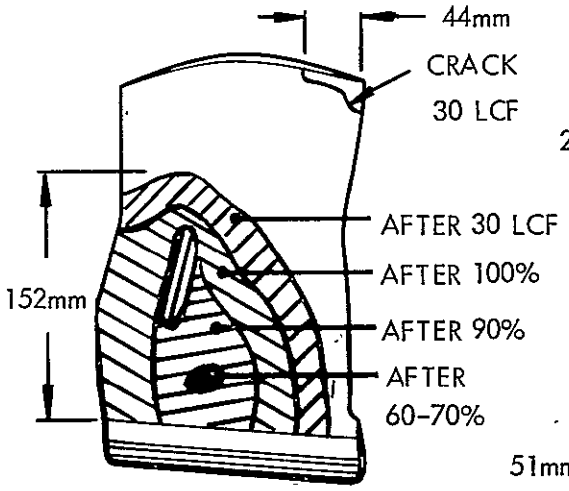

FIG. 40 S/N T-2

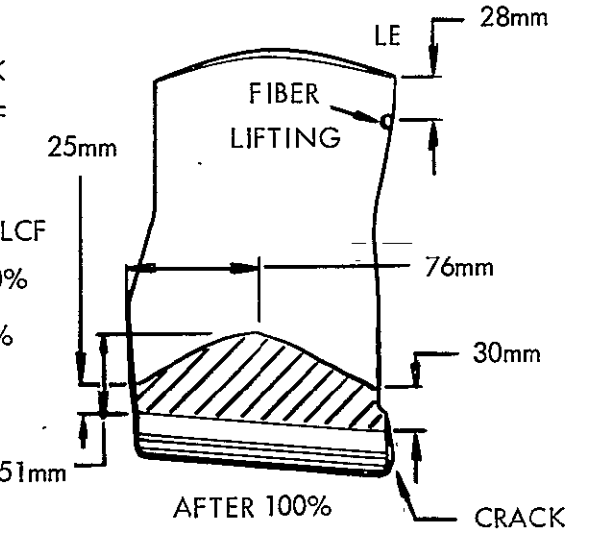

FIG. 41 S/N T-9

POST TEST BLADE EVALUATION

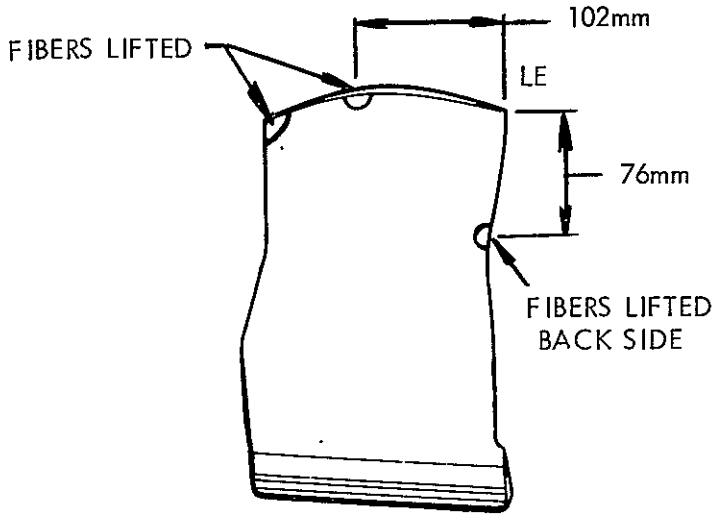

AFTER 80%

FIG. 42 S/N T-10

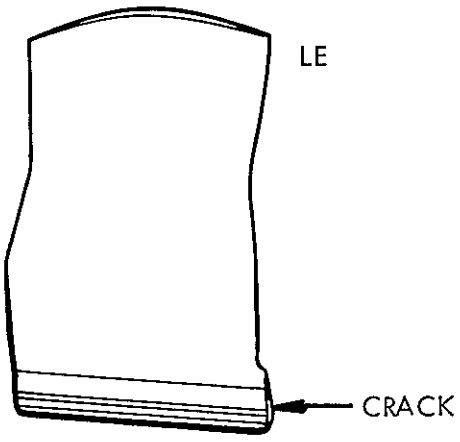

AFTER 100%

FIG. 43 S/N T-10

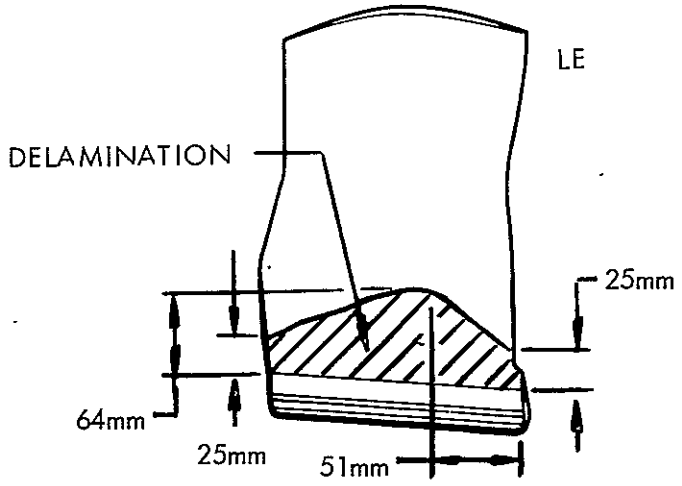

AFTER 110%

FIG. 44 S/N T-10

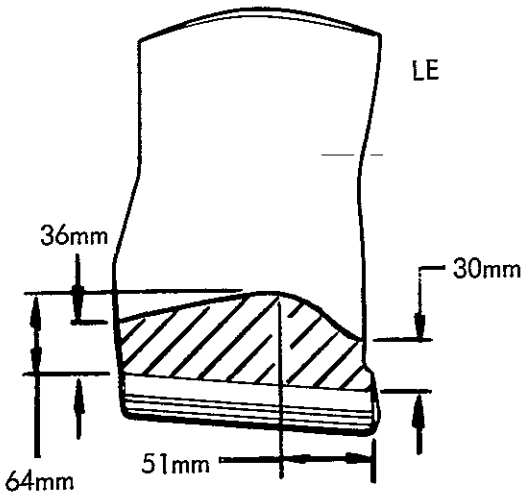

AFTER 10^7 HFF

FIG. 45 S/N T-10

POST TEST BLADE EVALUATION

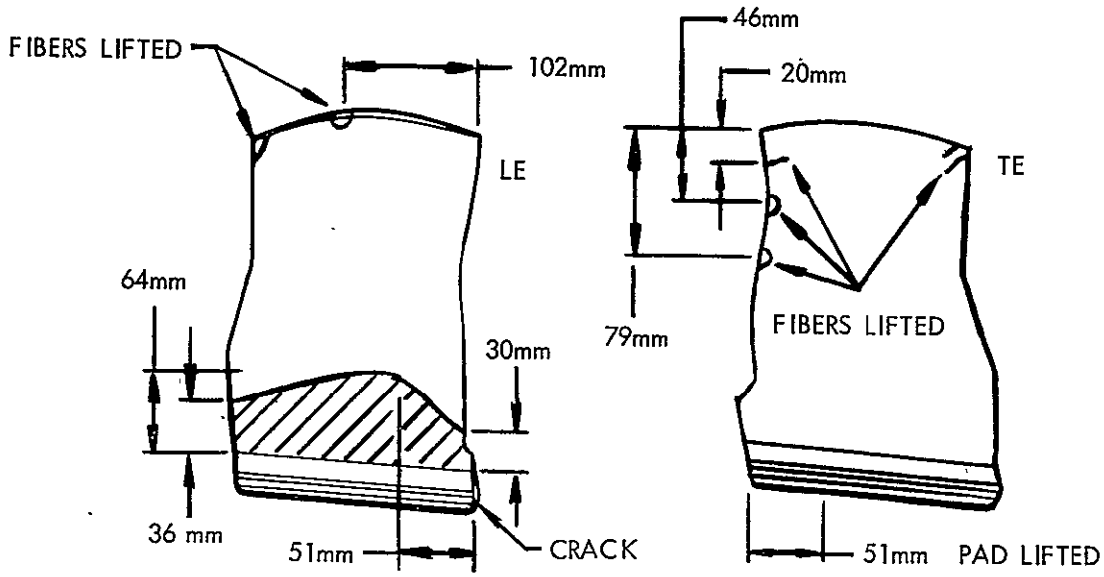

AFTER 10 LCF AT 110%

FIG. 46 S/N T-10

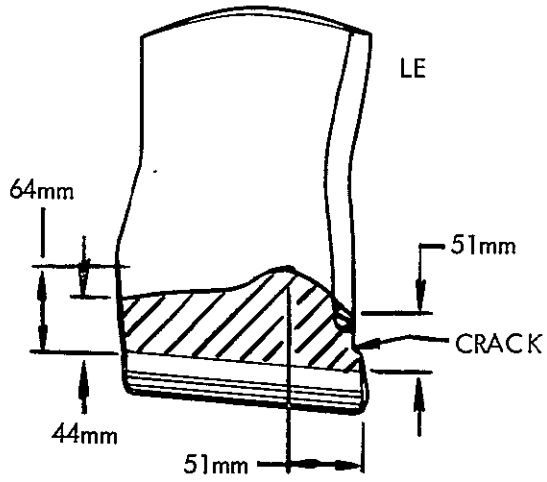

AFTER 105%

FIG. 47 S/N T-12

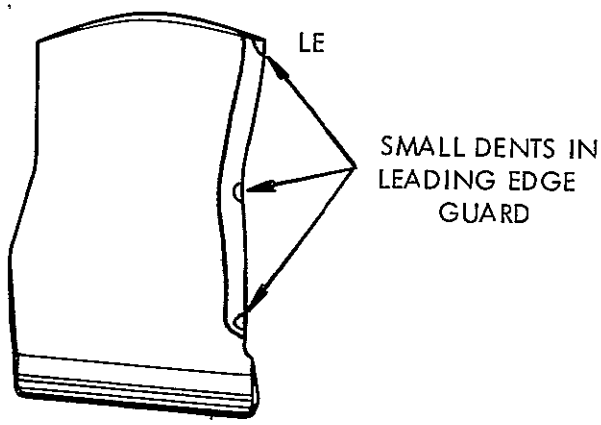

BEFORE TESTING

FIG. 48 S/N T-14

POST TEST BLADE EVALUATION

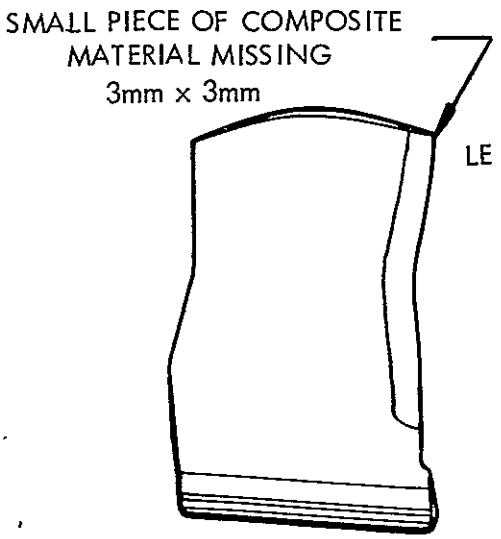

AFTER 80%

FIG. 49 S/N T-14

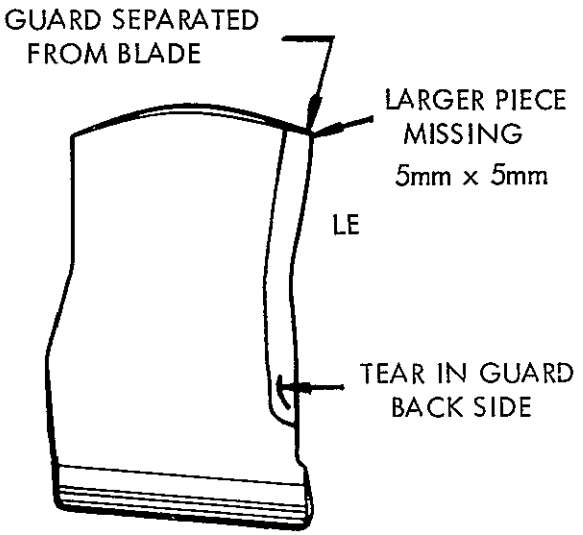

AFTER 105%

FIG. 50 S/N T-14

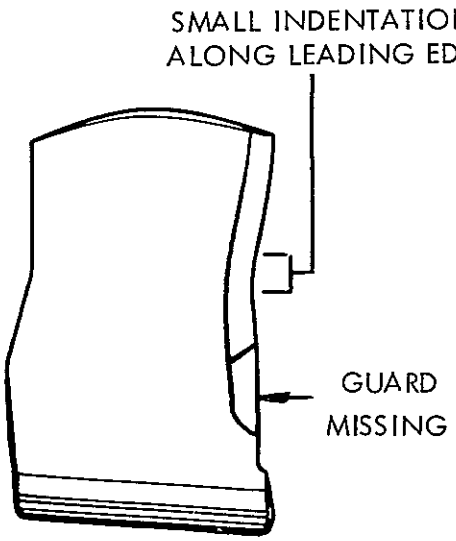

AFTER 110%

FIG. 51 S/N T-14

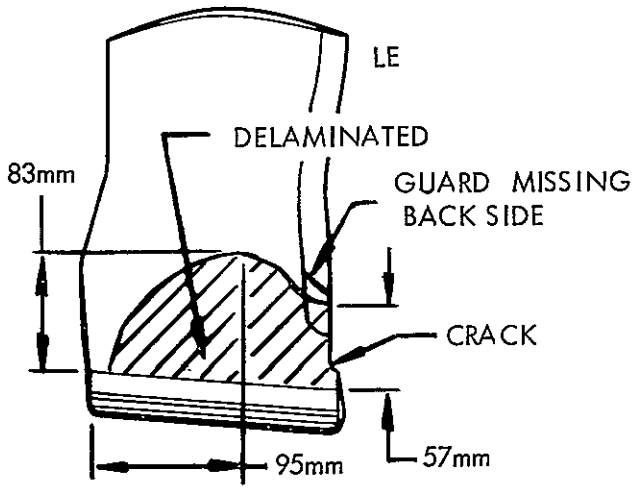

AFTER 50 LCF 105%

FIG. 52 S/N T-14

POST TEST BLADE EVALUATION

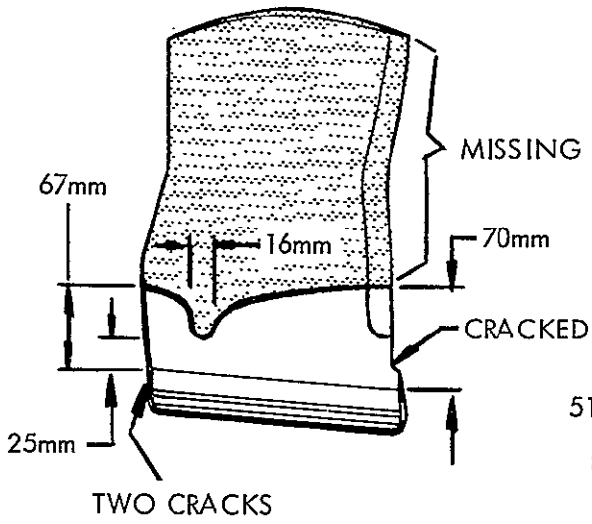

AFTER 7 SEC AT 100%

FIG. 53 S/N T-21

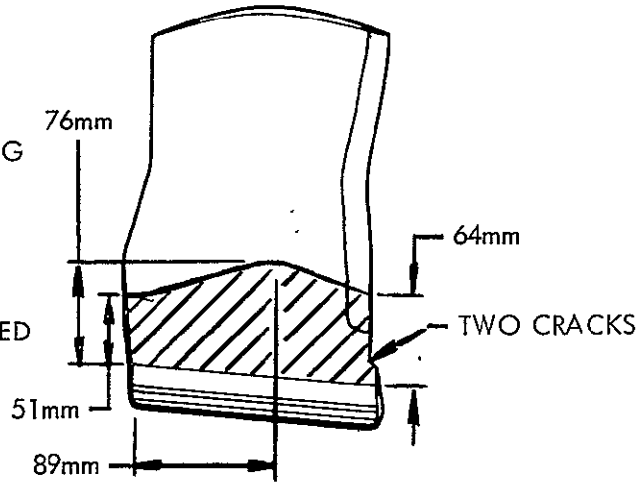

AFTER 100%

FIG. 54 S/N T-22

POST TEST BLADE EVALUATION

REFERENCES

1. Cavano, P. J., "Resin/Graphite Fiber Composites," NASA CR-134727, December 5, 1974.

2. Serafini, T. T. and Vannucci, R. D., "Tailor Making High Performance Graphite Fiber Reinforced PMR Polyimides," Proceedings of 30th Annual SPI Conference, February 1974.

3. Cavano, P. J., "Resin/Graphite Fiber Composites," NASA CR-121275, March 15, 1974.

4. Crane, L. W. et al, "Surface Treatment of Cured Epoxy Graphite Composites to Improve Adhesive Bonding," SAMPE JOURNAL, March/April 1974.

5. Fields, D., "Manufacturing Methods Development of Spot-Weld-Adhesive Bonded Joining for Titanium," AFML-TR-71-93, June 1971.

DISTRIBUTION LIST

	Copies
National Aeronautics and Space Administration Lewis Research Center 21000 Brookpark Road Cleveland, Ohio 44135	
Attn: Contracting Officer, J. E. Hickey, MS 500-313	1
Technical Report Control Office, MS 5-5	1
Technology Utilization Office, MS 3-16	1
AFSC Liaison Office, MS 4-1	2
Library, MS 60-3	2
Office of Reliability & Quality Assurance, MS 500-111	1
R. H. Kemp, MS 49-1	1
R. D. Vannucci, MS 49-1	25
N. T. Musial, MS 500-113	1
T. D. Gulko, MS 49-3	1
National Aeronautics and Space Administration Washington, D.C. 20546	
Attn: J. J. Gangler/Code RWM	1
B. G. Achhammer/Code RWM	1
NASA Scientific and Technical Information Facility Attn: Acquisitions Branch P. O. Box 33 College Park, Maryland 20740	10
National Aeronautics and Space Administration Ames Research Center Moffett Field, California 94035	
Attn: John Parker	1
National Aeronautics and Space Administration Flight Research Center P. O. Box 273 Edwards, California 93523	
Attn: Library	1
National Aeronautics and Space Administration Goddard Space Flight Center Greenbelt, Maryland 20771	
Attn: Library	1

DISTRIBUTION LIST (continued)

	Copies
National Aeronautics and Space Administration John F. Kennedy Space Center Kennedy Space Center, Florida 32899	
Attn: Library	1
National Aeronautics and Space Administration Langley Research Center Langley Station Hampton, Virginia 23365	
Attn: V. L. Bell, MS 226	1
N. Johnston, MS 226	1
National Aeronautics and Space Administration Manned Spacecraft Center Houston, Texas 77001	
Attn: Library	1
Code EP	1
National Aeronautics and Space Administration George C. Marshall Space Flight Center Huntsville, Alabama 35812	
Attn: J. Curry	1
J. Stuckey	1
Jet Propulsion Laboratory 4800 Oak Grove Drive Pasadena, California 91103	
Attn: Library	1
Office of the Director of Defense Research and Engineering Washington, D.C. 20301	
Attn: Dr. H. W. Schulz, Office of Assistant Director (Chem. Technology)	1
Defense Documentation Center Cameron Station Alexandria, Virginia 22314	1

	Copies
Research and Technology Division Bolling Air Force Base Washington, D.C. 20332	
Attn: RTNP	1
Bureau of Naval Weapons Department of the Navy Washington, D.C. 20360	
Attn: DLI-3	1
Director (Code 6180) U. S. Naval Research Laboratory Washington, D.C. 20390	
Attn: H. W. Carhart	1
SARPA-FR-MD Plastics Technical Evaluation Center Picatinny Arsenal Attn: A. M. Anzalone, Bldg. 176 Dover, New Jersey 07801	1
Structural Composites Industries, Inc. 6344 North Irwindale Avenue Azusa, California 91703	
Attn: Ira Petker	1
Aeronautic Division of Philco Corporation Ford Road Newport Beach, California 92600	
Attn: Dr. L. H. Linder, Manager Technical Information Department	1
Aerospace Corporation P. O. Box 95085 Los Angeles, California 90045	
Attn: Library Documents	1
Aerotherm Corporation 800 Welch Road Palo Alto, California 94304	
Attn: Mr. R. Rindal	1

DISTRIBUTION LIST (continued)

	Copies
Air Force Materials Laboratory Wright-Patterson Air Force Base, Ohio 45433	
Attn: AFML/MBC, T. J. Reinhart, Jr.	1
AFML/LNC, D. L. Schmidt	1
Office of Aerospace Research (RROSP) 1400 Wilson Boulevard Arlington, Virginia 22209	
Attn: Major Thomas Tomaskovic	1
Arnold Engineering Development Center Air Force Systems Command Tullahoma, Tennessee 37389	
Attn: AEOIM	1
Air Force Systems Command Andrews Air Force Base Washington, D.C. 20332	
Attn: SCLT/Capt. S. W. Bowen	1
Air Force Rocket Propulsion Laboratory Edwards, California 93523	
Attn: RPM	1
Air Force Flight Test Center Edwards Air Force Base, California 93523	
Attn: FTAT-2	1
Air Force Office of Scientific Research Washington, D.C. 20333	
Attn: SREP, Dr. J. F. Masi	1
American Cyanamid Company 1937 West Main Street Stamford, Connecticut 06902	
Attn: Security Officer	1
AVCO Corporation Space Systems Division Lowell Industrial Park Lowell, Massachusetts 01851	
Attn: W. Port	1

DISTRIBUTION LIST (continued)

	Copies
Battelle Memorial Institute 505 King Avenue Columbus, Ohio 43201	
Attn: Report Library, Room 6A	1
Bell Aerosystems, Inc. Box 1 Buffalo, New York 14205	
Attn: T. Reinhardt	1
The Boeing Company Aero Space Division P. O. Box 3999 Seattle, Washington 98124	
Attn: J. T. Hoggatt	1
Celanese Research Company Morris Court Summit, New Jersey	
Attn: Dr. J. R. Leal	1
University of Denver Denver Research Institute P. O. Box 10127 Denver, Colorado 80210	
Attn: Security Office	1
Dow Chemical Company Security Section Box 31 Midland, Michigan 48641	
Attn: Dr. R. S. Karpiuk, 1710 Building	1
E. I. DuPont De Nemours & Co. (Inc.) Fibers Department Experimental Station - Bldg. 262 Wilmington, Delaware 19898	
Attn: Dr. Carl Zweben	1

DISTRIBUTION LIST (continued)

	Copies
Ultrasystems, Inc. 2400 Michelson Drive Irvine, California 92664	
Attn: Dr. R. Kratzer	1
General Dynamics/Convair Dept. 643-10 Kerny Mesa Plant San Diego, California 92112	
Attn: J. Hertz	1
General Electric Company Re-Entry Systems Department P. O. Box 8555 Philadelphia, Pennsylvania 19101	
Attn: Library	1
General Electric Company Technical Information Center N-32, Building 700 Cincinnati, Ohio	
Attn: C. A. Steinhagen	1
C. L. Stotler	1
General Technologies Corporation 708 North West Street Alexandria, Virginia	
Attn: W. M. Powers	1
Grumman Aerospace Corporation Plant 12, Dept. 447 Bethpage, New York	
Attn: N. A. Sullo	1
Hercules Powder Company Allegheny Ballistics Laboratory P. O. Box 210 Cumberland, Maryland 21501	
Attn: Library	1

DISTRIBUTION LIST (continued)

	Copies
Hughes Aircraft Company Culver City, California	
Attn: N. Bilow	1
ITT Research Institute Technology Center Chicago, Illinois 60616	
Attn: C. K. Hersh, Chemistry Division	1
Lockheed Missiles & Space Company Propulsion Engineering Division (D.55-11) 111 Lockheed Way Sunnyvale, California 94087	1
McDonnell Douglas Aircraft Company Santa Monica Division 3000 Ocean Park Blvd. Santa Monica, California 90406	
Attn: N. Byrd	1
Monsanto Research Corporation Dayton Laboratory Station B, Box 8 Dayton, Ohio 45407	
Attn: Library	1
North American Rockwell Corporation Space & Information Systems Division 12214 Lakewood Blvd. Downey, California 90242	
Attn: Technical Information Center D/096-722 (AJ01)	1
Northrop Corporate Laboratories Hawthorne, California 90250	
Attn: Library	1
Rocketdyne, A Division of North American Rockwell Corporation 6633 Canoga Avenue Canoga Park, California 91304	
Attn: Library, Dept. 596-306	1

DISTRIBUTION LIST (continued)

	Copies
Union Carbide Corporation 12900 Snow Road Parma, Ohio	
Attn: Library	1
United Aircraft Corporation United Aircraft Research Laboratories East Hartford, Connecticut 06118	
Attn: D. A. Scola	1
United Aircraft Corporation Pratt and Whitney Aircraft East Hartford, Connecticut 06108	
Attn: G. Wood	1
United Aircraft Corporation United Technology Center P. O. Box 358 Sunnyvale, California 94088	
Attn: Library	1
Westinghouse Electric Corporation Westinghouse Research Laboratories Pittsburgh, Pennsylvania	
Attn: Library	1
Whittaker Corporation Research & Development/San Diego 3540 Aero Court San Diego, California 92123	
Attn: R. Gosnell	1
TRW Systems One Space Park Redondo Beach, California 90278	
Attn: Dr. E. A. Burns, Bldg. 01, Room 2020	3

DISTRIBUTION LIST (continued)

	Copies
General Dynamics Convair Aerospace Division P.O. Box 748 Fort Worth, Texas 76101	
Attn: Tech. Library, 6212	1
Material Science Corporation 1777 Walton Road Blue Bell, Pennsylvania 19422	
Attn: Ms. N. Sabia	1
Fiber Science Inc. 245 East 157 Street Gardena, California 90248	
Attn: L. J. Ashton	1
U.S. Army Air Mobility R&D Lab Fort Eustis, Virginia 23604	
Attn: Mr. H. L. Morrow, SAVDL-EU-TAP	1
U.S. Army Aviation Systems Command P.O. Box 209, Main Office St. Louis, Missouri 63166	
Attn: Mr. Ronald Evers	1
United States Air Force Aero Propulsion Laboratory Wright-Patterson AFB, Ohio 45433	
Attn: Mr. T. J. Norbut, AFAPL/TBP	1
Air Force Materials Laboratory Wright-Patterson AFB, Ohio 45433	
Attn: Mr. Paul Pirrung, AFML/LTN	1
Allison Division of Detroit Diesel Company P.O. Box 894 Department 5827, S42 Indianapolis, Indiana 46206	
Attn: John Spees	1